

©2009

Leilani Singson del Rosario

ALL RIGHTS RESERVED

PREPARATION AND EVALUATION OF AMPHIPHILIC MACROMOLECULES-
BASED CONJUGATES AND MICELLES FOR ANTICANCER DRUG DELIVERY

by

LEILANI SINGSON DEL ROSARIO

A dissertation submitted to the
Graduate School-New Brunswick
Rutgers, The State University of New Jersey
in partial fulfillment of the requirements

for the degree of

Doctor of Philosophy

Graduate Program in Chemistry and Chemical Biology

written under the direction of

Professor Kathryn E. Uhrich

and approved by

New Brunswick, New Jersey

May, 2009

ABSTRACT OF THE DISSERTATION

Preparation and Evaluation of Amphiphilic Macromolecules-Based Conjugates and
Micelles for Anticancer Drug Delivery
By LEILANI SINGSON DEL ROSARIO

Dissertation Director:
Professor Kathryn E. Uhrich

Micelles assembled from amphiphilic macromolecules (AM) or drug-conjugated AMs were evaluated as anticancer drug carriers in terms of drug content, sustained/controlled drug release and cytotoxicity of encapsulated/bound drug. Physical drug encapsulation was compared with chemical drug conjugation. The AM micelles were compared with known polymeric delivery systems, Pluronic P85 and Cremophor EL. Generally, AM micelles encapsulated drugs as efficiently (or better) than the established polymeric carriers.

Encapsulated hydrophobic drugs in AM micelles showed non-aggregation of drug and sustained drug release after lyophilization and resolubilization in aqueous solutions; indicating good solution and storage stability of drug-loaded AM micelles. Compared to the polymeric controls, the AM micelles showed faster resolubilization times and better pH/temperature micellar stability.

Cellular entry of AM micelles in human umbilical vein endothelial cells was observed to be endocytotic, observed from the colocalization of fluorescein-labeled AMs and

fluorescent dye-stained endosomes or lysosomes that were detected by confocal scanning microscopy.

Doxorubicin (DOX) was conjugated to AMs *via* acidic pH-sensitive hydrazone linkers and the DOX-AM micelles had ~ 30 nm sizes. DOX-AMs showed higher drug release at lysosomal pH 5.0 as compared to physiological pH 7.4. Cell proliferation assays of DOX-AM micelles showed better cytotoxicity compared to DOX-loaded AM micelles and free DOX against human hepatocellular carcinoma cells.

As another example of drug conjugation, camptothecin (CPT) was conjugated to AMs *via* glycine linkers. CPT-AM micelles showed CPT lactone stabilization, higher CPT solubilization, and increased stability against human serum albumin (HSA) on CPT release *in vitro*. However, cell proliferation assays on the CPT-AM micelles showed comparable cytotoxicity to CPT-loaded AM micelles against human colorectal carcinoma cells.

The placement of CPT conjugation was evaluated by CPT conjugation *via* mucic acid and functionalized alkyl chains. Carbodiimides were used to conjugate CPT to AM mucic acid, whereas click chemistry conjugated alkyne-terminated CPT to azide-terminated AM chains. Higher CPT conjugation was achieved *via* the functionalized chain ends (i.e. click chemistry) compared to the mucic acid (carbodiimide coupling). However, lesser HSA impact on CPT *in vitro* release was observed in CPT attached to the mucic acid.

Overall, the AM-based micelles showed good characteristics as anticancer drug carriers.

ACKNOWLEDGEMENTS

My deepest, most heartfelt thanks to Prof. Kathryn Uhrich, who is a warm, big-hearted and caring advisor, a kind mentor, an enthusiastic and brilliant scientist, an engaging speaker and a dynamic professor. Her encouragement and support especially during life-changing events in my graduate school life allowed me to continue and finish my Ph.D. studies. I will always be grateful for her faith in me, kindness and generosity. She is an inspiration to me and she will always be close to my heart.

My sincerest thanks to my thesis committee members: Prof. Ralf Warmuth, Prof. John Taylor and Prof. Barth Grant, for their valuable questions, comments and suggestions to my PhD thesis. My sincerest thanks to Prof. Joachim Kohn, Prof. Leslie Jimenez, Prof. John Taylor, Prof. Ralf Warmuth and Prof. David Talaga for their helpful critiques, questions, comments and suggestions in my in-field research proposal and out-of-field research proposal.

My warmest thanks to the Uhrich Group: Jinzhong, Michelle, Rob, Bryan, especially to Ashley and Sarah for all their help in the lab, with my in-field research proposal and my thesis. Many thanks to Melissa who helped me on some research experiments and to Nasreen for the friendly talks (with cookies and tea). My deepest thanks to Alex and Dave for the enjoyable, helpful talks, and for all their time, work and effort on the DOX and CPT projects.

Special thanks to Jelena for teaching me everything I know about cell culture, and for her encouragement in my research. Special thanks to Almudena for being a friend, for the laughs and talks. My heartfelt, sincerest thanks to Bahar for helping me a lot with my research experiments and for being my friend in the lab.

Warmest thanks to Min Jung, Jeremy and the friendly people in the Shreiber/Buettner lab (Gary, Harini, Shirley, Ian, Margaret and Andrew) for always being helpful and nice to me. I am also thankful to Jing and Frank for the laughs and friendly talks.

My sincerest thanks to Gary for his help with the SPSS software, to Matt for his help with the Image Pro Plus, to Ram for his help with the confocal scanning microscopy, to Karen for her help with the spectofluorimeter, and to Hanshella for her help with GPC analysis. My sincerest thanks to Kris Wetter, Melissa Grunweg and Ann Doeffinger for all their help.

Many happy thanks for the wonderful grads in chemistry: Patricia M, Karen S., Xue Jun, Lisa H., and James L. for their friendships. Special thanks to Sezgin, Joe and Kehinde for helping me with my research.

My warmest thanks to Krissy and Barry, for their friendship and for the memorable times we spent together. I look forward to seeing you both again. Warmest thanks also to Emel for her friendship and our enjoyable talks with yoghurt and tea.

My happy thanks to my dearest friend, Jennifer I., for all her help from simple things to taking care of Julia, for our enjoyable trips and our fun talks. Her friendship means a lot to me and I will keep it and cherish it in my life.

My deepest thanks to my bestfriend, Ahalya, who was always willing to help me especially during the toughest times in my graduate school life. She is very generous, caring, strong, admirable, and inspiring. I love her dearly.

My deepest thanks to my family: to Mama, Papa, Kuya Yani, Ate Joan, Gio, Yanna, and Kuya Mike for being my inspiration and strength. My sincerest thanks to Nanay Dinah, Tatay Jess and Ate Joyce for all their help to us especially in taking care of Julia. Warmest thanks to Ate Jasmin, Justine and Kuya James for playing with Julia and helping take care of her. Warm thanks to Alexandra for being a reliable and caring babysitter to Julia.

My deepest and heartfelt thanks to my husband Jasper, for his constant patience, his unending encouragement and support, his love and care. I could not have survived grad school without him by my side. My happy thanks to my darling Julia - my joy and inspiration. Her laughs, hugs and kisses strengthened me and inspired me to finish my grad studies.

Finally, I praise and thank GOD for all the wonderful blessings He has given us and I lift everything up to Him.

TABLE OF CONTENTS

ABSTRACT.....	ii
ACKNOWLEDGMENTS.....	iv
TABLE OF CONTENTS.....	vii
LIST OF FIGURES.....	xiii
LIST OF TABLES.....	xvii
CHAPTER 1: BACKGROUND AND SIGNIFICANCE	
1.1. Need for Drug Carriers.....	1
1.1.1. Indomethacin.....	2
1.1.2. Doxorubicin.....	3
1.1.3. Camptothecin.....	3
1.2. Drug Carriers: Polymeric Micelles.....	4
1.2.1. Polymeric Micelle Formation.....	5
1.2.2. Drug Loading.....	5
1.2.3. <i>In Vitro</i> Drug Release.....	7
1.3. Drug Carriers: Amphiphilic Macromolecules-based Conjugates and Micelles	7
1.3.1. Intracellular Drug Delivery.....	8
1.4. Drug Carriers: Pluronic P85 and Cremophor EL.....	10
1.5. Significance.....	10
1.6. References.....	12

CHAPTER 2: STORAGE AND SOLUTION STABILITY OF DRUG-LOADED
AMPHIPHILIC MACROMOLECULES-BASED MICELLES

2.1. Introduction.....	28
2.2. Materials.....	29
2.3. Methods.....	30
2.3.1. Drug Loading.....	30
2.3.2. Resolubilization of Lyophilized IMC-Loaded Polymeric Micelles.....	31
2.3.3. pH and Temperature Solution Stability.....	32
2.3.4. IMC <i>In Vitro</i> Release from Resolubilized Polymeric Micelles.....	33
2.4. Results and Discussion.....	33
2.4.1. Drug Loading.....	33
2.4.2. Resolubilization.....	34
2.4.3. pH and Temperature Solubility Stability.....	34
2.4.4. IMC <i>In Vitro</i> Release.....	35
2.5. Conclusions.....	36
2.6. References.....	37

CHAPTER 3: SUBCELLULAR LOCALIZATION OF FITC-LABELED AMPHIPHILIC
MACROMOLECULES (FITC-AM) IN HUVECS

3.1. Introduction.....	46
3.2. Materials.....	47
3.3. Methods.....	48
3.3.1. Cell Culture: Human Umbilical Vein Endothelial Cells.....	48

3.3.2. <i>In vitro</i> pH Stability of FITC-AM.....	48
3.3.3. Dynamic Light Scattering Measurements.....	48
3.3.4. Confocal Laser Scanning Microscopy (CLSM).....	49
3.3.4.1. Localization in Early and Recycling Endosomes.....	49
3.3.4.2. Localization in Endo-lysosomal Compartments.....	50
3.4. Results and Discussion.....	51
3.4.1. Preparation of FITC-AM.....	51
3.4.2. Subcellular Localization observed via CLSM.....	52
3.5. Conclusions.....	53
3.6. References.....	54

CHAPTER 4: PHYSICALLY ENCAPSULATED AND CHEMICALLY BOUND DOXORUBICIN IN AMPHIPHILIC MACROMOLECULES-BASED MICELLES

4.1. Introduction.....	62
4.2. Materials.....	64
4.3. Methods.....	65
4.3.1. Cell Culture: Human Liver Cancer Cells.....	65
4.3.2. Chemical Characterization of DOX-AM.....	65
4.3.3. Preparation of Hydrazide-AM.....	67
4.3.4. Preparation of DOX-AM.....	68
4.3.5. DOX Loading by Dialysis Method.....	68
4.3.6. Size Analysis of DOX-AM Micelles.....	69
4.3.7. <i>In Vitro</i> DOX Release.....	70

4.3.8. <i>In Vitro</i> Cytotoxicity Assay against HepG2 Human Liver Cancer Cells.....	70
4.3.9. Analysis of DOX-loaded DOX-AM Micelles.....	71
4.3.10. Comparison with Pluronic P85 and Cremophor EL.....	72
4.3.11. Statistical Analysis.....	72
4.4. Results and Discussion.....	72
4.4.1. Preparation and Characterization of DOX-AM.....	72
4.4.2. DOX Loading in AM micelles.....	74
4.4.3. Size Analysis of DOX-AM Micelles and DOX-loaded AM micelles.....	74
4.4.4. <i>In Vitro</i> DOX Release from DOX-AM.....	75
4.4.5. <i>In Vitro</i> Cytotoxicity Assay of DOX-loaded AMs and DOX-AMs.....	75
4.4.6. Analysis of DOX-Loaded DOX-AM Micelles.....	76
4.4.7. Comparison with Pluronic P85 and Cremophor EL.....	78
4.5. Conclusions.....	78
4.6. References.....	80

CHAPTER 5: PHYSICALLY ENCAPSULATED AND CHEMICALLY BOUND
CAMPTOTHECIN IN AMPHIPHILIC MACROMOLECULES-BASED MICELLES

5.1. Introduction.....	97
5.2. Materials.....	99
5.3. Methods.....	100
5.3.1. Cell Culture: Human Colon Cancer Cells.....	100
5.3.2. Chemical Characterization of CPT-AM.....	100
5.3.3. Synthesis of CPT-AM... ..	101

5.3.4. Size Analysis of CPT-AM Micelles.....	102
5.3.5. CPT-Loading by Solvent Evaporation.....	103
5.3.6. Impact of HSA on CPT Release <i>In Vitro</i>	104
5.3.7. <i>In Vitro</i> Cytotoxicity Assay against Human Colon Cancer Cells.....	105
5.3.8. Analysis of CPT-loaded CPT-AM Micelles.....	105
5.3.9. Comparison with Pluronic P85 and Cremophor EL.....	106
5.3.10. Statistical Analysis of Data.....	106
5.4. Results and Discussion.....	106
5.4.1. Synthesis and Characterization of CPT-AM Conjugates	106
5.4.2. Size Analysis of CPT-AM Micelles.....	107
5.4.3. CPT Content in AM micelles vs CPT-AM micelles.....	108
5.4.4. Impact of HSA on CPT Release <i>In Vitro</i>	108
5.4.5. <i>In Vitro</i> Cytotoxicity Assay.....	109
5.4.6. Analysis of CPT-loaded CPT-AM Micelles.....	109
5.4.7. Comparison with Pluronic P85 and Cremophor EL.....	110
5.5. Conclusions.....	110
5.6. References.....	111

CHAPTER 6: CAMPTOTHECIN-CONJUGATED AMPHIPHILIC

MACROMOLECULES: CPT-MUCIC-AM VS CPT-ALKYL-AM

6.1. Introduction.....	124
6.2. Materials.....	125
6.3. Methods.....	126

6.3.1. Chemical Characterization of CPT-Mucic/Alkyl AM Conjugates.....	126
6.3.2. Preparation of CPT-Mucic-AM Conjugates by Direct Conjugation.....	127
6.3.3. Preparation of CPT-Alkyl-AM Conjugates by Click Chemistry.....	128
6.3.4. Impact of HSA on CPT Release <i>In Vitro</i>	129
6.3.5. Impact of HSA on CPT-Mucic/Alkyl Micellar Sizes <i>In Vitro</i>	130
6.4. Results and Discussion.....	130
6.4.1. Preparation and Characterization of CPT-Mucic/Alkyl-AM Conjugates.....	130
6.4.2. Impact of HSA on CPT Release <i>In Vitro</i>	132
6.4.3. Impact of HSA on CPT-Mucic/Alkyl-AM Micellar Sizes <i>In Vitro</i>	132
6.5. Conclusions.....	133
6.6. References.....	134
FUTURE WORK.....	143
CURRICULUM VITA.....	147

LIST OF FIGURES

CHAPTER 1

Figure 1-1. Chemical structure of indomethacin.....	21
Figure 1-2. Chemical structure of doxorubicin.....	22
Figure 1-3. Chemical structures of CPT lactone and CPT carboxylate.....	23
Figure 1-4. Cartoon of unimer-micelle equilibrium at critical micelle concentration.....	24
Figure 1-5. Physical encapsulation of hydrophobic drugs into polymeric micelles: I. Dialysis method; II Oil-in-water emulsion method.....	25
Figure 1-6. Drug release mechanisms from polymeric micelles.....	26
Figure 1-7. Lysosomotropic drug delivery of polymer-drug conjugates.....	27

CHAPTER 2

Figure 2-1. Chemical structures of amphiphilic macromolecules: self-assembled micelles AM 1 and AM 2, unimolecular micelles AM 3 and AM 4.....	40
Figure 2-2. UV analysis of pH and temperature stability of representative CPT-loaded AM 4 micelles.....	41
Figure 2-3. DLS analysis of CPT-loaded polymeric micelle stability with pH: a-b) AM 1, c-d) AM 4, e-f) Pluronic P85, g-h) Cremophor EL.....	42
Figure 2-4. <i>In vitro</i> IMC cumulative release profile from polymeric micelles within 48 h.....	43

CHAPTER 3

Figure 3-1. Chemical structures of a) Texas Red and b) LysoTracker Red.....	56
Figure 3-2. Chemical structure of FITC-AM.....	57
Figure 3-3. Micelle size number-weight distribution from dynamic light scattering studies: (a) AM micelles and (b) FITC-labeled micelles.....	58
Figure 3-4. Confocal images demonstrating the co-localization of FITC-labeled micelles with Texas Red-stained endosomes in HUVECs.....	59
Figure 3-5. Confocal images demonstrating the co-localization of FITC-labeled micelles with LysoTracker Red-stained lysosomes in HUVECs.....	60
Figure 3-6. Confocal images demonstrating the contrast in fluorescence of FITC control and FITC-labeled micelles in HUVECs.....	61

CHAPTER 4

Figure 4-1. Cartoon of micelle formation of DOX-AM conjugates.....	87
Figure 4-2. Preparation of DOX-AM conjugate.....	88
Figure 4-3. Detection of hydrazide end groups by TNBSA assay ($\lambda = 500$ nm)....	89
Figure 4-4. Gel permeation chromatograms before and after DOX conjugation....	90
Figure 4-5. UV-vis absorption spectra of hydrazide-AM, free DOX, DOX conjugated to AM, and DOX physically admixed with AM.....	91
Figure 4-6. Spectrofluorometric spectra of DOX admixed with AM (free drug) and DOX-AM (conjugated drug).....	92
Figure 4-7. TEM images showing spherical morphology of (a) mixed micelles assembled from aqueous solutions (100 μ M) of DOX-AM conjugates	

containing unconjugated AMs and (b) AM micelles with physically encapsulated and chemically bound DOX.....	93
Figure 4-8. <i>In vitro</i> DOX release from DOX-AM (9) at 37°C (pH 7.4 and 5.0)...	94
Figure 4-9. <i>In vitro</i> cytotoxicity of DOX in AM-based micelles against HepG2 cells after 72 h incubation.....	95
 CHAPTER 5	
Figure 5-1. Chemical structures of CPT lactone and CPT carboxylate.....	116
Figure 5-2. Cartoons of micelle assembly: (a) CPT-AM conjugates and (b) CPT loading AM micelles.....	117
Figure 5-3. Synthesis of CPT-AM conjugates.....	118
Figure 5-4. UV spectra of CPT derivatives and AM alone.....	119
Figure 5-5. Transmission electron micrograph of CPT-AM/AM mixed micelles in water (1 mg/mL) negatively stained with 1% uranyl acetate.....	120
Figure 5-6. Impact of HSA on CPT release from AM-based micelles.....	121
Figure 5-7. <i>In vitro</i> cytotoxicity of CPT and CPT-carrier versions against HT-29 cells after 72 h incubation.....	122
 CHAPTER 6	
Figure 6-1. Cartoon of AM showing possible sites of CPT attachment.....	136
Figure 6-2. Preparation of CPT-mucic-AM.....	137
Figure 6-3. Preparation of CPT-alkyl-AM.....	138
Figure 6-4. UV spectra of the two CPT forms and CPT-mucic-AM.....	139

Figure 6-5. UV spectra of the two CPT forms and CPT-alkyl-AM..... 140

LISTS OF TABLES

Table 2-1. Drug (CPT, IMC) loading capability of polymeric micelles.....	44
Table 2-2. Resolubilization time of lyophilized IMC-loaded polymeric micelles...	45
Table 4-1. DOX encapsulation capability and micellar sizes of AM-based micelles.....	96
Table 5-1. CPT encapsulation capability and solubility enhancement of AM- based micelles.....	123
Table 6-1. Impact of HSA on CPT <i>in vitro</i> release from AM-based micelles.....	141
Table 6-2. Impact of HSA on micellar sizes of AM-based CPT micelle carriers....	142

Chapter 1

BACKGROUND AND SIGNIFICANCE

1.1. Need for Drug Carriers

Several drugs such as indomethacin (IMC) [1, 2] and camptothecin (CPT) [3] have poor water solubility resulting in decreased bioavailability upon injection into the body. Other drugs such as doxorubicin (DOX) [4] have toxic side effects (e.g. cardiotoxicity) leading to dose limitations. Carriers are needed to improve the therapeutic efficacy of these drugs. Examples of drug carriers include liposomes [5-7], nanoparticles [3, 5, 8], nanospheres [9-11] and polymeric micelles [12-16]. As drug carriers, the following characteristics are generally important: water solubility, non-toxicity, non-immunogenicity, lack of long-term host accumulation, *in vivo* stability, targeted delivery, encapsulation ability of poorly water-soluble drugs and controlled drug release [17].

Alternatively, drug carriers also include polymer-drug conjugates wherein drugs are attached within the polymer backbone or to the polymer side chains [11, 18-24]. Polymer-drug conjugation improves the cell specificity of low molecular weight compounds [18] and leads to “radical changes in the pharmacokinetics” of drugs at cellular and body levels [18]. However, these systems must include the following characteristics: *i*) water solubility; *ii*) prolonged plasma circulation; *iii*) stability during transport then drug release at an optimum rate; *iv*) adequate drug capacity related to drug potency; and *v*) targeting ability by active (receptor-ligand) or passive (pathophysiological) mechanisms [11, 18, 20, 23, 24].

Another form of drug carrier includes PEGylated drugs which are drugs attached to high molecular weight poly(ethylene glycol) or PEG. PEGylated drugs are observed to have low urinary clearance, increased drug circulatory retention and tumor accumulation [25]. In addition, PEG conjugation reduces drug toxicity and increases drug therapeutic index [25]. However, limitations of PEGylated drug conjugates include low drug loading (e.g. 1.7 wt % for PEG-CPT conjugates [18]) as the drug can only be attached *via* one or two PEG chain ends.

1.1.1. Indomethacin (IMC)

Indomethacin (**Figure 1-1**) is an anti-pyretic, analgesic, potent non-steroidal anti-inflammatory drug for the treatment of conditions such as rheumatoid arthritis, ankylosing spondylitis, and osteoarthritis [26]. It also induces antitumor immunity to murine carcinoma cells and reduces tumor load in mice, with the antitumor effect associated with its capability to restore impaired immunosurveillance in tumor-bearing mice [27]. However, it is highly hydrophobic ($\log P = 4.18$) and has side effects of gastrointestinal mucosity irritation and central nervous system toxicity [26].

Current delivery systems for IMC include physical encapsulation in polymeric micelles [26, 28, 29] for improved water solubility. Other delivery systems include conjugation to β -cyclodextrins [1, 2] to improve IMC water solubility and bioavailability. IMC was also conjugated to chitosan [30] or PEG [31] but IMC was used only as a model drug in these systems designed for mucosal drug delivery.

1.1.2. Doxorubicin (DOX)

Doxorubicin (**Figure 1-2**), also known as adriamycin (ADR) has antitumor activity [32], belongs to the class of anthracycline antibiotics, and has dose limitations resulting from non-specific cardiotoxicity [4].

Current delivery systems for DOX include micelles [33-37] and liposomes [6, 7] and other carriers. Polymer-DOX conjugates include N-(2-hydroxypropyl)methacrylamide (HPMA)-DOX conjugates [38, 39], PEG-poly(lactic-*co*-glycolic acid)-DOX [40] and PEG-poly(aspartic acid)-DOX [41], among others. DOX conjugation reportedly led to longer sustained release profile and higher cytotoxic activity than free drug [40], long blood circulation times and low liver/spleen uptake *in vivo* [41]. However, toxicity problems arise from accumulation of non-biodegradable polymers if administered intravenously with molecular weights higher than the renal threshold [18].

1.1.3. Camptothecin (CPT)

CPT was first isolated from the Chinese tree *Camptotheca acuminata* [3, 42] and inhibits Topoisomerase I during the S-phase of the cell cycle [43]. In biological systems, there is a pH-dependent equilibrium (**Figure 1-3**), wherein the active CPT lactone form predominant at pH 4.0-5.0, converts to the inactive carboxylate form in a more basic environment [43]. Preferential binding of CPT carboxylate to human serum albumin (HSA) limits the therapeutic efficacy of CPT [44].

Current delivery systems for CPT include liposomes [45], polymeric micelles [46-49] nanoparticles [8, 50-52] and microspheres [53, 54]. Polymer-CPT conjugates include linear β -cyclodextrin-based polymers with amino acid/peptide linkers [55], phthalimide-based polymers [56, 57], poly(L-glutamic acid)-based polymers with glycine linkers [44], and HPMA-based polymers with peptide spacers [43]. CPT conjugation reportedly led to higher cytotoxicity than free drug [56, 57], and improved pharmacological profile of the conjugates in animal models compared to the free drug [43]. However, problems were reported in clinical trials on low drug loading of HPMA copolymer-CPT conjugates [18] and dose-limiting cumulative bladder toxicity of methacrylate-CPT conjugates [18].

1.2. Drug Carriers: Polymeric Micelles

Polymeric micelles have many desirable characteristics for anticancer drug delivery [16]: *i*) hydrophobic-core-hydrophilic-shell structure allowing water solubilization of water-insoluble drugs; *ii*) hydrophilic shells which minimize uptake by macrophages; *iii*) high molecular weight that prevents renal excretion; and *iv*) accumulation of micelle-incorporated drugs in tumors compared to free drug that is explained by the “enhanced permeability and retention effect or EPR effect” [16, 58]. The EPR effect is considered a “universal solid tumor phenomenon for macromolecular drugs” [25] wherein greater accumulation of high MW molecules in tumors than in normal tissues result from increased tumor vascular permeability and impaired lymphatic drainage [16, 17, 25, 58, 59]. Compared to other delivery systems, polymeric micelles have small sizes and the advantages of sterilization by filtration and no capillary embolism [17, 58]. Consequently, polymeric micelles are widely studied as carriers of hydrophobic drugs.

1.2.1. Polymeric Micelle Formation

Micelle formation from amphiphilic block copolymers is the result of two forces: an attractive force leading to the association of molecules and a repulsive force preventing unlimited growth to a distinct macroscopic phase [16]. At very low concentrations, the polymers exist as unimers in solution (**Figure 1-4**). At the critical micelle concentration (CMC), the hydrophobic chains assemble in solution to avoid contact with water [16], and form spherical [17, 58] micelles (**Figure 1-4**). This equilibrium process is entropy-driven [59]; there is an increase in disorder as water molecules move from around the hydrophobic chains into the bulk solution.

1.2.2. Drug loading

The core-shell structure of polymeric micelles (shown in **Figure 1-4**) allows solubilization of water-insoluble drugs in the micellar core [16, 58]. Physical entrapment of drugs is generally performed by oil-in-water emulsion [60, 61], dialysis [26, 62] or solvent evaporation [63, 64], depending on the characteristics of the polymer and the drug (**Figure 1-5**).

For water-soluble polymers and highly water-insoluble drugs, the oil-in-water emulsion method is preferred, as the polymer is first dissolved in water (or buffer solution) and the drug dissolved in a volatile solvent (e.g. dichloromethane) is added. The dialysis method is preferred for less water-soluble polymers, as both the drug and polymer are first dissolved in a water-miscible organic solvent (e.g. dimethyl sulfoxide)

and then dialyzed against water. Solvent evaporation method is an alternative for the dialysis method, as disposal of the large amount of dialysate (solution outside the dialysis bags) containing the anticancer drug can be a problem. In the solvent evaporation method, both the drug and polymer are first dissolved in a relatively volatile solvent (e.g. tetrahydrofuran). The solvent is then removed, and replaced with buffer solution.

The extent of drug loading is dependent on factors such as the molecular volume of the drug and its interfacial tension against water, the length of the core- and shell-copolymer blocks, and the drug/polymer concentration [17]. The amount of drug encapsulated in the micelles is detected by UV-visible spectrophotometry or by reverse phase high pressure liquid chromatography (RP-HPLC). Drug loading is often reported in terms of weight % loading, encapsulation efficiency (%) and solubility enhancement (-fold).

Weight % loading is the amount of drug physically encapsulated in a given amount of the polymer and indicative of the drug loading capability of the polymer micelle. Encapsulation efficiency is the amount of drug effectively loaded into the micelles and shows the efficiency of the drug loading process. Solubility enhancement indicates the increase (-fold) in drug solubility in the presence of the polymer; it is evidence of drug water solubilization by the polymeric micelle. These terms are calculated as follows:

$$\text{Weight \% Loading} = \frac{\text{Concentration of drug detected}}{\text{Concentration of polymer}} \times 100$$

$$\text{Encapsulation Efficiency (\%)} = \frac{\text{Concentration of drug detected}}{\text{Initial concentration of drug}} \times 100$$

$$\text{Solubility Enhancement (-fold)} = \frac{\text{Solubility of drug in the presence of polymer}}{\text{Solubility of drug alone}}$$

1.2.3. *In Vitro* Drug Release

Physically encapsulated drugs are released from stable micelles by diffusion or by the dissociation of the micelles into the unimers (**Figure 1-6**) [16, 17]. Controlled or slow release of the drug is ideal, (i.e. the depot effect [58]) as sudden release of the drug or “dose dumping” may lead to intra-vascular precipitation of the drug [16, 58]. Alternatively, favorable interaction between drug and micellar core may result in low diffusion rates [17].

1.3. Drug Carriers: Amphiphilic Macromolecules (AM)-based Conjugates and Micelles

Micelles assembled from amphiphilic macromolecules (AM) show excellent micellar characteristics of low CMC [65, 66], small sizes [65, 67], biodegradability [68] and non-cytotoxicity [65, 69]. Consequently, AM micelles were investigated as carriers of anticancer drugs (DOX, CPT). AM micelles have also shown high IMC wt % loading and sustained IMC release *in vitro* within 48 h [65, 70]. Thus, the storage/solution stability of AM micelles was investigated using IMC as a model drug. As polymer-drug conjugation offers several advantages to improve drug delivery, anticancer drugs (DOX, CPT) were also conjugated to amphiphilic macromolecules (AMs). Micelles assembled from the

drug-AM conjugates were then compared with AM micelles containing physically encapsulated drugs.

1.3.1. Intracellular Drug Delivery

One way to improve the efficiency of drug-loaded AM micelles is to determine their cellular internalization and enhance their intracellular drug delivery. Polymeric micelles typically enter the cell *via* the endocytic pathway [16] (**Figure 1-7**). Likewise, AM micelles are also expected to enter cells *via* the endocytotic pathway. Endocytosis involves invagination of the cell membrane upon interaction with the macromolecules leading to the formation of membrane-bound vesicles that mature to endosomes and fuse with acidic lysosomes (pH ~5.0) that contain degrading enzymes (proteases, esterases, glycosidases, phosphatases and nucleases) [71].

In the absence of drug carriers, drug molecules enter cells by diffusion through the cell membranes [71, 72]. However, drug efflux can occur wherein the drug is pumped out of the cell by P-glycoprotein pumps resulting to multidrug resistance in cancer cells [73]. In contrast, drugs internalized by endocytosis bypass efflux pumps [74]. Furthermore, polymeric micelles assembled from poly(caprolactone)-*b*-poly(ethylene oxide) showed increased delivery of 5-dodecanoylaminofluorescein (DAF) inside rat pheochromocytoma cells compared to DAF alone, suggesting the potential of polymeric micelles for subcellular drug delivery [75]. In addition, polymeric micelles assembled from triblock copolymers of poly(ethylene oxide)-poly(propylene oxide)-poly(ethylene oxide) (Pluronic P105) showed a “drug-shielding effect”, wherein the drugs that entered

promyelocytic cells remained inside the micelles and internalized inside the cells *via* endocytosis [76]. Thus, it is possible that AM micelles increase cellular drug uptake and provide drug shielding effect, resulting in increased cytotoxicity of encapsulated drugs compared to free drug.

Polymer-drug conjugates also enter cells by endocytosis i.e. “piggy-back endocytosis” [59, 77]. To enhance intracellular drug delivery of polymer-drug conjugates, linkers sensitive to lysosomal pH (~5.0) or lysosomal enzymes (e.g. cathepsin) are used in polymer-drug conjugation to allow drug release inside the lysosomes (**Figure 1-7**) [18, 24]. Nuclear accumulation of DOX bound to HPMA copolymers *via* lysosomally degradable linkers was observed in epithelial ovarian carcinoma cells [78]. Similarly, DOX-AM conjugates were designed with acidic pH-sensitive hydrazone linkers for enhanced intracellular DOX delivery in cancer cells.

Delivery of the drug to the subcellular target site is important, and studies have shown accumulation of HPMA polymers (and some of DOX-HPMA polymers attached via nondegradable spacers) in the nucleus of human hepatocellular carcinoma cells after endocytosis and endosomal/lysosomal escape [73, 77]. This nuclear accumulation was unexpected as the polymers were uncharged, but this observation shows the potential of polymers for the nuclear delivery of drugs that are active on nuclear components [73, 77]. Thus, it is possible for AMs or drug-AM conjugates to deliver drugs to the nucleus. However, it is still not understood why the HPMA copolymer or DOX-HPMA conjugates partition to the nucleus [73, 77] and further understanding about the nuclear entry of

polymers is necessary before nuclear drug delivery of AMs or drug-AM conjugates can be explored.

1.4. Drug Carriers: Pluronic P85 and Cremophor EL

In this dissertation, the AM-based micelles were compared with Pluronic P85 and Cremophor EL to determine if their drug carrier capabilities compare with these widely used drug carriers.

Pluronic systems are composed of triblock copolymers of poly(ethylene oxide)-poly(propylene oxide)-poly(ethylene oxide) and are used for drug and gene delivery [76, 79, 80]. However, limitations result from high CMC values of the Pluronic micelles resulting in “moderately stable to relatively unstable micelles” [80].

Cremophor EL is a mixture of glycerol-PEG ricinoleate, fatty acid esters of PEG, PEG and ethoxylated glycerols (BASF, Ludwigshafen, Germany). Cremophor EL is commonly used in the pharmaceutical field in the aqueous preparation of hydrophobic substances [81, 82]. However, problems with hypersensitivity, neurotoxicity and nephrotoxicity are reported [81, 82].

1.5. Significance

Even though numerous drug carriers are currently evaluated for the delivery of hydrophobic drugs, several problems still persist, arising from polymer non-biodegradability [18], polymer toxicity [82] or micellar instability [80]. Micelles

assembled from amphiphilic macromolecules (AM) have shown excellent micellar properties of low CMC (10^{-7} M) [65, 66], small micellar sizes [65, 67], high drug encapsulation [65], sustained drug release [65, 70], biodegradability [68] and non-cytotoxicity [65, 69]. Clearly, these micelles show potential as anticancer drug carriers.

In this dissertation, the storage/solution stability of drug-loaded AM micelles was first evaluated to determine the effect of lyophilization and resolubilization on drug aggregation and drug release (Chapter 2). Next, cellular internalization of AMs was analyzed (Chapter 3) with the aim of developing drug-AM conjugates for intracellular drug delivery. Anticancer drugs DOX (Chapter 4) and CPT (Chapter 5) were conjugated to AMs to improve drug solubility (CPT) and control drug release (DOX). In Chapters 4 and 5, physical encapsulation of drug was compared with chemical conjugation in AM micelles in terms of: *i*) drug content/drug solubility enhancement, *ii*) micellar sizes, *iii*) drug release and *iv*) cytotoxicity against cancer cells. Furthermore, in Chapters 2, 4 and 5, the AM-based micelles were compared with two widely-used polymeric carriers: Pluronic P85 and Cremophor EL. Finally, the effect of drug attachment to AMs (carboxylic end of micellar core vs alkyl side chains) on conjugation yield, micellar sizes and drug release was investigated (Chapter 6). This dissertation therefore evaluated all the important features of amphiphilic macromolecules-based micelles as anticancer drug carriers.

1.6 References

- 1 N. Wang, Q. Wu, Y. M. Xiao, C. X. Chen, and X. F. Lin. Regioselective synthesis of cyclodextrin mono-substituted conjugates of non-steroidal anti-inflammatory drugs at C-2 secondary hydroxyl by protease in non-aqueous media. *Bioorganic and Medicinal Chemistry* **13**: 3667-3671 (2005).
- 2 H. Namazi, S. Bahrami, and A. A. Entezami. Synthesis and controlled release of biocompatible prodrugs of β -cyclodextrin linked with PEG containing ibuprofen or indomethacin. *Iranian Polymer Journal* **14**: 921-927 (2005).
- 3 A. Hatefi and B. Amsden. Camptothecin delivery methods. *Pharmaceutical Research* **19**: 1389-1399 (2002).
- 4 D. L. Hershman, R. B. McBride, A. Eisenberger, W. Y. Tsai, V. R. Grann, and J. S. Jacobson. Doxorubicin, Cardiac Risk Factors, and Cardiac Toxicity in Elderly Patients with Diffuse B-Cell Non-Hodgkin's Lymphoma. *Journal of Clinical Oncology* **26**: 3159-3165 (2008).
- 5 C. Monfardini and F. M. Veronese. Stabilization of substances in circulation. *Bioconjug. Chem.* **9**: 418-450 (1998).
- 6 R. I. Pakunlu, Y. Wang, M. Saad, J. Khandare, V. Starovoytov, and T. Minko. *In vitro* and *in vivo* intracellular liposomal delivery of antisense oligonucleotides and anticancer drug. *Journal of Controlled Release* **114**: 153-162 (2006).
- 7 R. M. Rifkin, S. A. Gregory, A. Mohrbacher, and M. A. Hussein. Pegylated Liposomal Doxorubicin, Vincristine, and Dexamethasone Provide Significant Reduction in Toxicity Compared with Doxorubicin, Vincristine, and Dexamethasone in Patients with Newly Diagnosed Multiple Myeloma. *Cancer* **106**: 848-858 (2006).
- 8 J. Williams, R. Lansdown, R. Sweitzer, M. Romanowski, R. LaBell, R. Ramaswami, and E. Unger. Nanoparticle drug delivery system for intravenous delivery of topoisomerase inhibitors. *Journal of Controlled Release* **91**: 167-172 (2003).

- 9 K. Letchford and H. Burt. A review of the formation and classification of amphiphilic block copolymer nanoparticulate structures: micelles, nanospheres, nanocapsules and polymersomes. *Eur. J. Pharm. Biopharm.* (2007).
- 10 Y. Hu, Y. Ding, D. Ding, M. Sun, L. Zhang, X. Jiang, and C. Yang. Hollow Chitosan/Poly(acrylic acid) Nanospheres as Drug Carriers. *Biomacromolecules* **8**: 1069-1076 (2007).
- 11 R. Tong and J. Cheng. Anticancer Polymeric Nanomedicines. *Polymer Reviews* **47**: 345-381 (2007).
- 12 H. M. Aliabadi, M. Shahin, D. R. Brocks, and A. Lavasanifar. Disposition of drugs in block copolymer micelle delivery systems: from discovery to recovery. *Clin. Pharmacokinet.* **47**: 619-634 (2008).
- 13 V. P. Torchilin. Structure and design of polymeric surfactant-based drug delivery systems. *Journal of Controlled Release* **73**: 137-172 (2001).
- 14 V. P. Torchilin. Micellar Nanocarriers: Pharmaceutical Perspectives. *Pharm. Res* **24**: 1-16 (2007).
- 15 K. Kataoka, A. Harada, and Y. Nagasaki. Block copolymer micelles for drug delivery: design, characterization and biological significance. *Advanced drug delivery reviews* **47**: 113-131 (2001).
- 16 M. C. Jones and J. C. Leroux. Polymeric micelles- a new generation of colloidal drug carriers. *European Journal of Pharmaceutics and Biopharmaceutics* **48**: 101-111 (1999).
- 17 A. Lavasanifar, J. Samuel, and G. S. Kwon. Poly(ethylene oxide)-*block*-poly(L-amino acid) micelles for drug delivery. *Advanced Drug Delivery Reviews* **54**: 169-190 (2002).
- 18 R. Duncan. The dawning era of polymer therapeutics. *Nature Reviews Drug Discovery* **2**: 347-360 (2003).
- 19 K. Hoste, K. D. Winne, and E. Schacht. Polymeric prodrugs. *International Journal of Pharmaceutics* **277**: 119-131 (2004).

- 20 J. Khandare and T. Minko. Polymer-drug conjugates: Progress in polymeric prodrugs. *Prog. Polym. Sci.* **31**: 359-397 (2006).
- 21 C. Li and S. Wallace. Polymer-drug conjugates: recent development in clinical oncology. *Advanced drug delivery reviews* **60**: (2008).
- 22 J. H. Park, S. Lee, J.-H. Kim, K. Park, K. Kim, and I. C. Kwon. Polymeric nanomedicine for cancer therapy. *Progress in Polymer Science* **33**: 113-137 (2008).
- 23 G. Pasut and F. M. Veronese. Polymer-drug conjugation, recent achievements and general strategies. *Progress in Polymer Science* **32**: 933-961 (2007).
- 24 K. Ulbrich, T. Etrych, P. Chytil, M. Pechar, M. Jelinkova, and B. Rihova. Polymeric anticancer drugs with pH-controlled activation. *International Journal of Pharmaceutics* **277**: 63-72 (2004).
- 25 R. B. Greenwald, C. D. Conover, A. Pendri, Y. H. Choe, A. Martinez, D. Wu, S. Guan, Z. Yao, and K. L. Shum. Drug delivery of anticancer agents: water soluble 4-poly(ethylene glycol) derivatives of the lignan, podophyllotoxin. *Journal of Controlled Release* **61**: 281-294 (1999).
- 26 S. B. La, T. Okano, and K. Kataoka. Preparation and characterization of the micelle-forming polymeric drug indomethacin-incorporated poly(ethylene oxide)-poly(β -benzyl-L-aspartate) block copolymer micelles. *Journal of Pharmaceutical Sciences* **85**: 85-90 (1996).
- 27 S. Morecki, E. Yacovlev, Y. Gelfand, V. Trembovler, E. Shohami, and S. Slavin. Induction of antitumor immunity by indomethacin. *Cancer Immunology and Immunotherapy* **48**: 613-620 (2000).
- 28 S. Y. Kim, I. G. Shin, Y. M. Lee, C. S. Cho, and Y. K. Sung. Methoxy poly(ethylene glycol) and caprolactone amphiphilic block copolymeric micelle containing indomethacin. II. Micelle formation and drug release behaviors. *J. Control. Release* **51**: 13-22 (1998).
- 29 W.-J. Lin, Y.-C. Chen, C.-C. Lin, C.-F. Chen, and J.-W. Chen. Characterization of pegylated copolymeric micelles and *in vivo* pharmacokinetics and biodistribution studies. *Journal of Biomedical Materials Research Part B: Applied Biomaterials* **77B**: 188-194 (2006).

- 30 I. Orienti, K. Aiedeh, E. Gianasi, C. Ponti, and V. Zecchi. Chitosan-indomethacin conjugates. Effect of different substituents on the polysaccharide molecule on drug release. *Arch. Pharm. Pharm. Med. Chem.* **329**: 245-250 (1996).
- 31 B. S. Lele and A. S. Hoffman. Mucoadhesive drug carriers based on complexes of poly(acrylic acid) and PEGylated drugs having hydrolysable PEG-anhydride-drug linkages. *J. Controlled Release* **69**: 237-248 (2000).
- 32 K. Yoshimatsu, A. Yamaguchi, H. Yoshino, N. Koyanagi, and K. Kitoh. Mechanism of action of E7010, an orally active sulfonamide antitumor agent: inhibition of mitosis by binding to the colchicine site of tubulin. *Cancer Research* **57**: 3208-3213 (1997).
- 33 E. S. Lee, K. Na, and Y. H. Bae. Doxorubicin loaded pH-sensitive polymeric micelles for reversal of resistant MCF-7 tumor. *Journal of Controlled Release* **103**: 405-418 (2005).
- 34 C. L. Lo, C. K. Huang, K. M. Lin, and G. H. Hsiue. Mixed micelles formed from graft and diblock copolymers for application in intracellular drug delivery. *Biomaterials* **28**: 1225-1235 (2007).
- 35 F. Kohori, M. Yokoyama, K. Sakai, and T. Okano. Process design for efficient and controlled drug incorporation into polymeric micelle carrier systems. *Journal of Controlled Release* **78**: 155-163 (2002).
- 36 Y.-Q. Ye, F.-L. Yang, F.-Q. Hu, Y.-Z. Du, H. Yuan, and H.-Y. Yu. Core-modified chitosan-based polymeric micelles for controlled release of doxorubicin. *International Journal of Pharmaceutics* **352**: 294-301 (2008).
- 37 J. You, F.-Q. Hu, Y.-Z. Du, and H. Yuan. Improved cytotoxicity of doxorubicin by enhancing its nuclear delivery mediated via nanosized micelles. *Nanotechnology* **19**: 1-8 (2008).
- 38 T. Etrych, M. Jelinkova, B. Rihova, and K. Ulbrich. New HPMA copolymers containing doxorubicin bound via pH-sensitive linkage: synthesis and preliminary in vitro and in vivo biological properties. *Journal of Controlled Release* **73**: 89-102 (2001).
- 39 T. Etrych, P. Chytil, M. Jelinkova, B. Rihova, and K. Ulbrich. Synthesis of HPMA Copolymers Containing Doxorubicin Bound via a Hydrazone Linkage.

- Effect of Spacer on Drug Release and in vitro Cytotoxicity. *Macromolecular Bioscience* **2**: 43-52 (2002).
- 40 H. S. Yoo and T. G. Park. Biodegradable polymeric micelles composed of doxorubicin conjugated PLGA-PEG block copolymer. *Journal of Controlled Release* **70**: 63-70 (2001).
- 41 M. Yokoyama, S. Fukushima, R. Uehara, K. Okamoto, K. Kataoka, Y. Sakurai, and T. Okano. Characterization of physical entrapment and chemical conjugation of adriamycin in polymeric micelles and their design for in vivo delivery to a solid tumor. *Journal of Controlled Release* **50**: 79-92 (1998).
- 42 J. Cheng, K. T. Khin, and M. E. Davis. Antitumor activity of β -cyclodextrin polymer-camptothecin conjugates. *Molecular Pharmaceutics* **1**: 183-193 (2004).
- 43 V. R. Caiolfa, M. Zamai, A. Fiorino, E. Frigerio, C. Pellizzoni, R. d'Argy, A. Ghiglieri, M. G. Castelli, M. Farao, E. Pesenti, M. Gigli, F. Angelucci, and A. Suarato. Polymer-bound camptothecin: initial biodistribution and antitumour activity studies. *Journal of Controlled Release* **65**: 105-119 (2000).
- 44 J. W. Singer, R. Bhatt, J. Tulinsky, K. R. Buhler, E. Heasley, P. Klein, and P. de Vries. Water-soluble poly(L-glutamic acid)-gly-camptothecin conjugates enhance camptothecin stability and efficacy in vivo. *Journal of Controlled Release* **74**: 243-247 (2001).
- 45 M. Watanabe, K. Kawano, K. Toma, Y. Hattori, and Y. Maitani. In vivo antitumor activity of camptothecin incorporated in liposomes formulated with an artificial lipid and human serum albumin. *Journal of Controlled Release* **127**: 231-238 (2008).
- 46 R. Barreiro-Iglesias, L. Bromberg, M. Temchenko, T. A. Hatton, A. Concheiro, and C. Alvarez-Lorenzo. Solubilization and stabilization of camptothecin in micellar solutions of pluronic-g-poly(acrylic acid) copolymers. *Journal of Controlled Release* **97**: 537-549 (2004).
- 47 L. Li and Y. B. Tan. Preparation and properties of mixed micelles made of Pluronic polymer and PEG-PE. *Journal of Colloid and Interface Science* **317**: 326-331 (2008).

- 48 P. Opanasopit, M. Yokoyama, M. Watanabe, K. Kawano, Y. Maitani, and T. Okano. Block Copolymer Design for Camptothecin Incorporation into Polymeric Micelles for Passive Tumor Targeting. *Pharmaceutical Research* **21**: 2001-2008 (2004).
- 49 K. Kawano, M. Watanabe, T. Yamamoto, M. Yokoyama, P. Opanasopit, T. Okano, and Y. Maitani. Enhanced antitumor effect of camptothecin loaded in long-circulating polymeric micelles. *Journal of Controlled Release* **112**: 329-332 (2006).
- 50 L. Zhang, Y. Hu, X. Jiang, C. Yang, W. Lu, and H. H. Yang. Camptothecin derivative-loaded poly(caprolactone-co-lactide)-b-PEG-b-poly(caprolactone-co-lactide) nanoparticles and their biodistribution in mice. *Journal of Controlled Release* **96**: 135-148 (2004).
- 51 K. H. Min, K. Park, Y.-S. Kim, S. M. Bae, S. Lee, H. G. Jo, R.-W. Park, I.-S. Kim, S. Y. Jeong, K. Kim, and I. C. Kwon. Hydrophobically modified glycol chitosan nanoparticles-encapsulated camptothecin enhance the drug stability and tumor targeting in cancer therapy. *Journal of Controlled Release* **127**: 208-218 (2008).
- 52 R. Kunii, H. Onishi, K.-i. Ueki, K.-i. Koyama, and Y. Machida. Particle characteristics and biodistribution of camptothecin-loaded PLA/(PEG-PPG-PEG) nanoparticles. *Drug Delivery* **15**: 3-10 (2008).
- 53 A. Shenderova, T. G. Burke, and S. P. Schwendeman. The Acidic Microclimate in Poly(lactide-co-glycolide) Microspheres Stabilizes Camptothecins. *Pharmaceutical Research* **16**: 241-248 (1999).
- 54 B. Ertl, P. Platzner, M. Wirth, and F. Gabor. Poly(D,L-lactic-co-glycolic acid) microspheres for sustained delivery and stabilization of camptothecin. *Journal of Controlled Release* **61**: 305-317 (1999).
- 55 J. Cheng, K. T. Khin, G. S. Jensen, A. Liu, and M. E. Davis. Synthesis of linear, β -cyclodextrin-based polymers and their camptothecin conjugates. *Bioconjugate Chemistry* **14**: 1007-1017 (2003).
- 56 N.-J. Lee and E. A. Theodorakis. Synthesis and Antitumor Activity of Phthalimide-Based Polymers Containing Camptothecin. *Macromolecular Research* **11**: 47-52 (2003).

- 57 N.-J. Lee, S.-J. Lee, S.-H. Kim, Y.-S. Kang, S.-B. Moon, H. Sohn, K.-T. Kang, and E. A. Theodorakis. Synthesis and in vitro antitumor activity of phthalimide-based polymers containing camptothecin. *European Polymer Journal* **40**: 1291-1296 (2004).
- 58 G. S. Kwon and T. Okano. Polymeric micelles as new drug carriers. *Advanced Drug Delivery Reviews* **21**: 107-116 (1996).
- 59 G. S. Kwon and K. Kataoka. Block copolymer micelles as long-circulating drug vehicles. *Advanced Drug Delivery Reviews* **16**: 295-309 (1995).
- 60 S. Cammas, K. Suzuki, C. Sone, Y. Sakurai, K. Kataoka, and T. Okano. Thermo-responsive polymer nanoparticles with a core-shell micelle structure as site-specific drug carriers. *Journal of Controlled Release* **48**: 157-164 (1997).
- 61 L. Tian, L. Yam, J. Wang, H. Tat, and K. E. Uhrich. Core crosslinkable polymeric micelles from PEG-lipid amphiphiles as drug carriers. *Journal of Materials Chemistry* **14**: 2317-2324 (2004).
- 62 M. F. Francis, M. Piredda, and F. M. Winnik. Solubilization of poorly water soluble drugs in micelles of hydrophobically modified hydroxypropylcellulose copolymers. *Journal of Controlled Release* **93**: 59-68 (2003).
- 63 A. Lavasanifar, J. Samuel, and G. S. Kwon. The effect of fatty acid substitution on the in vitro release of amphotericin B from micelles composed of poly(ethylene oxide)-*block*-poly(N-hexyl stearate-*L*-aspartamide). *Journal of Controlled Release* **79**: 165-172 (2002).
- 64 A. Lavasanifar, J. Samuel, and G. S. Kwon. Micelles self-assembled from poly(ethylene oxide)-*block*-poly(N-hexyl stearate *L*-aspartamide) by a solvent evaporation method: effect on the solubilization and haemolytic activity of amphotericin B. *Journal of Controlled Release* **77**: 155-160 (2001).
- 65 J. Djordjevic, M. Barch, and K. E. Uhrich. Polymeric micelles based on amphiphilic scorpion-like macromolecules: novel carriers for water insoluble drugs. *Pharmaceutical Research* **22**: 24-32 (2005).
- 66 L. Tian, L. Yam, N. Zhou, H. Tat, and K. E. Uhrich. Amphiphilic scorpion-like macromolecules: design, synthesis and characterization. *Macromolecules* **37**: 538-543 (2004).

- 67 L. Tao and K. E. Uhrich. Novel amphiphilic macromolecules and their in vitro characterization as stabilized micellar drug delivery systems. *Journal of Colloid and Interface Science* **298**: 102-110 (2006).
- 68 B. Demirdirek. MS Thesis, *Dept. of Chemistry and Chemical Biology*, Rutgers University, Piscataway, NJ, 2009.
- 69 A. M. Harmon and K. E. Uhrich. In vitro evaluation of amphiphilic macromolecular nanocarriers for systemic drug delivery. *Journal of Bioactive and Compatible Polymers* **24**: 185-197 (2009).
- 70 J. Wang, L. S. d. Rosario, B. Demirdirek, A. Bae, and K. E. Uhrich. Comparison of PEG chain length and density on amphiphilic macromolecular nanocarriers: self-assembled and unimolecular micelles. *Acta Biomaterialia* **5**: 883-892 (2009).
- 71 R. J. Christie and D. W. Grainger. Design strategies to improve soluble macromolecular delivery constructs. *Advanced Drug Delivery Reviews* **55**: 421-437 (2003).
- 72 J. Kopecek, P. Kopeckova, T. Minko, and Z.-R. Lu. HEMA copolymer-anticancer drug conjugates: design, activity, and mechanism of action. *European Journal of Pharmaceutics and Biopharmaceutics* **50**: 61-81 (2000).
- 73 K. D. Jensen, A. Nori, M. Tijerina, P. Kopeckova, and J. Kopecek. Cytoplasmic delivery and nuclear targeting of synthetic macromolecules. *Journal of Controlled Release* **87**: 89-105 (2003).
- 74 N. Rapoport, A. Marin, Y. Luo, G. D. Prestwich, and M. Muniruzzaman. Intracellular uptake and trafficking of pluronic micelles in drug-sensitive and MDR cells: effect on the intracellular drug localization. *Journal of Pharmaceutical Sciences* **91**: 157-170 (2002).
- 75 R. Savic, L. Luo, A. Eisenberg, and D. Maysinger. Micellar nanocontainers distribute to defined cytoplasmic organelles. *Science* **300**: 615-618 (2003).
- 76 M. Muniruzzaman, A. Marin, Y. Luo, G. D. Prestwich, W. G. Pitt, G. Husseini, and N. Y. Rapoport. Intracellular uptake of Pluronic copolymer: effects of the aggregation state. *Colloids and Surfaces B: Biointerfaces* **25**: 233-241 (2002).

- 77 K. Jensen, P. Kopeckova, J. Bridge, and J. Kopecek. The cytoplasmic escape and nuclear accumulation of endocytosed and microinjected HPMA copolymers and a basic kinetic study in Hep G2 cells. *AAPS Pharm. Sci.* **3**: 1-14 (2001).
- 78 V. Omelyanenko, C. Gentry, P. Kopeckova, and J. Kopecek. HPMA copolymer-anticancer drug-ov-t116 antibody conjugates. II processing in epithelial ovarian carcinoma cells in vitro. *Int. J. Cancer* **75**: 600-608 (1998).
- 79 E. V. Batrakova, H. Han, D. W. Miller, and A. Kabanov. Effects of Pluronic P85 unimers and micelles on drug permeability in polarized BBMEC and Caco-2 cells. *Pharm. Res.* **15**: 1525-1531 (1998).
- 80 A. V. Kabanov, E. V. Batrakova, and V. Y. Alakhov. Pluronic block copolymers as novel polymer therapeutics for drug and gene delivery. *Journal of Controlled Release* **82**: 189-212 (2002).
- 81 S. C. Lee, C. Kim, I. C. Kwon, H. Chung, and S. Y. Jeong. Polymeric micelles of poly(2-ethyl-2-oxazoline)-block-poly(ϵ -caprolactone) copolymer as a carrier for paclitaxel. *Journal of Controlled Release* **89**: 437-446 (2003).
- 82 J. Szebeni, F. M. Muggia, and C. R. Alving. Complement Activation by Cremophor EL as a Possible Contributor to Hypersensitivity to Paclitaxel: an In Vitro Study. *Journal of the National Cancer Institute* **90**: 300-306 (1998).

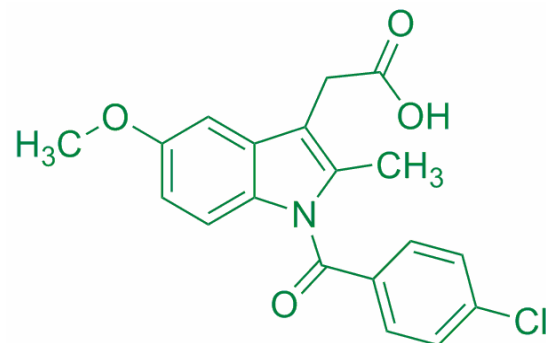


Figure 1-1. Chemical structure of indomethacin.

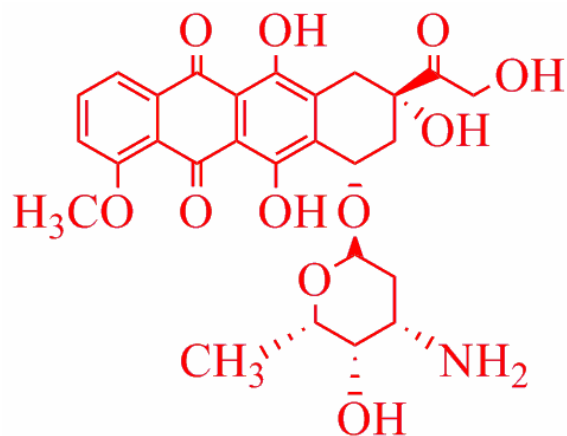


Figure 1-2. Chemical structure of doxorubicin.

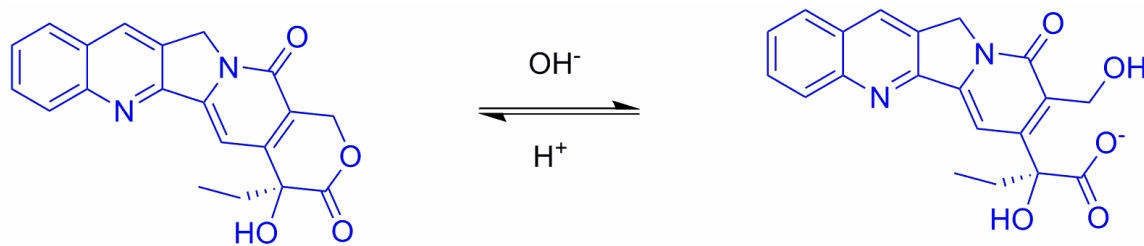


Figure 1-3. Chemical structures of CPT lactone (left) and CPT carboxylate (right) [43].

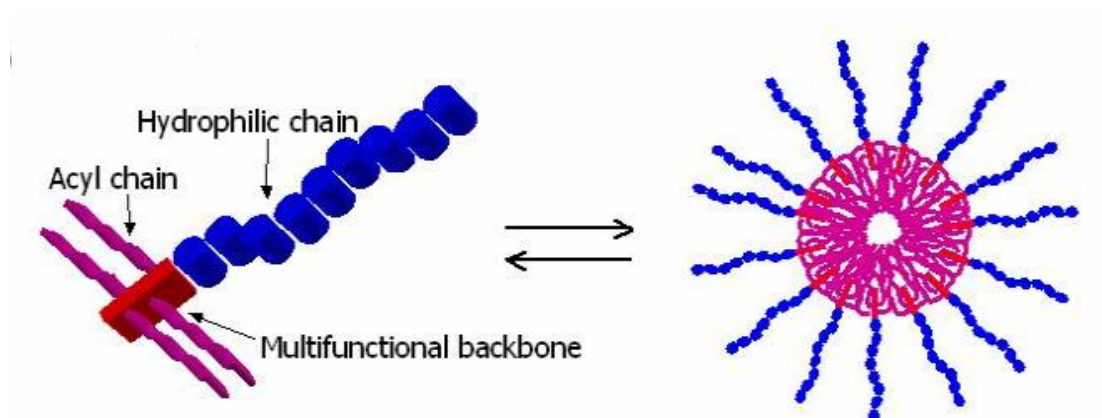
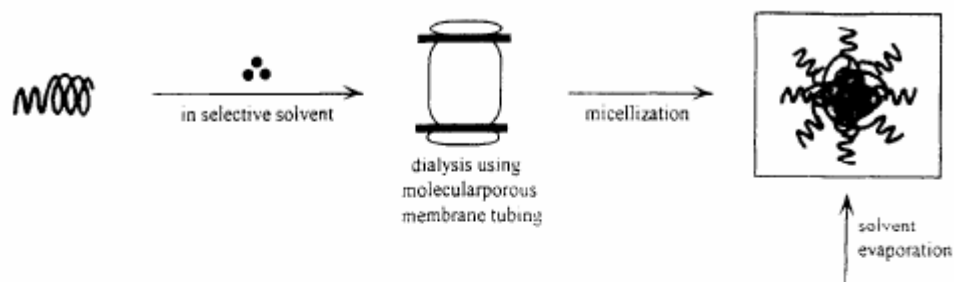


Figure 1-4. Cartoon of unimer-micelle equilibrium at critical micelle concentration [65].

I. Dialysis method



II. O/W emulsion method

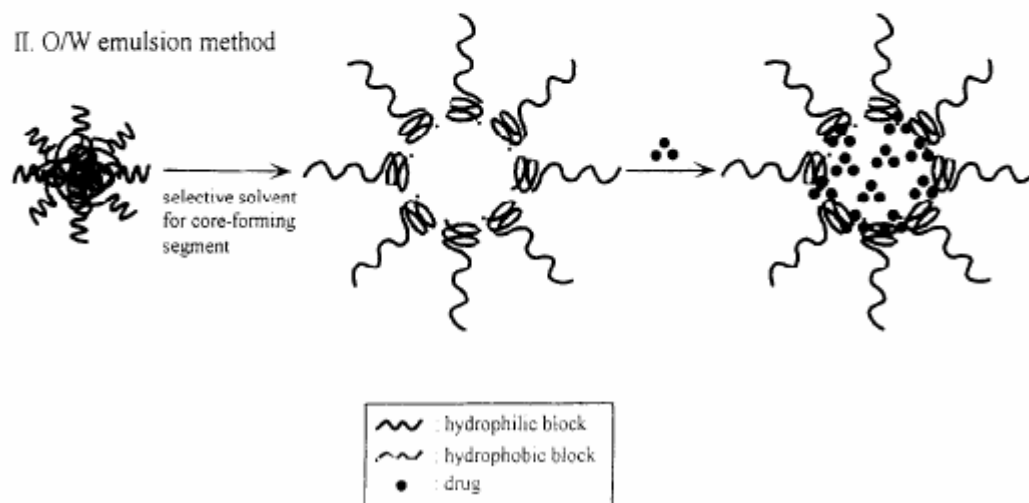


Figure 1-5. Physical encapsulation of hydrophobic drugs into polymeric micelles: I.

Dialysis method, II. Oil in water emulsion method [58].

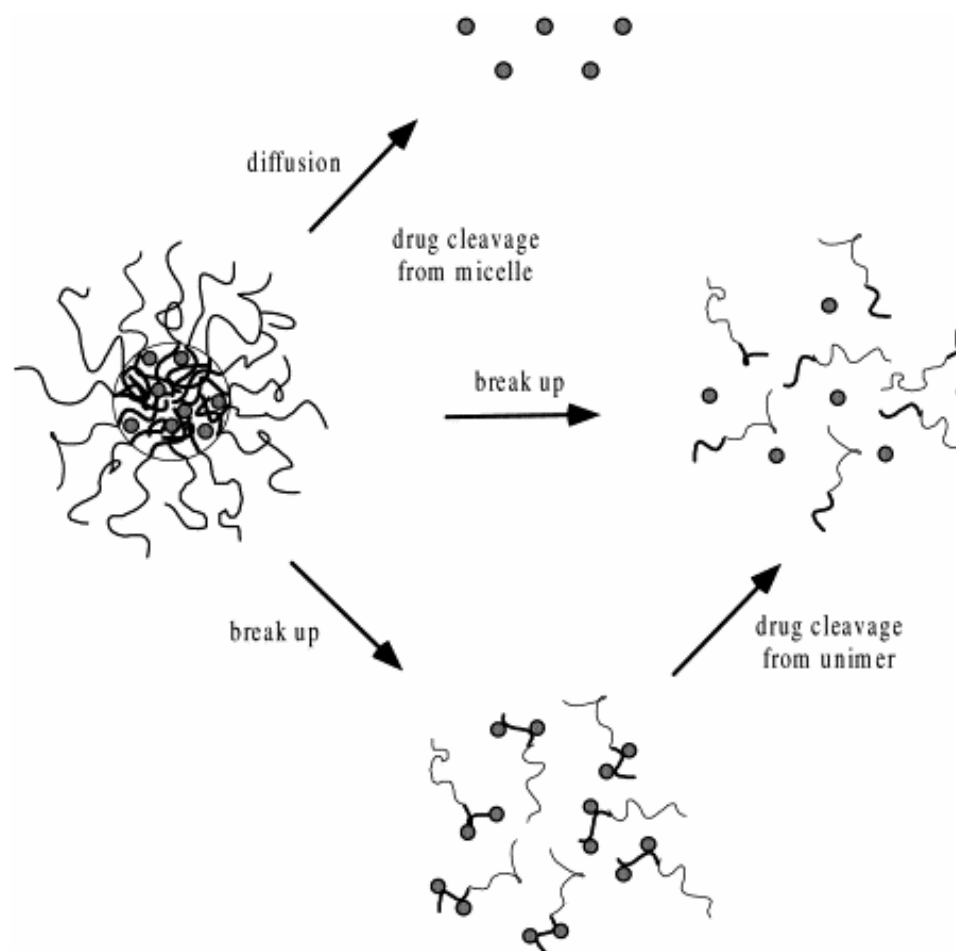


Figure 1-6. Drug release mechanisms from polymeric micelles [17].

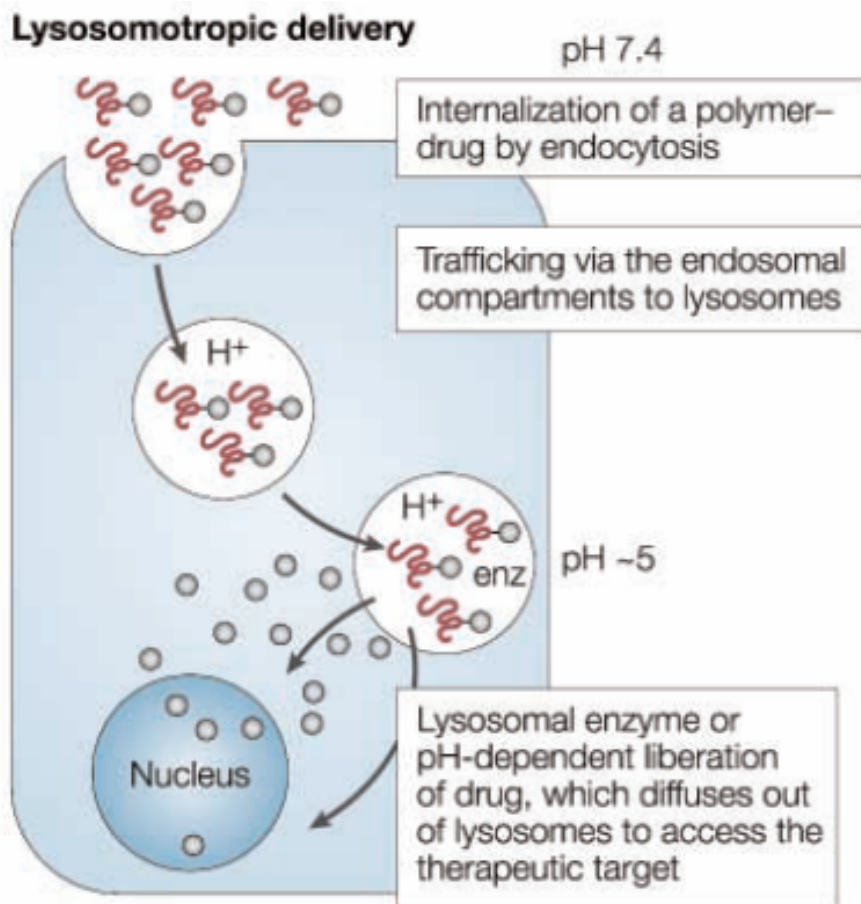


Figure 1-7. Lysosomotropic drug delivery of polymer-drug conjugates [18].

Chapter 2

STORAGE AND SOLUTION STABILITY OF DRUG-LOADED AMPHIPHILIC MACROMOLECULES-BASED MICELLES

2.1. Introduction

Freeze-drying (also known as lyophilization) is a commonly used process of converting pharmaceutical solutions or suspensions into solids for easy handling, distribution and storage [1, 2]. It is used to improve the stability and long-term storage of labile drugs, viruses, vaccines, proteins, peptides, liposomes, nanoparticles, and nanoemulsions [1-3]. However, the lyophilized solids should have rapid reconstitution time and conserved physico-chemical characteristics (e.g. drug entrapment for a carrier; as drug leaking can occur during the lyophilization process) [2].

A limiting factor for intravenous (injection) administration of pharmaceuticals (such as drug delivery systems) is the particle size $< 5 \mu\text{m}$, as larger particles can potentially block capillaries [3]. Drugs with limited solubility pose a formulation challenge, particularly in controlling drug aggregation behavior [4]. For example, loading tetracaine and etomidate in solid lipid nanoparticles led to increased number and sizes of aggregates after lyophilization and reconstitution [3]. However, encapsulation in polymeric micelles allows non-aggregation and sustained release of drug [2, 4]. For example, the aggregation state of amphotericin B was preserved in PEO-*b*-p(L-Asp) micelles during lyophilization and reconstitution [4].

Indomethacin (IMC) is a non-steroidal anti-inflammatory drug [5] that induces antitumor immunity in certain carcinoma cells [6]. However, its hydrophobicity and side effects of gastrointestinal mucosa irritation and central nervous system toxicity have led to studies of IMC encapsulation in polymeric micelles [5]. IMC is frequently used in the polymeric micelle field as the model hydrophobic drug [5, 7-10]. Similarly, camptothecin (CPT) is an anticancer drug with potent antitumor activity but with extreme hydrophobicity; consequently polymeric micelles are studied as carriers of CPT [11-16].

In this chapter, IMC and CPT were used as model drugs in the evaluation of storage and solution stability of micelles assembled from amphiphilic macromolecules (AM). The AM micelles were loaded with drug and lyophilized to form a powder. The resolubilized drug-loaded micelles were then evaluated for ease of resolubilization, pH and temperature solution stability, and sustained drug release upon rehydration. Four amphiphilic macromolecules (**AM 1-4**) were evaluated in this study (**Figure 2-1**); **AM 1** and **AM 2** self-assemble to micelles while **AM 3** and **AM 4** are unimolecular micelles.

The aim of this study was to evaluate the storage and solution stability of the **AM 1-4** micelles in comparison to polymeric carriers Pluronic P85, a gene and drug carrier, [17] and Cremophor EL, an emulsifier for hydrophobic molecules [18].

2.2. Materials

Regenerated cellulose membranes (Spectra/Por MWCO 3,500 Da, flat sheets) and acrylic dialysis cells were purchased from Fisher Scientific (Atlanta, GA). Indomethacin

(IMC), camptothecin (CPT), phosphate buffered saline (PBS) tablets, phosphate citrate tablets and all other reagents and solvents were purchased from Sigma-Aldrich (St. Louis, MO) and used as received. Pluronic P85 and Cremophor EL were kindly given by BASF Corporation (Mount Olive, NJ). All amphiphilic macromolecules (**AM 1-4**) were prepared by Jinzhong Wang [19] and Bahar Demirdirek [20].

2.3. Methods

2.3.1. Drug Loading

IMC was loaded by the oil-in-water water emulsion method and CPT by the solvent evaporation method.

IMC Loading: IMC (10 mg) was dissolved in dichloromethane (4.0 mL) to make a 2.5 mg/mL solution. IMC aliquots (1.0 mL) were added dropwise into 50.0 mL polymer solutions (0.50 mg/mL) in HPLC-grade water (wt/wt drug:polymer 1:10) with continuous stirring at room temperature. The mixtures were capped and stirred in the dark at room temperature for 24 h to equilibrate. The solutions were uncapped and stirred for another 24 h to allow evaporation of CH₂Cl₂. The resulting aqueous mixture was suction filtered to remove precipitated drug. All measurements were performed in triplicate. IMC was detected by UV-Vis spectrophotometry ($\lambda = 318$ nm) as used elsewhere [10] after complete disruption of the drug-loaded micelles with N,N-dimethylacetamide (DMA) (1:1 dilution). Indomethacin standard solutions were prepared in 1:1 DMA: H₂O.

CPT Loading: CPT and polymer were dissolved (1:1 or 0.1:1 w/w drug:polymer ratio) in a solution of methanol:chloroform (4:1 v/v), and after complete dissolution, the solvents were removed by rotary evaporation at room temperature. PBS (pH 7.4) was added to obtain a 1.5 mg/mL final polymer concentration. The solution was sonicated at room temperature for 5 min, stirred for 4 h at 37 °C, and the resulting mixtures filtered through 0.45 µm PVDF syringe filters. CPT was detected by UV vis spectrophotometry ($\lambda = 365$ nm) as used elsewhere [16], after dilution with dimethylsulfoxide (DMSO) (9:1) and using CPT calibration standards in DMSO.

Drug loading capability of micellar carriers was calculated as follows:

$$\text{Weight \% Loading} = \frac{\text{Concentration of free drug detected}}{\text{Concentration of polymer}} \times 100\%$$

2.3.2. Resolubilization of Lyophilized IMC-Loaded Polymeric Micelles

Freshly prepared IMC-loaded polymeric micelles were frozen at -20°C and lyophilized at $< 133 \times 10^{-3}$ mBar (condenser T = -50°C) for 48-72 h using the Labconco Freeze Dry System (Freezone 4.5). HPLC water was then added to the lyophilized solids to obtain a final indomethacin concentration of 1 mg/mL. The rate of resolubilization was determined using a timer (from time of water addition to complete particle dissolution) and visually assessed with the solutions shaken by hand.

2.3.3. pH and Temperature Solution Stability

The pH and temperature solution stability of resolubilized lyophilized CPT-loaded polymeric micelles was analyzed by *i*) UV vis spectrophotometry and *ii*) dynamic light scattering (DLS) measurements.

UV analysis: Lyophilized CPT-loaded micelles were redissolved in PBS (pH 7.4) or phosphate citrate buffer (pH 5.0) to obtain a final polymer concentration of 1 mg/mL. Samples were placed in quartz cuvettes equipped with outer water reservoirs connected to a chemical transfer pump to allow circulation of heated water through the cuvette outer reservoirs. At specific temperatures within the 25°C - 50°C range, samples were analyzed at 365 nm for drug detection and 285 nm for polymer detection using a Beckman DU 520 UV vis spectrophotometer. Samples were equilibrated for 5 min at each temperature before UV analysis.

DLS analysis: Lyophilized CPT-loaded micelles were redissolved in PBS (pH 7.4) or phosphate citrate buffer (pH 5.0) and briefly equilibrated at 37 °C, then analyzed (unfiltered) for particle size distribution using a Malvern Instruments Zetasizer Nano ZS-90 instrument (Southboro, MA). The temperature trend (size vs temperature) method was used with 10 runs for each measurement (total of ~20 measurements) set at a 90° scattering angle and 37 °C reading temperature.

2.3.4. IMC *In Vitro* Release from Resolubilized Polymeric Micelles

Lyophilized IMC-loaded micelles were resolubilized in PBS (pH 7.4) to obtain a final polymer concentration of $\sim 1 \times 10^{-4}$ M. The release protocol consisted of pre-soaked (PBS pH 7.4, ~ 18 h) regenerated cellulose flat sheets (MWCO 3.5 kDa) placed between the donor cell and receptor cell of equilibrium dialysis cells (Bel-Art Products, Pequannock, NJ) incubated in a 37 °C water bath. Samples were added into 5-mL donor cells and fresh PBS solutions into the 5-mL receptor cells. Receptor solutions were retrieved (5 mL) at specific time intervals and replaced with the same amount of fresh PBS. IMC concentration was determined by UV-vis spectrophotometry ($\lambda = 318$ nm) using PBS solution (pH 7.4) as blank.

2.4. Results and Discussion

2.4.1. Drug Loading

IMC was loaded into polymeric micelles using the oil-in-water emulsion method. The AM micelles (**AM 1-4**) showed comparable wt % loading (~ 6 wt %) comparable to Cremophor EL but 6x higher than the Pluronic P85 control (**Table 2-1**).

CPT was encapsulated in representative micelles **AM 1** (as representative self-assembled micelle) and **AM 4** (as representative unimolecular micelle) and control polymeric carriers using the solvent evaporation method. Results showed comparable wt % loading for all micellar carriers (**Table 2-1**).

2.4.2. Resolubilization

As injectibles, a possible drug formulation involves the drug and polymer as solids or powders that are resolubilized prior to use. Thus the capability of a drug carrier to be easily resolubilized to clear solutions, with no drug aggregation, is important in its practical applications. Results (**Table 2-2**) showed faster resolubilization times for the amphiphilic macromolecules **AM 1-4** compared to Pluronic P85 and Cremophor EL. Notably, the unimolecular AMs (**3** and **4**) were approximately 3x faster for resolubilization than the micellar AMs (**1** and **2**).

2.4.3. pH and Temperature Solution Stability

Resolubilized CPT-loaded **AM 4** micelles (as representative AM) were analyzed for pH and temperature stability. As injectibles, the drug-AM solutions would be resolubilized from powder form and upon injection into the body, a sudden temperature change from room temperature 25°C to body temperature 37°C will occur; thus any detected phase transition or aggregation at this temperature change will show micellar instability as well as drug aggregation. The wavelengths used were those relevant for drug detection 365 nm, and AM detection 285 nm. Results (**Figure 2-2**) showed good thermal stability for CPT-loaded **AM 4** micelles within the temperature range (25°C - 50°C), with no drug nor macromolecule aggregations. As drug carriers, the CPT-loaded **AM 4** micelles were also evaluated for micellar stability at relevant pH: physiological pH 7.4 and lysosomal pH 5.0. Results (**Figure 2-2**) showed good pH stability for CPT-loaded **AM 4** micelles; no phase transition nor drug or AM aggregations were seen from UV analysis.

The pH solution stability of resolubilized CPT-loaded polymeric micelles was also analyzed by dynamic light scattering. Small sizes (10 – 100 nm) of polymeric micelles are reportedly advantageous compared to other larger drug delivery systems due to simple sterilization by filtration, no concern for capillary embolism and extravasation of the carriers [21]. Results of DLS analysis (**Figure 2-3**) showed micellar sizes of **AM 1-4** micelles within the 10-100 nm ideal micellar size at both pH conditions (**Figure 2-3 a-d**), although a few aggregations were detected. In contrast, Pluronic P85 (**Figure 2-3 e-f**) displayed aggregations (100-1000 nm) at pH 5.0 and had lower micellar stability at pH 7.4 (1-500 nm sizes). Likewise, Cremophor EL (**Figure 2-3 g-h**) also had large aggregations at both pH conditions, with particle sizes > 100 nm.

2.4.4. IMC *In Vitro* Release

IMC release from resolubilized IMC-loaded **AM 1-4** micelles showed sustained release behavior over 48 hours (**Figure 2-4**) relative to free IMC, and slower IMC release compared to Pluronic P85 and Cremophor EL. This effect is likely due to higher IMC interactions with the hydrophobic AM micelle cores compared to the control polymeric carriers. Even though IMC-loaded AM micelles were lyophilized and resolubilized, sustained IMC release was still observed. This data suggests that the drug remained intact within the AM micelles while in solid, lyophilized form which is a good indication of the storage stability of the drug-loaded AM micelles.

2.5. Conclusions

Drug-loaded AM micelles showed good storage and solution stability: non-aggregation of drug and sustained drug release. Faster resolubilization time was observed for drug-loaded AM micelles compared to drug-loaded polymeric carriers Pluronic P85 and Cremophor EL. Furthermore, after lyophilization and resolubilization, drug-loaded AM-based micelles showed better pH and temperature stability, micellar sizes within 10-100 nm, and slightly slower IMC release compared to the model polymeric carriers.

2.6. References

- 1 X. C. Tang and M. J. Pikal. Design of Freeze-Drying Processes for Pharmaceuticals: Practical Advice. *Pharm Res* **21**: 191-200 (2004).
- 2 W. Abdelwahed, G. Degobert, S. Stainmesse, and H. Fessi. Freeze-drying of nanoparticles: Formulation, process and storage considerations. *Adv. Drug Del. Rev.* **58**: 1688-1713 (2006).
- 3 C. Schwarz and W. Mehnert. Freeze-drying of drug-free and drug-loaded solid lipid nanoparticles (SLN). *Int. J. Pharm.* **157**: 171-179 (1997).
- 4 M. Adams and G. S. Kwon. Spectroscopic investigation of the aggregation state of amphotericin B during loading, freeze-drying, and reconstitution of polymeric micelles. *Journal of Pharm Pharmaceutical Sciences* **7**: 1-6 (2004).
- 5 S. B. La, T. Okano, and K. Kataoka. Preparation and characterization of the micelle-forming polymeric drug indomethacin-incorporated poly(ethylene oxide)-poly(β -benzyl-L-aspartate) block copolymer micelles. *Journal of Pharmaceutical Sciences* **85**: 85-90 (1996).
- 6 S. Morecki, E. Yacovlev, Y. Gelfand, V. Trembovler, E. Shohami, and S. Slavin. Induction of antitumor immunity by indomethacin. *Cancer Immunology and Immunotherapy* **48**: 613-620 (2000).
- 7 S. Y. Kim, Y. M. Lee, and J. S. Kang. Indomethacin-loaded methoxy poly(ethylene glycol)/ poly(D,L-lactide) amphiphilic diblock copolymeric nanospheres: Pharmacokinetic and toxicity studies in rodents. *Journal of Biomedical Materials Research* **74A**: 581-590 (2005).
- 8 S. Y. Kim, I. G. Shin, Y. M. Lee, C. S. Cho, and Y. K. Sung. Methoxy poly(ethylene glycol) and caprolactone amphiphilic block copolymeric micelle containing indomethacin. II. Micelle formation and drug release behaviors. *J. Control. Release* **51**: 13-22 (1998).
- 9 J. X. Zhang, X. J. Li, L. Y. Qiu, X. H. Li, M. Q. Yan, Y. Jin, and K. J. Zhu. Indomethacin-loaded polymeric nanocarriers based on amphiphilic polyphosphazenes with poly(N-isopropylacrylamide) and ethyl tryptophan as side

- groups: preparation, in vitro and in vivo evaluation. *Journal of Controlled Release* **116**: 322-329 (2006).
- 10 W.-J. Lin, Y.-C. Chen, C.-C. Lin, C.-F. Chen, and J.-W. Chen. Characterization of pegylated copolymeric micelles and *in vivo* pharmacokinetics and biodistribution studies. *Journal of Biomedical Materials Research Part B: Applied Biomaterials* **77B**: 188-194 (2006).
 - 11 R. Barreiro-Iglesias, L. Bromberg, M. Temchenko, T. A. Hatton, A. Concheiro, and C. Alvarez-Lorenzo. Solubilization and stabilization of camptothecin in micellar solutions of pluronic-g-poly(acrylic acid) copolymers. *Journal of Controlled Release* **97**: 537-549 (2004).
 - 12 A. Hatefi and B. Amsden. Camptothecin delivery methods. *Pharmaceutical Research* **19**: 1389-1399 (2002).
 - 13 K. Kawano, M. Watanabe, T. Yamamoto, M. Yokoyama, P. Opanasopit, T. Okano, and Y. Maitani. Enhanced antitumor effect of camptothecin loaded in long-circulating polymeric micelles. *Journal of Controlled Release* **112**: 329-332 (2006).
 - 14 P. Opanasopit, M. Yokoyama, M. Watanabe, K. Kawano, Y. Maitani, and T. Okano. Block Copolymer Design for Camptothecin Incorporation into Polymeric Micelles for Passive Tumor Targeting. *Pharmaceutical Research* **21**: 2001-2008 (2004).
 - 15 P. Opanasopit, M. Yokoyama, M. Watanabe, K. Kawano, Y. Maitani, and T. Okano. Influence of serum and albumins from different species on stability of camptothecin-loaded micelles. *Journal of Controlled Release* **104**: 313-321 (2005).
 - 16 M. Watanabe, K. Kawano, M. Yokoyama, P. Opanasopit, T. Okano, and Y. Maitani. Preparation of camptothecin-loaded polymeric micelles and evaluation of their incorporation and circulation stability. *International Journal of Pharmaceutics* **308**: 183-189 (2006).
 - 17 A. V. Kabanov, E. V. Batrakova, and V. Y. Alakhov. Pluronic block copolymers as novel polymer therapeutics for drug and gene delivery. *Journal of Controlled Release* **82**: 189-212 (2002).

- 18 J. Szebeni, F. M. Muggia, and C. R. Alving. Complement Activation by Cremophor EL as a Possible Contributor to Hypersensitivity to Paclitaxel: an In Vitro Study. *Journal of the National Cancer Institute* **90**: 300-306 (1998).
- 19 J. Wang. Synthesis and Evaluation of Novel Amphiphilic Macromolecules as Drug Carriers and Therapeutics (Ph.D. Thesis), *Dept. of Chemistry and Chemical Biology*, Rutgers University, Piscataway, NJ, 2007.
- 20 B. Demirdirek. MS Thesis, *Dept. of Chemistry and Chemical Biology*, Rutgers University, Piscataway, NJ, 2009.
- 21 M. C. Jones and J. C. Leroux. Polymeric micelles- a new generation of colloidal drug carriers. *European Journal of Pharmaceutics and Biopharmaceutics* **48**: 101-111 (1999).

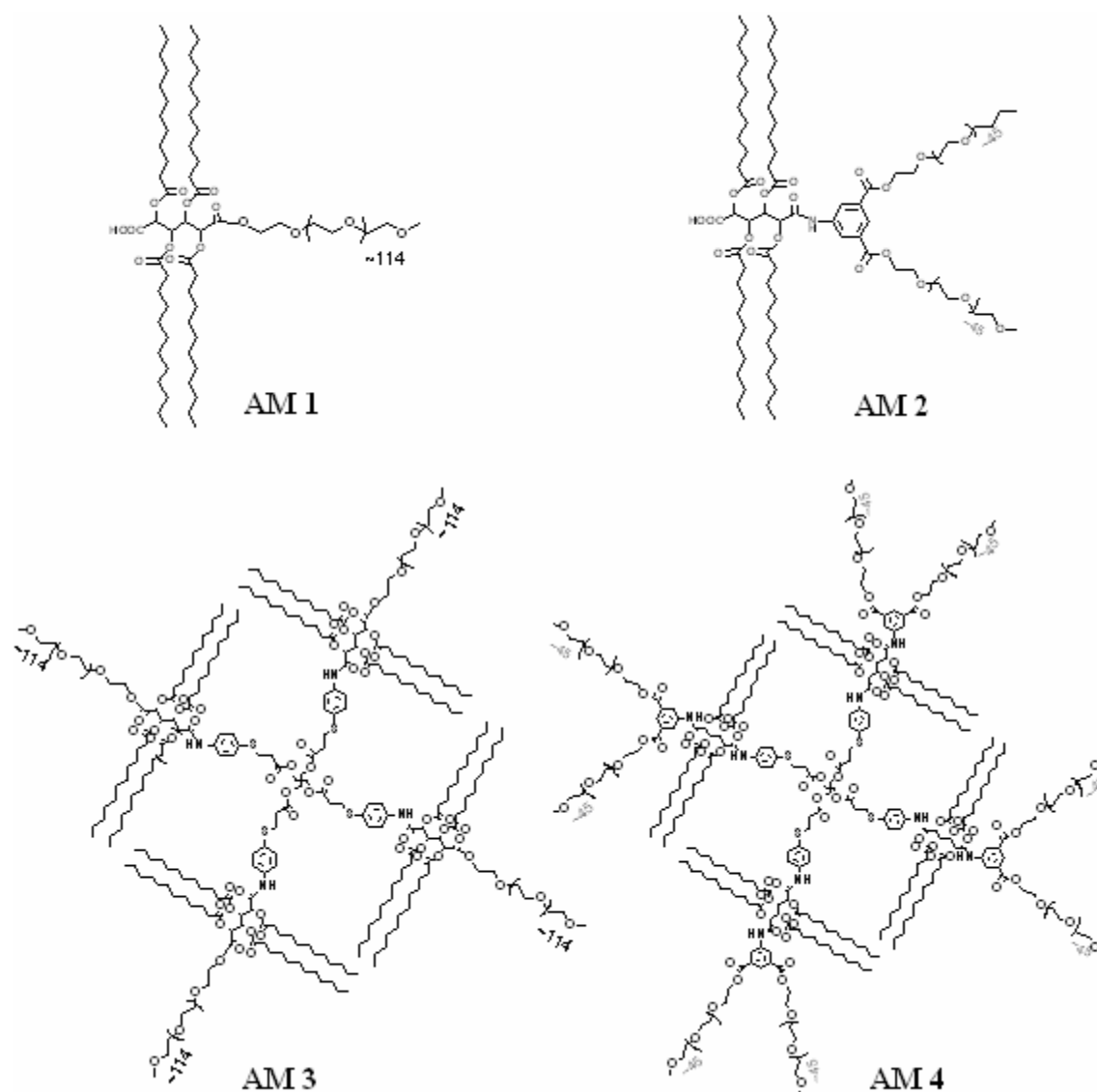


Figure 2-1. Chemical structures of amphiphilic macromolecules: self-assembled micelles AM 1 and AM 2, unimolecular micelles AM 3 and AM 4 [19].

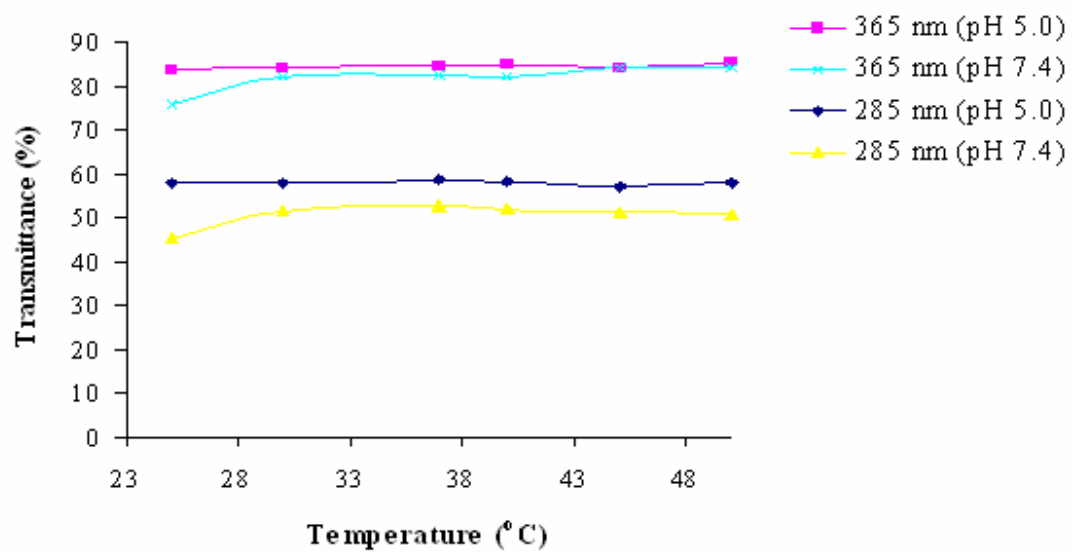


Figure 2-2. UV analysis of pH and temperature stability of representative CPT-loaded **AM 4** micelles. CPT was monitored at 365 nm and AM at 285 nm.

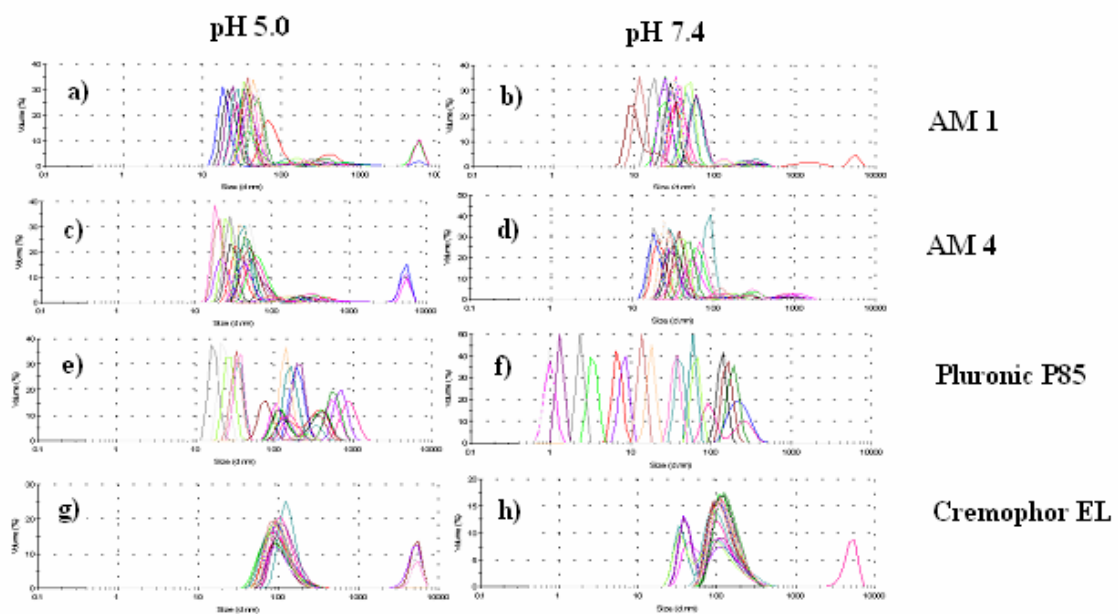


Figure 2-3. DLS analysis of CPT-loaded polymeric micelle stability with pH: *a-b)* AM 1, *c-d)* AM 4, *e-f)* Pluronic P85, *g-h)* Cremophor EL. Each line represents a DLS measurement of the CPT-loaded micelle.

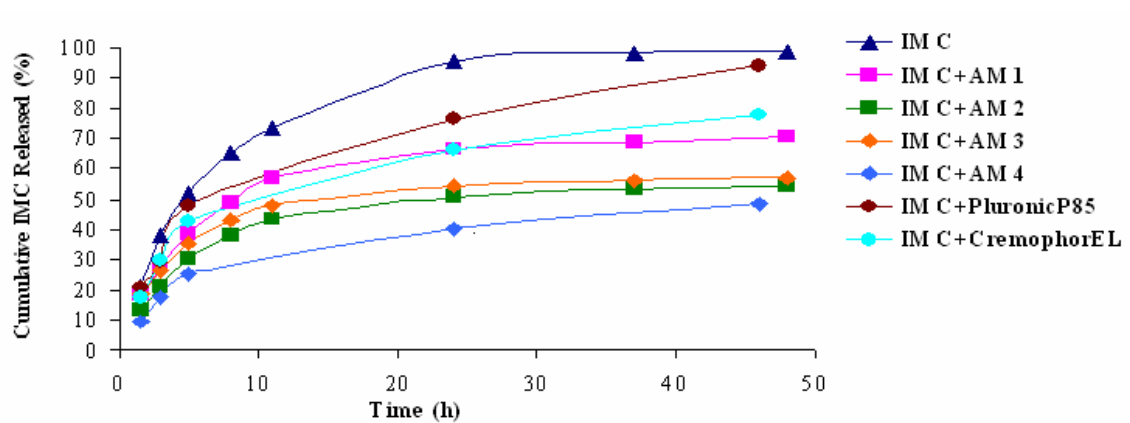


Figure 2-4. *In vitro* IMC cumulative release profile from polymeric micelles within 48

h.

Table 2-1. Drug (CPT, IMC) loading capability of polymeric micelles.

Sample	IMC Wt % Loading	CPT Wt % Loading
drug-loaded AM 1	5 ± 1	1 ± 0.3
drug-loaded AM 2	3 ± 1	-
drug-loaded AM 3	4 ± 1	-
drug-loaded AM 4	4 ± 1	0.5 ± 0.1
drug-loaded Pluronic P85	0.6 ± 0.1	0.3 ± 0.1
drug-loaded Cremophor EL	3 ± 1	0.5 ± 0.1

Table 2-2. Resolubilization time of lyophilized IMC-loaded polymeric micelles.

Lyophilized sample	Time (sec)
IMC + AM 1	50
IMC + AM 2	40
IMC + AM 3	12
IMC + AM 4	15
IMC + Pluronic P85	56
IMC + Cremophor EL	73

Chapter 3

SUBCELLULAR LOCALIZATION OF FITC-LABELED AMPHIPHILIC MACROMOLECULES (FITC-AM) IN HUVECS

3.1. Introduction

In the evaluation of AM-based micelles as drug carriers, this study focuses on their capability for intracellular drug delivery. As the target sites of several therapeutic compounds occur at the subcellular level [1, 2], the mode of cellular entry of the AM must be determined.

Several methods are used to study cellular internalization of polymers or nanoparticles including fluorescence microscopy [3, 4] and transmission electron microscopy [5, 6]. Confocal scanning microscopy allows the use of multiple fluorescent dyes at a time and is commonly used in cellular internalization studies [6-12]. The fluorescent dyes are either physically encapsulated in nanoparticles [6, 10, 12] or chemically conjugated to the macromolecules [8, 11]. However, chemical conjugation of fluorescent dyes should not drastically change the physico-chemical properties of the drug carriers, such as particle size. Furthermore, the dye-macromolecule conjugation should be stable in physiological (pH 7.4) and lysosomal (pH 5.0) conditions.

Human umbilical vein endothelial cells (HUVECs) were used as the cell line in this study as endothelium is an important target for drug and gene therapy [12]. HUVECS are

involved in angiogenesis and tumor growth [12] and thus relevant in the evaluation of the AM micelles for anticancer drug delivery.

Macromolecules assembling into polymer micelles typically enter the cells by endocytosis [4, 10, 11, 13, 14]. The aim of this study was to confirm endocytotic entry of amphiphilic macromolecules (AMs) in human umbilical vein endothelial cells. The AMs were conjugated with fluorescein isothiocyanate (FITC), while the endosomes and lysosomes of HUVECs were stained with fluorescent dyes specific for those organelles. Confocal scanning microscopy was used to confirm endocytotic uptake of AMs in HUVECs from co-localization evidences of FITC-AMs and fluorescent dye-stained organelles.

3.2. Materials

Phosphate buffer tablets, heparin sodium salt (Grade I-A from porcine intestinal mucosa), endothelial cell growth factor (ECGF), and endothelial cell attachment factor (ECAAF) were purchased from Sigma-Aldrich (St. Louis, MO). Fetal bovine serum (FBS, non heat-inactivated), Ham's F-12K media, penicillin-streptomycin 100x solution and human umbilical vein endothelial cells (HUVECs) were obtained from American Tissue Culture Collection (ATCC, Manassas, VA). Fluorescein isothiocyanate (FITC), LysoTracker Red, Texas Red-conjugated transferrin from human serum were purchased from Invitrogen (Carlsbad, CA). Tissue culture plates, flasks, Spectra/Por dialysis tubings and DispoDialyzer bags {molecular weight cut-off (MWCO) 3500 Da} and all

solvents (HPLC grade) were purchased from Fisher Scientific (Atlanta, GA). The amine-terminated AM and FITC-AM **5** were synthesized by Jinzhong Wang [15].

3.3. Methods

3.3.1. Cell Culture: Human Umbilical Vein Endothelial Cells

HUVECs were grown in Ham's F-12K media supplemented with 1 % ECGF, 1 % heparin, 10 % FBS and 1 % penicillin-streptomycin solution. The cells were plated in tissue culture flasks or plates initially added with 300 μ L ECAF. The cells were grown at 37 $^{\circ}$ C, 5% CO₂ for several passages prior to seeding in petri dishes for the confocal scanning microscopy experiments.

3.3.2. *In vitro* pH Stability of FITC-AM

The pH stability of the FITC-AM linkage was analyzed using dialysis methods and UV-vis spectrophotometry. Solutions of FITC control and FITC-labeled micelles containing equivalent FITC concentrations were separately placed in DispoDialyzer bags and dialyzed against phosphate buffer solutions (pH 7.4 or pH 4.0) for 27 h at room temperature. The resulting solutions inside the DispoDialyzers were analyzed with UV vis spectrophotometer (FITC $\lambda_{\text{max}} = 492$ nm) to calculate % FITC released at each pH buffer system.

3.3.3. Dynamic Light Scattering Measurements

FITC-labeled micelles were prepared by mixing 10 mol % FITC-AM (**5**) and 90 mol % AM (**1**). The number-weighted Nicomp distribution of FITC-labeled mixed micelles

was determined by dynamic light scattering (DLS) using Particle Size Systems Nicomp 380 Submicron Particle Sizer (Santa Barbara, CA) equipped with helium-neon laser, with measurements obtained at a 90° detector angle to incident beam. The solutions were filtered using 0.45 µm PTFE syringe filters (Whatman, USA) prior to DLS analysis.

3.3.4. Confocal Laser Scanning Microscopy (CLSM)

For cell studies, FITC-labeled mixed micelles were prepared by mixing 10 mol % FITC-AM (**5**) and 90 mol % AM (**1**). HUVECs maintained in complete growth media were harvested and seeded into glass-bottomed petri dishes (35 mm dish, 14 mm microwell; MatTek Corporation, Ashlan, MA) in 1 mL of complete growth media at a density of 90,000 cells/well and incubated for 48 hours to allow cell attachment.

CLSM studies were performed using a Zeiss confocal laser-scanning microscopy workstation (LSM410) fitted with 40x objective. Different mol % ratios (5:95, 10:90, 15:85) of FITC-AM (**5**) to AM (**1**) were analyzed to determine the minimum amount of FITC-AM in the mixed micelles that gave detectable fluorescence under the microscope. An average of 100 cells per image (40x magnification) were counted.

3.3.4.1. Localization in Early and Recycling Endosomes

Texas Red (**Figure 3-1**)-conjugated transferrin from human serum was used because of the characteristic binding of transferrin (a monomeric serum glycoprotein) to iron cations for receptor-mediated endocytotic delivery [16]. Thus, labeled transferrin is used in investigating endocytosis or endocytotic recycling pathways [16]. HUVECs were

seeded in glass-bottomed petri dishes (35 mm dish, 14 mm microwell: MatTek Corporation, Ashlan, MA) in 1 mL of complete growth media at a density of 90,000 cells/well and incubated with complete growth media for 60 h (37°C) followed by treatment for 12 h with FITC-labeled micelles or FITC (as control) prepared in complete growth media. The cells were then stained with Texas red-conjugated transferrin (50 µg/mL; excitation λ 595 nm) for 45 min. The cells were washed with Dulbecco's PBS (3x) and fixed using 0.5 mL 4% paraformaldehyde in methanol for 20 minutes. After washing again, cells were visualized in Dulbecco's PBS by CLSM using Texas Red filter (568 nm) and FITC filter (488 nm). The fluorescent images were overlaid with the differential interference contrast images to determine localization of the amphiphilic macromolecules in early and recycling endosomes. Semi-quantitative analysis was performed on the fluorescent images using Image-Pro Plus 5.1 software (Media Cybernetics, San Diego, CA) to quantify the co-localization of fluorescence intensities. An average of 100 cells per image (40x magnification) were counted.

3.3.4.2. Localization in Endo-lysosomal Compartments

LysoTracker Red dye (**Figure 3-1**) emits red fluorescence in the acidic vesicles of the cells but not at physiological pH; it is used as a marker for late-stage endosomes and lysosomes [16, 17]. HUVECs were seeded in glass-bottomed petri dishes (35 mm dish, 14 mm microwell: MatTek Corporation, Ashlan, MA) in 1 mL of complete growth media at a density of 90,000 cells/well and incubated with complete media for 60 h (37 °C), followed by treatment for 12 h with FITC-labeled micelles or FITC (as control) prepared in complete growth media. The cells were then stained with LysoTracker Red (50 nM;

excitation λ 577 nm) for 45 min, washed with 1 mL sterile Dulbecco's PBS (3x) and fixed using 0.5 mL 4 % paraformaldehyde in methanol for 20 min. After washing again, cells were visualized in Dulbecco's PBS by CLSM using LysoTracker Red filter (568 nm) and FITC filter (488 nm). The fluorescent images were overlaid with the differential interference contrast images to determine localization of the amphiphilic macromolecules in endolysosomal compartments. Semi-quantitative analysis was performed on the fluorescent images using Image-Pro Plus 5.1 software (Media Cybernetics, San Diego, CA) to quantify the co-localization of fluorescence intensities. An average of 100 cells per image (40 x magnification) were counted.

3.4. Results and Discussion

3.4.1. Preparation of FITC-AM

As nanocarriers for hydrophobic anticancer drugs, the amphiphilic macromolecular micelles were further evaluated for intracellular drug delivery. As these polymers do not have fluorescence detectable under the confocal laser scanning microscope, the AMs were conjugated with fluorescein isothiocyanate (FITC) (**Figure 3-2**) to allow observation of their cellular uptake and subcellular localization in HUVECs. FITC-AM (**5**) was purified by gel permeation chromatography (Sephadex G-75) that showed two distinct bands indicating separation of FITC-AM (**5**) and free FITC. Successful FITC conjugation was also confirmed by the *i*) shift in the UV absorption peak of the FITC-AM (**5**) at 498 nm relative to free FITC at 492 nm, and *ii*) appearance of FITC-associated proton peaks in the nuclear magnetic resonance spectra (*NMR performed by Jinzhong Wang* [15]). FITC-labeled micelles consisting of 90 mol % AM (**1**) and 10 mol % FITC-

AM (5) showed detectable fluorescence under the confocal scanning microscope but without any difference in micellar property observed. In particular, the micellar size distribution of FITC-labeled micelles detected from dynamic light scattering analysis, was similar to that of AM micelles (**Figure 3-3**).

The stability of FITC-AM linkage for 27 h was analyzed by dialysis and UV-vis spectrophotometry methods which showed only 7 % FITC was released at pH 4.0 and only 30 % FITC was released at pH 7.4. This data supports our expectation that FITC fluorescence pertains to the amphiphilic macromolecules and not free/released FITC.

3.4.2. Subcellular Localization observed via CLSM

Endocytosis is reportedly the mechanism of macromolecular cellular entry, as interaction with the plasma membrane leads to endosomal vesicle formation, and then lysosomal fusion or recycled in endosomes back to cell surface [18]. Confocal scanning microscopy was used to confirm the endocytotic entry of amphiphilic macromolecules in HUVECs. Confocal images showed co-localization of the FITC-labeled micelles with Texas Red-stained organelles, indicating their subcellular location in early and recycling endosomes (**Figure 3-4**). Furthermore, confocal images showing co-localization of the FITC-labeled micelles with LysoTracker Red-stained organelles indicated their presence in late endosomes and lysosomes (**Figure 3-5**). Combined, these data indicate that the amphiphilic macromolecules enter cells by endocytosis. Further support of the endocytotic entry of the amphiphilic macromolecules was observed from the difference in fluorescence of free FITC and FITC-labeled micelles (**Figure 3-6**) since cellular entry

of free FITC is likely by diffusion. Semi-quantitative analysis of the co-localized images (**Figures 3-4 and 3-5**) using the Image-Pro Plus 5.1 software showed that 30% of the internalized polymers were located within the lysosomes and 47% within the endosomes. By difference, the remaining 23% of the polymer was located within the rest of the cell.

Similar results were observed with related polymeric micelles. For example, poly(ethylene oxide)-*block*-poly(caprolactone) copolymer micelles entered human adenocarcinoma breast cancer cells [10], PC12 cells [13, 14] and NIH 3T3 cells [14] by endocytosis. Similarly, FITC-labeled cross-linked polymer micelles from poly(ethylene oxide)-*b*-poly(methacrylic acid) copolymers were internalized in human A2780 ovarian carcinoma cells [19] by endocytosis. However, it is not clear for the amphiphilic macromolecular micelles evaluated in this study, whether the entire micelle or the individual unimers were transported or diffused into the cytoplasm.

3.5. Conclusions

Evaluation of the amphiphilic macromolecules-based micelles as drug delivery systems includes analysis of their cellular entry or internalization mechanism. Intracellular drug delivery is an important parameter in their development as nanocarriers of hydrophobic anticancer drugs. Confirmation of the endocytotic cellular entry of AMs led to the development of drug-AM conjugates designed for enhanced intracellular drug release, as described in **Chapter 4**.

3.6. References

- 1 K. D. Jensen, A. Nori, M. Tijerina, P. Kopeckova, and J. Kopecek. Cytoplasmic delivery and nuclear targeting of synthetic macromolecules. *Journal of Controlled Release* **87**: 89-105 (2003).
- 2 P. Watson, A. Jones, and D. Stephens. Intracellular trafficking pathways and drug delivery: fluorescence imaging of living and fixed cells. *Adv. Drug Del. Rev.* **57**: 43-61 (2005).
- 3 N. Rapoport, A. Marin, Y. Luo, G. D. Prestwich, and M. Muniruzzaman. Intracellular uptake and trafficking of pluronic micelles in drug-sensitive and MDR cells: effect on the intracellular drug localization. *Journal of Pharmaceutical Sciences* **91**: 157-170 (2002).
- 4 M. Muniruzzaman, A. Marin, Y. Luo, G. D. Prestwich, W. G. Pitt, G. Hussein, and N. Y. Rapoport. Intracellular uptake of Pluronic copolymer: effects of the aggregation state. *Colloids and Surfaces B: Biointerfaces* **25**: 233-241 (2002).
- 5 S. K. Lai, K. Hida, S. T. Man, C. Chen, C. Machamer, T. A. Schroer, and J. Hanes. Privilege delivery of polymer nanoparticles to the perinuclear region of live cells via a non-clathrin, non-degradative pathway. *Biomaterials* **28**: 2876-2884 (2007).
- 6 J. Panyam, S. Sahoo, S. Prabha, T. Barger, and V. Labhasetwar. Fluorescence and electron microscopy probes for cellular and tissue uptake of poly(d,l-lactide-co-glycolide) nanoparticles. *Int. J. Pharm.* **262**: 1-11 (2003).
- 7 F. Chiellini, D. Dinucci, C. Bartoli, A. M. Piras, and E. Chiellini. Intracellular fate investigation of bio-eliminable polymeric nanoparticles by confocal laser scanning microscopy. *Journal of Bioactive and Compatible Polymers* **22**: 667-685 (2007).
- 8 A. Nori, K. D. Jensen, M. Tijerina, P. Kopeckova, and J. Kopecek. Subcellular trafficking of HPMA copolymer-Tat conjugates in human ovarian carcinoma cells. *Journal of Controlled Release* **91**: 53-59 (2003).
- 9 K. Jensen, P. Kopeckova, J. Bridge, and J. Kopecek. The cytoplasmic escape and nuclear accumulation of endocytosed and microinjected HPMA copolymers and a basic kinetic study in Hep G2 cells. *AAPS Pharm. Sci.* **3**: 1-14 (2001).

- 10 A. Mahmud and A. Lavasanifar. The effect of block copolymer structure on the internalization of polymeric micelles by human breast cancer cells. *Colloids Surf. B: Biointerfaces* **45**: 82-89 (2005).
- 11 G. Sahay, E. V. Batrakova, and A. V. Kabanov. Different internalization pathways of polymeric micelles and unimers and their effects on vesicular transport. *Bioconjugate Chemistry* **10**: 2023-2029 (2008).
- 12 J. Davda and V. Labhasetwar. Characterization of nanoparticle uptake by endothelial cells. *Int. J. Pharm.* **233**: 51-59 (2002).
- 13 C. Allen, Y. Yu, A. Eisenberg, and D. Maysinger. Cellular internalization of PCL20-b-PEO44 block copolymer micelles. *Biochim. and Biophys. Acta* **1421**: 32-38 (1999).
- 14 R. Savic, L. Luo, A. Eisenberg, and D. Maysinger. Micellar nanocontainers distribute to defined cytoplasmic organelles. *Science* **300**: 615-618 (2003).
- 15 J. Wang. Synthesis and evaluation of novel amphiphilic macromolecules as drug carriers and therapeutics (PhD Thesis), *Department of Chemistry and Chemical Biology*, Rutgers University, Piscataway, NJ, 2007.
- 16 J. Panyam, W. Z. Zhou, S. Prabha, S. Sahoo, and V. Labhasetwar. Rapid endo-lysosomal escape of poly(DL-lactide-co-glycolide) nanoparticles: implications for drug and gene delivery. *FASEB* **16**: 1217-1226 (2002).
- 17 J. Panyam and V. Labhasetwar. Dynamic of endocytosis and exocytosis of poly(D,L-lactide-co-glycolide) nanoparticles in vascular smooth muscle cells. *Pharm. Res.* **20**: 212-220 (2003).
- 18 M. K. Pratten and J. B. Lloyd. Micelle-forming block copolymers: Pinocytosis by macrophages and interaction with model membranes. *Makromol. Chem.* **186**: 725-733 (1985).
- 19 S. Bontha, A. V. Kabanov, and T. K. Bronich. Polymer micelles with cross-linked ionic cores for delivery of anticancer drugs. *J. Control. Release* **114**: 163-174 (2006).

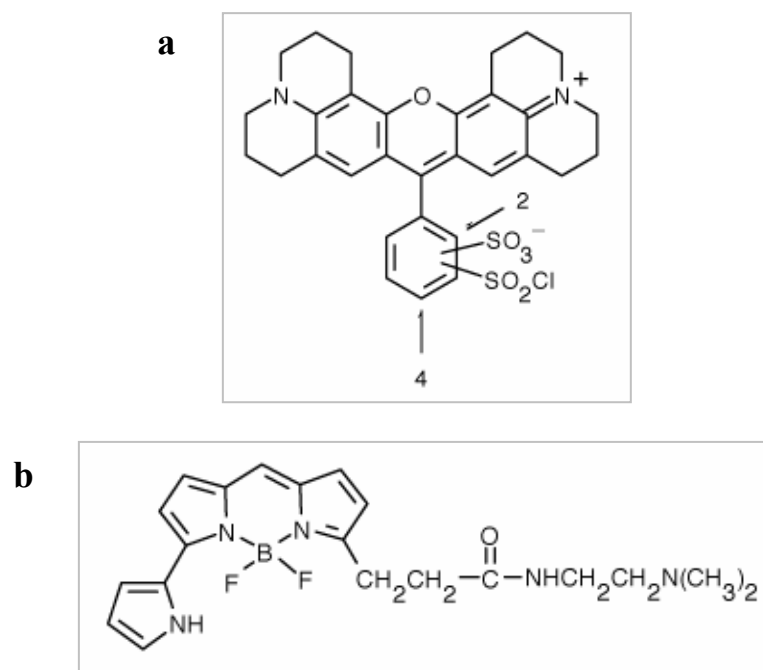


Figure 3-1. Chemical structures of a) Texas Red and b) LysoTracker Red (Invitrogen Catalog, Invitrogen, Carlsbad, CA).

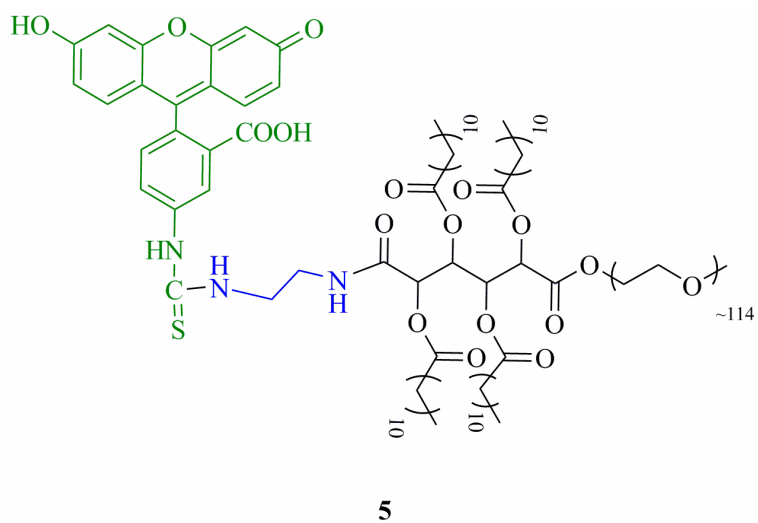


Figure 3-2. Chemical structure of FITC-AM.

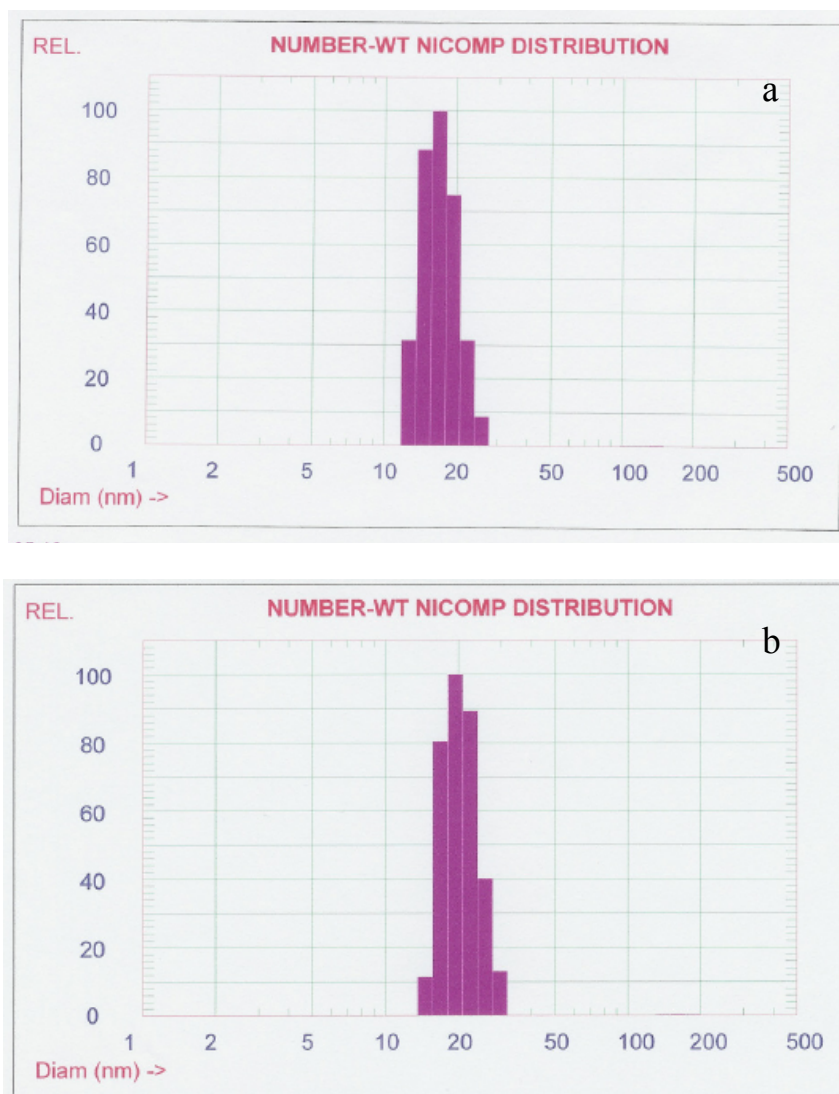


Figure 3-3. Micelle size number-weight distribution from dynamic light scattering studies: (a) AM micelles and (b) FITC-labeled micelles.

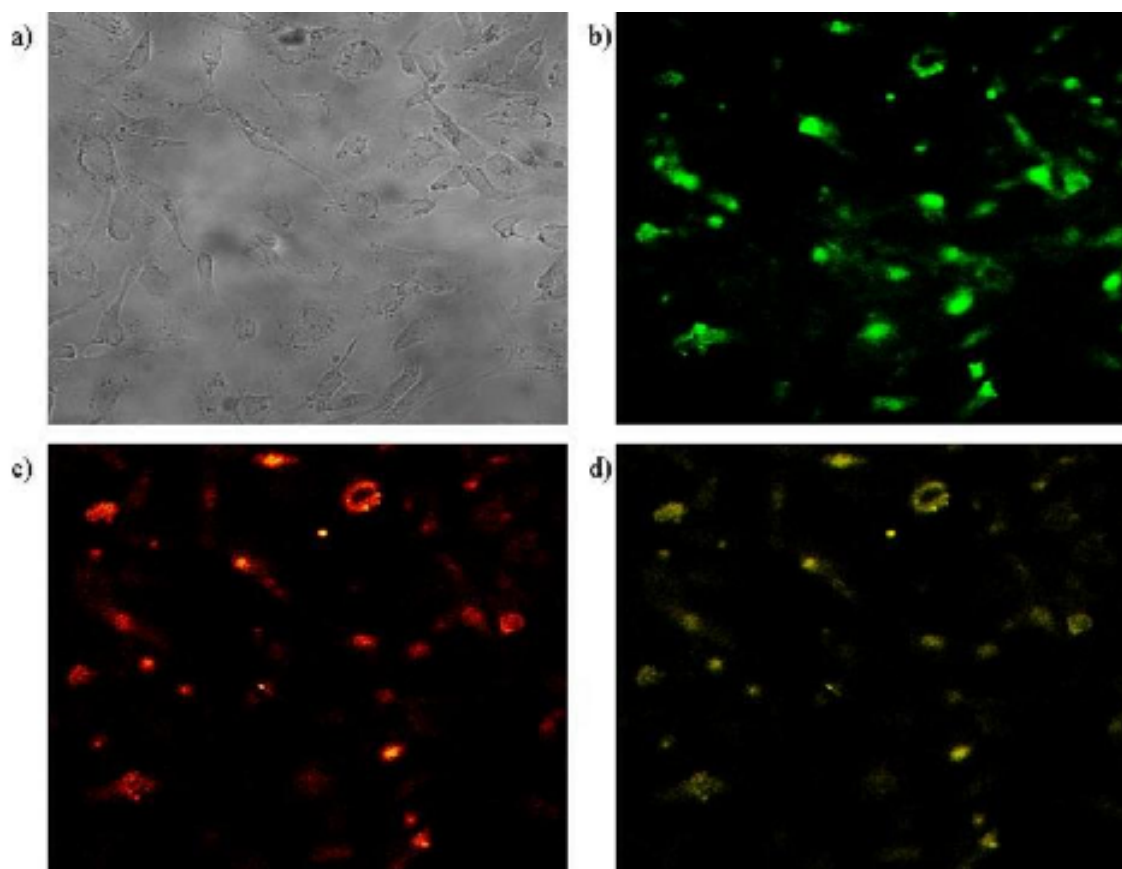


Figure 3-4. Confocal images demonstrating the subcellular localization of FITC-labeled micelles in HUVECs: (a) Differential interference contrast image showing the outline of the cells; (b) appearance of FITC-labeled micelles indicate cellular uptake; (c) presence of Texas Red-stained conjugate identifies endosomes; and (d) overlay showing the colocalization of FITC-labeled micelles with Texas Red-stained endosomes.

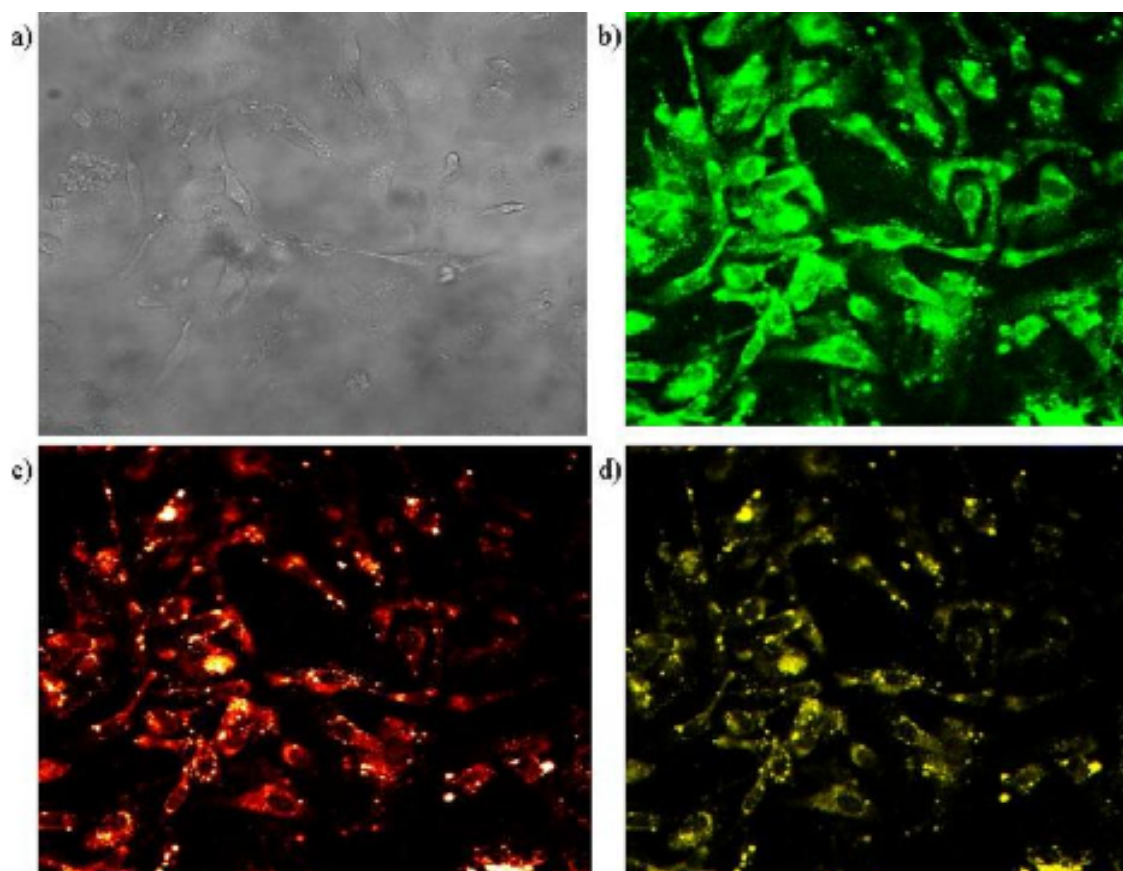


Figure 3-5. Confocal images demonstrating the subcellular localization of FITC-labeled micelles in HUVECs: (a) Differential interference contrast image showing the outline of the cells; (b) appearance of FITC-labeled micelles indicate cellular uptake; (c) presence of LysoTracker Red identifies lysosomes; and (d) overlay showing the co-localization of FITC-labeled micelles with LysoTracker Red-stained lysosomes.

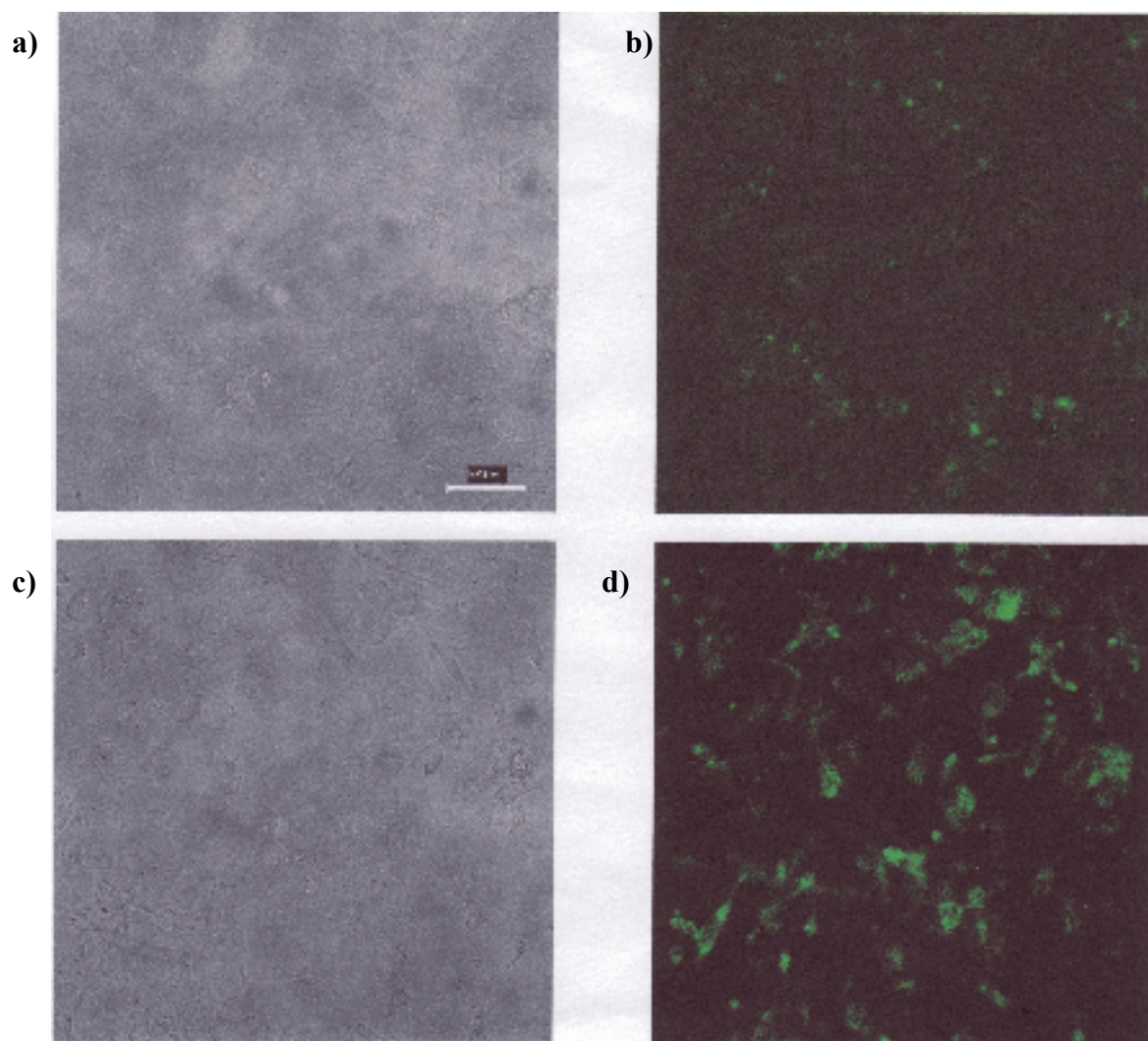


Figure 3-6. Confocal images demonstrating the contrast in fluorescence of FITC control and FITC-labeled micelles in HUVECs: (a) Differential interference contrast image showing the outline of cells incubated with FITC control; (b) fluorescence of FITC control; (c) differential interference contrast image showing the outline of cells incubated with FITC-labeled micelles (d) fluorescence of FITC-labeled micelles.

Chapter 4

PHYSICALLY ENCAPSULATED AND CHEMICALLY BOUND DOXORUBICIN IN AMPHIPHILIC MACROMOLECULES-BASED MICELLES

4.1. Introduction

Doxorubicin (DOX) is an antitumor drug and anthracycline antibiotic that has dose limitations resulting from non-specific cardiotoxicity [1]. Efforts to minimize the negative effects of the drug for intravenous administration have focused on delivery systems, such as polymer-based carriers. Polymer carriers for doxorubicin include liposomes [2, 3] and polymeric micelles [4-19] which focus on physical encapsulation of the drug. Other polymer-based drug delivery systems for doxorubicin involve chemical conjugation of the drug directly onto the polymer side chains of graft copolymers, chain ends of dendrimers or hydrophobic blocks of amphiphilic diblock copolymers [20-24]. Several polymeric micellar carriers containing both chemically conjugated or physically encapsulated doxorubicin have also been reported [25-28]. Other examples of drug carriers include polymer-drug conjugates, nanospheres, dendrimers, nanogels and vesicles, all are referred to as “nanomedicines” [29, 30].

It has been reported that drug conjugation to a polymer has many advantages: *i*) improved pharmacokinetics [31] *ii*) increased hydrodynamic volume resulting in slower renal excretion and longer blood circulation [32] and *iii*) tumor accumulation by the enhanced permeability and retention (EPR) effect resulting from defective tumor vascular architecture and impaired lymphatic drainage [33]. Polymer-conjugated drugs are

reported to have prolonged half-life, higher stability, and lower immunogenicity and antigenicity [34].

This study focuses on doxorubicin conjugates of amphiphilic macromolecules that self-assemble in aqueous solution to form micelles, with doxorubicin attached to the hydrophobic core (see **Figure 4-1**). Doxorubicin was covalently attached *via* hydrazone linker to the hydrophobic chain end of the amphiphilic macromolecule (**Figure 4-2**). This amphiphilic macromolecule (AM) was chosen because of its excellent nanocarrier properties including low critical micelle concentration (1.3×10^{-7} M) [35, 36], small micellar size (~ 20 nm) [35, 37], good water solubility (15 mg/mL) [38], drug encapsulation capability [35], non-cytotoxicity [35] and simple synthetic route [36]. The pH-sensitivity of the hydrazone linker at lysosomal pH (5.0) over physiological pH (7.4) has been well documented [39-48]. The unique micellar carrier properties of AMs and pH sensitivity of the hydrazone drug-polymer linker combine to form a unique doxorubicin delivery system. Consequently, this study evaluates micelles assembled from doxorubicin conjugates (DOX-AM) as nanocarriers of doxorubicin.

The AM micelles were first evaluated by comparing physical encapsulation of DOX and chemical conjugation of DOX in terms of DOX content, micellar sizes and cytotoxicity against human liver cancer cells (as DOX is widely used for the treatment of hepatocellular carcinoma) [49]. Next, AM micelles with both physically encapsulated and chemically bound DOX were analyzed. Finally, AM micelles were compared with two polymeric drug delivery systems: *i*) Pluronic P85, a popular micellar drug and gene

carrier [50, 51], and *ii*) Cremophor EL, a commonly used solubilizing agent for hydrophobic molecules [52].

4.2. Materials

Doxorubicin hydrochloride (DOX·HCl), hydrazine monohydrate, phosphate buffered saline tablets (PBS), phosphate citrate buffer tablets, carbonate-bicarbonate buffer capsules, 4Å <5 μm molecular sieves, triethylamine (TEA), N,N-dimethylformamide (DMF), 2,4,6-trinitrobenzene-1-sulfonic acid (TNBSA) (5% w/v in H₂O), and ethyl carbazate were purchased from Sigma-Aldrich (St. Louis, MO). Sephadex LH-20 was purchased from Amersham Biosciences GE Healthcare (Piscataway, NJ). Regenerated cellulose (RC) membranes (Spectra/Por molecular weight cut-off MWCO 3500 Da), Scienceware acrylic equilibrium dialysis cells (Bel-Art Products, NJ), Whatman polytetrafluoroethylene (PTFE) and poly(vinylidene fluoride) (PVDF) syringe filters, Corning cell culture T-75 flasks, sterile serological pipets, BD Falcon 15-mL graduated tubes, BD Falcon 96-well tissue culture plates, and Vialab reagent reservoirs were purchased from Fisher Scientific (Pittsburg, PA). Hepatocellular carcinoma (HepG2) cells, Modified Eagle's Minimum Essential Media (MEM), fetal bovine serum (FBS), penicillin-streptomycin solution, trypsin-EDTA (1x) solution, Dulbecco's phosphate buffered saline and MTT Cell Proliferation Assay kit were purchased from ATCC (Manassas, VA). Pluronic P85 and Cremophor EL were kindly given by BASF Corporation (Mount Olive, NJ). All other reagents and solvents were purchased from Sigma-Aldrich and used as received.

4.3. Methods

4.3.1. Cell Culture: Human Liver Cancer Cells

Human hepatocellular carcinoma cells (HepG2) were grown in Modified Eagle's Minimum Essential Media supplemented with 10% FBS and 1% penicillin-streptomycin solution. The cells were grown at 37 °C, 5% CO₂ for 2 passages prior to the 3-(4,5-dimethylthiazol-2-yl)-2,5-diphenyl-2H-tetrazolium bromide (MTT) experiment. The cells growing in the exponential phase, were seeded (10,000 cells/well) in 96-well plates for the MTT assay.

4.3.2. Chemical Characterization of DOX-AM

¹H NMR spectroscopy was performed in samples (~ 10-20 mg/ml) in CDCl₃-*d* using tetramethylsilane as the reference signal. NMR experiments were completed using a 300 MHz Varian spectrometer.

Gel permeation chromatography (GPC) was used for molecular weight determination. Samples were injected into a Waters 510 HPLC equipped with a 5 μm gel precolumn, two PL columns with pore size 10³-10⁵ Å (Polymer Labs), and Waters 410 Differential Refractometer. DMF containing 0.1 % v/v trifluoroacetic acid was used as the mobile phase (flow rate 0.8 mL/min) and solvent for sample dissolution (~10 mg/mL). Before injection, the samples were filtered through a 0.45 μm PTFE filter (Whatman, Clifton, NJ). The GPC system was calibrated using polystyrene standards (Polymer Labs, UK) to obtain number-average molecular weights and polydispersity indices (PDI).

UV-vis spectrophotometry was used to confirm DOX conjugation. Samples {DOX-AM (8), hydrazide-AM (7) admixed with DOX, and hydrazide-AM (7)} dissolved in DMF (~1 mg/mL) were analyzed on a Beckman DU520 General Purpose UV/VIS Spectrophotometer over 190-1100 nm wavelength range. DOX has a characteristic wavelength peak at 480 nm [47, 53].

Steady state fluorescence spectroscopic analysis was performed to further confirm DOX conjugation. Samples {hydrazide-AM (7) admixed with DOX, and DOX-AM (8)} in DMF (~1 mg/mL) were analyzed on a Shimadzu RF-5301PC Spectrofluorophotometer equipped with a Xenon lamp using the excitation wavelength at 480 nm [47, 53] and the emission wavelength at 586 nm [47, 53].

A modified TNBSA assay was performed to confirm AM hydrazide functionalization using UV-vis spectrophotometry. TNBSA reacts with primary amines in aqueous medium at pH 8 and room temperature without any undesirable secondary reactions [54]. For hydrazide-terminated polymer side chains, hydrazide content is determined by incubation with TNBSA in borate buffer (pH 9.3) for 100 min, measuring absorbance of the N-nitrophenyl derivative at $\lambda=500$ nm, and using the model reaction of TNBSA and ethyl carbazate [47]. In this study, instead of borate buffer, carbonate buffer (pH 9.6) was used as it was readily available.

4.3.3. Preparation of Hydrazide-AM (7).

Compound **6** is an N-hydroxysuccinimide-activated amphiphilic macromolecule and prepared according to published procedures [38]. Compound **6** (1.2 g, 0.20 mmol) was reacted with 10 molar excess of hydrazine monohydrate (0.10 mL) in methanol (25 mL) for 3 hours at room temperature. The reaction mixture was dialyzed against deionized water using regenerated cellulose membranes MWCO 3500 Da for 12 h then lyophilized for 48 h at $<133 \times 10^{-3}$ mBar with the condenser temperature at -50 °C (FreeZone Benchtop and Console Freeze Dry System, Labconco, Kansas City, MI).

The hydrazide end group of the product **7** was quantified using a modified TNBSA assay for primary amine detection, similarly used by Etrych *et al.* [47]. Briefly, **7** was dissolved in carbonate buffer pH 9.6 (10 mg/mL), then an aliquot (0.125 mL) added to 0.125 mL of 1 w/v % aqueous TNBSA solution and 4.75 mL carbonate buffer (pH 9.6). After incubation for 100 h in the dark at room temperature, the solution was analyzed at λ 500 nm by UV spectrophotometry (Beckman DU 520 UV vis spectrophotometer) to confirm the transformation. The hydrazide-AM (**7**) was obtained as white powder: 0.78 g, 63 % yield. ^1H NMR (DMSO- d_6 , TMS): δ 9.8 (s, 1H, **AM** - NH_2), 9.4 (s, 1H, **AM** - NH_2), 8.2 (s, 1H, **AM** - NH-NH_2), 5.0 - 5.8 (m, 4H, **AM** CH), 3.60 (m, ~ 0.4 kH, **AM** CH_2O), 2.3 (m, 8H, **AM** CH_2), 1.5 (m, 8H, **AM** CH_2), 1.2 (m, 64H, **AM** CH_2), 0.9 (t, 12H, **AM** CH_3). MW:6.1 kDa, PDI: 1.1.

4.3.4. Preparation of DOX-AM (8)

Compound **7** (0.10 g, 0.020 mmol), DOX·HCl (0.010 g, 0.020 mmol) and TEA (0.010 mL, 4 molar equiv excess) in flame-activated 4Å molecular sieves (36 mg) were added to anhydrous DMF (16 mL). The reaction proceeded in the dark under argon for 24 h at 60 °C. DOX-AM (**8**) was isolated by precipitation into diethyl ether (40 mL), followed by redissolution of the precipitate in methanol (4 mL), filtration through 0.45µm PTFE filters to remove molecular sieves, then methanol removed by rotary evaporation. The DOX-AM concentrate was purified by gel filtration chromatography (Sephadex LH-20) using methanol as the mobile phase. The first red fraction was collected, solvent removed by rotary evaporation and product **8** obtained as a reddish purple solid: 0.98 g, 46 % yield (overall yield 29 %) ¹H NMR (DMSO-d₆, TMS): δ 7.6 – 8.0 (m, 3H, **DOX** Ar-H), 5.1 - 5.8 (m, 4H, **AM** CH), 4.6 (t, 1H, **DOX** CH), 4.2 (t, 1H, **DOX** CH), 3.4 (m, ~0.4 kH, **AM** CH₂O), 2.4 (m, 8H, **AM** CH₂), 2.0 (t, 2H, **DOX** CH₂), 1.9 (d, 2H, **DOX** CH₂), 1.5 (m, 8H, **AM** CH₂), 1.3 (m, 64H, **AM** CH₂), 1.1 (m, 3H, **DOX** CH₃), 0.9 (t, 12H, **AM** CH₃).

4.3.5. DOX Loading by Dialysis Method

Samples (1 mg) were dissolved in DMF (3.8 ml) and added to DOX·HCl (2 mg) dissolved in DMF (0.2 mL) to a drug-polymer ratio of 2:1 w/w. TEA (1.0 µL, 2.0 mol equiv) was added to neutralize the HCl salt of DOX and enhance drug encapsulation into the hydrophobic micellar core. The samples were covered with aluminum foil and parafilm, and shaken using vortex mixer for about two minutes. Controls were DOX

alone and polymer alone dissolved in DMF. Samples were dialyzed 24 h against 1 L distilled water using cellulose membranes.

DOX loading was quantified by UV-visible spectrophotometry at 480 nm. Calibration was performed using DOX standards in DMF (1-60 $\mu\text{g/mL}$). Calculation of DOX content for DOX-loaded AMs was as follows:

$$\text{Weight \% loading} = \frac{\text{Concentration of free drug detected}}{\text{Polymer concentration}} \times 100$$

4.3.6. Size Analysis of DOX-AM Micelles

Dynamic light scattering (DLS) measurements were performed using a Malvern Instruments Zetasizer Nano ZS-90 (Southboro, MA). The scattering angle for the instrument was set at 90° and solutions of DOX-AM or AM (~1 mg/mL) were prepared in deionized water, filtered through 0.2 μm PVDF filters into disposable sizing cuvettes and analyzed at 25°C. DLS measurements were done in triplicate, with 10 runs per measurement at 60-sec run duration, using water (viscosity 1.02 cp and refractive index of 1.335) as the dispersant medium. Particle size distributions were reported by volume-weight.

Transmission electron microscopy (TEM) measurements were done using a JEM-100 CXII (Jeol Ltd, Japan). Samples were dissolved in HPLC-grade water (100 μM) and one drop placed onto a wax plate. A circular copper grid (Formvar/carbon film, Electron Microscopy Sciences, Hatfield, PA) was placed on the drop surface. After one minute, the grid was removed, tapped with filter paper to remove excess water, and negatively

stained using 1% uranyl acetate for one minute. The grid was air dried for 20 min and then analyzed under the electron microscope at 80 kV. Analysis of the samples was done in triplicate.

4.3.7. *In Vitro* DOX Release

These experiments were performed with the assistance of Bahar Demirdirek.

The drug release system consisted of a regenerated cellulose membrane (soaked in PBS for 12 h) placed between the donor and receptor cells of acrylic equilibrium dialysis cells (Scienceware, Bel-Art Products, NJ) immersed in a constant temperature bath (37 °C). Samples were separately dissolved in PBS (pH 7.4) and phosphate citrate buffer (pH 5.0). Aliquots (5 mL) of the solutions were separately added into donor dialysis cells and fresh PBS or citrate buffer (5 mL) was added into their corresponding receptor cells. At specific time intervals, the receptor cell solutions were retrieved, analyzed by UV-vis spectrophotometry (DOX $\lambda_{\text{max}} = 480 \text{ nm}$ [47, 53]) and replaced with fresh PBS or citrate buffer solutions (5 mL). PBS or citrate buffer was used as blank and a calibration curve was generated from doxorubicin solutions in DMF (1- 60 $\mu\text{g/mL}$).

4.3.8. *In Vitro* Cytotoxicity Assay Against HepG2 Human Liver Cancer Cells

Hepatocellular carcinoma (HepG2) cells were maintained in Modified Eagle's Minimum Essential Media supplemented with 10% v/v fetal bovine serum and 1% v/v penicillin-streptomycin solution at 37 °C in a humidified atmosphere containing 5% CO₂. The MTT cell proliferation assay was performed to measure cell proliferation rates, and conversely, the reduction in cell viability, based on the reduction of yellow tetrazolium

MTT (3,4,5-dimethylthiazoly-2)-2,5-diphenyltetrazolium bromide) by metabolically active cells resulting in purple formazan salts that can be quantified spectrophotometrically (ATCC, Manassas, VA). Briefly, 10,000 cells/well were plated in BD Falcon 96-well tissue culture plates (Fisher Scientific, PA) and incubated in 37°C, 5% CO₂ for 24 h with complete media containing 10 % FBS. The medium was replaced with fresh complete medium containing DOX ± polymer samples with equivalent DOX concentrations ranging from 0.01 to 10 µM. Four wells were treated at each concentration of each sample. The cells were incubated with samples for 72 h, the MTT reagent added, and the plates incubated for 3 h at 37 °C. The MTT detergent was added and the plates left for 2 h at room temperature in the dark. Absorbance values were obtained from the EL808 Ultra Microplate Reader (Biotek Instruments, Winooski, VT) at 570 nm using the KC Junior program. The IC₅₀ values were calculated from logarithmic equations generated from % cell viability vs. DOX concentration (nM) plots.

4.3.9. Analysis of DOX-loaded DOX-AM Micelles

*DOX-AM (8) micelles were also loaded with free DOX molecules using the dialysis loading method described in **Section 4.3.5.**, this work was performed by Bahar Demirdirek. The resulting micelles consisted of both physically encapsulated and chemically bound drug and referred to as DOX-loaded DOX-AM micelles.* The size distribution of DOX-loaded DOX-AM micelles was measured by dynamic light scattering, and micellar morphology by TEM, using the methods described in **Section 4.3.6.** Finally, using the same methods described in **Section 4.3.8,** the *in vitro* cytotoxicity of DOX-loaded DOX-AM micelles were analyzed against HepG2 cells.

4.3.10 Comparison with Pluronic P85 and Cremophor EL

Two polymeric drug delivery systems Pluronic P85 and Cremophor EL were loaded with DOX using the methods described in **Section 4.3.5**. The resulting samples were analyzed for *in vitro* cytotoxicity against HepG2 cells using the methods described in **Section 4.3.8**.

4.3.11. Statistical Analysis

Data are reported as means \pm standard deviation. Differences among the % cell viability results for DOX \pm polymer samples were compared by univariate analysis of variance (ANOVA) followed by the Tukey and LSD post hoc tests for multiple comparisons at each DOX concentration using SPSS for Windows v.16 (SPSS, Chicago, IL), with the level of significance set at $\alpha = 0.05$.

4.4. Results and Discussion

4.4.1. Preparation and Characterization of DOX-AM

A major difference between free and polymer-bound DOX is cellular internalization: free DOX is internalized by passive diffusion, and polymer-bound DOX by endocytosis [26, 42, 43, 55]. Current interest is on intracellular pH-controlled DOX release, particularly with utilizing pH-sensitive drug-polymer linkages stable in physiological pH (7.4) that hydrolyze at lysosomal pH (5.0). The hydrazone linkage is a popular choice because the released DOX molecule remains intact in structure [42].

Previously, we reported the endocytotic internalization of AMs in human umbilical vein endothelial cells [38]. In this chapter, we designed DOX-AM conjugates (**8**) with this endocytotic pathway in mind: the endo-lysosomal delivery of DOX using pH-sensitive hydrazone linkages between DOX and AMs. In this study, the drug delivery system under investigation consisted of DOX-AMs that assembled to polymeric micelles (**Figure 4-1**). DOX was conjugated to AM through a two-step reaction scheme shown in **Figure 4-2**: NHS-activated AM (**6**) was reacted with hydrazine hydrate to form hydrazide-AM (**7**), then DOX was covalently bound through the formation of a hydrazone bond to form DOX-AM (**8**).

To confirm hydrazone functionalization, the hydrazide group was quantified from the reaction of TNBSA with primary amines e.g. ethyl carbazate in basic pH [47, 48]. Using this protocol, 63% of AMs were calculated to be functionalized (**Figure 4-3**), using equivalent amounts of ethyl carbazate as the standard. Given that the solubility of **7** and unfunctionalized AMs **6** are similar, their separation is extremely difficult. Thus, the mixture of **6** and **7** was reacted with DOX·HCl. DOX conjugation was confirmed by the appearance of DOX protons from ^1H NMR analysis in the 7.6 – 8.0 ppm region corresponding to DOX aromatic protons; no aromatic peaks were observed for AM (**1**) nor hydrazide-AM (**7**). Furthermore, an increase in molecular weight was observed by GPC (**Figure 4-4**). DOX conjugation to AM was further confirmed from UV analysis by a 95-nm λ red shift that was clearly not observed when the DOX was physically admixed with hydrazide-AM (**Figure 4-5**). DOX also has a characteristic fluorescence spectra, and fluorescence variations is reportedly attributed to association of DOX with a less

polar environment [56]; thus a change in fluorescence spectra further supports polymer-drug conjugation (**Figure 4-6**).

Conjugated DOX was quantified by UV vis spectrophotometry ($\lambda = 480$ nm) and indicated a 46 % yield of DOX-AM conjugation (29 % overall yield). This lower conjugation efficiency is likely due to the steric hindrance in the reactive end groups. However, DOX conjugation to AMs (6.5 wt %) *via* hydrazone linkage was still higher than other DOX-polymer conjugates containing hydrazone linkers: DOX-pullulan conjugates (3.18 wt %) [25] and PolymerIV-DOX conjugates (3 wt %) [44].

4.4.2. DOX Loading in AM micelles

DOX was physically encapsulated in AM micelles using the dialysis method. DOX physically encapsulated in AM micelles (12 wt %) showed higher DOX content than when chemically bound in AMs (6 wt %) likely due to the steric hindrances in DOX conjugation compared to physical encapsulation (**Table 4-1**). Notably, the highest DOX content was for physically loaded DOX into DOX-AMs.

4.4.3. Size Analysis of DOX-AM Micelles and DOX-loaded AM Micelles

Micellar formation of DOX-AM (**8**) was confirmed by dynamic light scattering (DLS) measurements with micellar sizes of 30 ± 1 nm. Micelles assembled from AMs alone were of 20 ± 2 nm sizes and upon DOX physical encapsulation slightly decreased to 16 ± 1 nm, possibly due to increased hydrophobic interactions in the micellar core (**Table 4-1**). The hydrophobic interactions possibly correlate to the DOX content and the

micellar sizes: AM micelles have higher DOX content and smaller sizes; DOX-AM micelles have lower DOX content and bigger sizes. All of these micellar sizes (< 100 nm) are appropriate for simple sterilization by filtration, minimized capillary embolism and extravasation to tumors as reported elsewhere [57].

Further support of DOX-AM micellar formation was obtained from TEM measurements, showing spherical morphologies and similar to DLS-detected sizes of the DOX-AM micelles (**Figure 4-7a**) and DOX-loaded DOX-AM micelles (**Figure 4-7b**)

4.4.4. *In Vitro* DOX Release from DOX-AM

The *in vitro* release of DOX from DOX-AMs was analyzed at two different buffered solutions (pH 5.0 and 7.4) to detect pH-sensitivity of the hydrazone linker. **Figure 4-8** shows that DOX released faster at pH 5.0 (lysosomal pH) compared to pH 7.4 (physiological pH), similar to data reported elsewhere [25, 42-44, 47]. This acidic pH enhanced DOX *in vitro* release indicates the potential of DOX-AMs for endo-lysosomal DOX delivery; further studies are needed to explore this capability of intracellular DOX release (see **FUTURE WORK**).

4.4.5. *In Vitro* Cytotoxicity Assay of DOX-loaded AMs and DOX-AMs

DOX is widely used as the therapeutic drug for hepatocellular carcinoma [49], consequently, HepG2 is a commonly used cell line in cell proliferation assays to assess DOX therapeutic efficacy *in vitro* [9, 49, 53, 58, 59]. The cytotoxic effects of AM with physically encapsulated DOX (DOX-loaded AMs) and AMs with chemically bound

DOX (DOX-AMs) were compared with DOX alone using the MTT assay (**Figure 4-9**). Statistical analysis of data ($p < 0.05$) showed that chemically bound DOX was significantly more cytotoxic than physically encapsulated DOX. Furthermore, compared to DOX alone (IC_{50} : 84 nM), DOX-loaded AM (IC_{50} : 230 nM) was about 3-fold less cytotoxic whereas DOX-AMs (IC_{50} : 8 nM) was 10-fold more cytotoxic against HepG2 cells after 72 h incubation (**Figure 4-9**).

Similar to DOX physically encapsulated in AMs, it was reported that DOX-loaded PEO-*b*-PBCL micelles (IC_{50} : 1.54 $\mu\text{g/mL}$) were less cytotoxic than free DOX (IC_{50} : 0.03 $\mu\text{g/mL}$) against B16F10 murine melanoma cells after 48 h incubation [28]. Other micelle systems assembled from DOX-conjugated polymers with hydrazone linkages were found to be more cytotoxic than free DOX after 48 h incubation: CF-FLU-DOX (IC_{50} : 1.2 μM) showed greatly enhanced cytotoxicity than free DOX (IC_{50} : 18.5 μM) against MCF-7 human breast cancer cells [43], and DOX-PLLA-mPEG (IC_{50} : 10 μM) showed higher cytotoxicity than free DOX (IC_{50} : 50 μM) against human lymphoblast cells [42]. In summary, the cytotoxicity data suggest the advantage of DOX-AM conjugation over DOX physical encapsulation in the AMs: the pH-controlled DOX release from DOX-AMs in the liver cancer cells.

4.4.6. Analysis of DOX-loaded DOX-AM Micelles

AM micelles with both physically encapsulated and chemically bound DOX were analyzed for DOX content, micellar sizes/morphology, and *in vitro* cytotoxicity against HepG2 cells.

DOX-loaded DOX-AM micelles showed higher DOX content (24 wt %) compared to AM micelles with only physically encapsulated drug (12 wt %) or AM micelles with chemically bound drug (6 wt %) (**Table 4-1**). This phenomenon is likely due to the DOX initially present and chemically bound in the micellar core, where increased π - π interactions in the micellar core led to higher DOX physical encapsulation. This result is similar to observations reported elsewhere: DOX loading was enhanced in PEO-b-PBCL micelles [28] and PEG-PBLA micelles [4] resulting from π - π stacking with benzyl groups in the micelle core.

Micellar sizes detected by dynamic light scattering showed smaller sizes for DOX-loaded DOX-AM micelles (18 ± 2 nm) than DOX-AM micelles (30 ± 1 nm) but similar to DOX-loaded AM micelles (16 ± 1) as shown in **Table 4-1**. The spherical morphology of DOX-loaded DOX-AM micelles was observed (**Figure 4-7b**) from TEM analysis.

Although AM micelles with both physically encapsulated and chemically bound DOX had higher DOX content than AM micelles (physically encapsulated DOX) or DOX-AM micelles (chemically bound DOX), equivalent DOX concentrations in the different micelle systems were used against HepG2 cells in the MTT assay. The cytotoxicity of DOX-loaded DOX-AM micelles (IC_{50} 24 nM) was lower than DOX-AM micelles (IC_{50} : 8 nM), but higher than free DOX (IC_{50} : 84 nM) and DOX-loaded AM micelles (IC_{50} : 230 nM). As DOX-AMs had more chemically bound DOX than DOX-loaded DOX-AM micelles, this data further supports the advantage of pH-controlled

release from DOX-AM conjugation over DOX physical encapsulation in AMs, as mentioned in **Section 4.4.5**.

4.4.7. Comparison with Pluronic P85 and Cremophor EL

DOX was also physically encapsulated in two polymeric carrier systems, Pluronic P85 and Cremophor EL, using the dialysis method. The DOX-loaded model carriers containing equivalent DOX concentrations to AM-based micelles and DOX control were analyzed against HepG2 cells using the MTT assay.

Results showed lower DOX loading in Pluronic P85 (8 wt %) and Cremophor EL (9 wt %) compared to DOX-loaded AM micelles (12 wt %) and DOX-loaded DOX-AM micelles (18 wt % physically encapsulated DOX). Furthermore, DOX-loaded Cremophor EL showed lower cytotoxicity (IC_{50} : 60 nM) than DOX-loaded DOX-AM micelles (IC_{50} : 24 nM) and DOX-AM micelles (IC_{50} : 8 nM). However, the IC_{50} of DOX-loaded Pluronic P85 could not be calculated because the results showed poor correlation between % cell viability and DOX dose.

4.5. Conclusions

Chemical conjugation of DOX to AMs was better than physical encapsulation as DOX-AM micelles were significantly more cytotoxic than DOX-loaded AM micelles against HepG2 cells. Loading DOX into the DOX-AM micelles resulted in even higher DOX content. However, the increased DOX content did not show increased cytotoxic

activity against HepG2 cells. The AM-based micelles showed better wt % loading and enhanced DOX cytotoxicity than Cremophor EL.

4.6. References

- 1 D. L. Hershman, R. B. McBride, A. Eisenberger, W. Y. Tsai, V. R. Grann, and J. S. Jacobson. Doxorubicin, Cardiac Risk Factors, and Cardiac Toxicity in Elderly Patients with Diffuse B-Cell Non-Hodgkin's Lymphoma. *J. Clinical Oncol.* **26**: 3159-3165 (2008).
- 2 R. M. Rifkin, S. A. Gregory, A. Mohrbacher, and M. A. Hussein. Pegylated Liposomal Doxorubicin, Vincristine, and Dexamethasone Provide Significant Reduction in Toxicity Compared with Doxorubicin, Vincristine, and Dexamethasone in Patients with Newly Diagnosed Multiple Myeloma. *Cancer* **106**: 848-858 (2006).
- 3 R. I. Pakunlu, Y. Wang, M. Saad, J. Khandare, V. Starovoytov, and T. Minko. *In vitro* and *in vivo* intracellular liposomal delivery of antisense oligonucleotides and anticancer drug. *J. Controlled Release* **114**: 153-162 (2006).
- 4 K. Kataoka, T. Matsumoto, M. Yokoyama, T. Okano, Y. Sakurai, S. Fukushima, K. Okamoto, and G. S. Kwon. Doxorubicin-loaded poly(ethylene glycol)-poly(β -benzyl-L-aspartate) copolymer micelles: their pharmaceutical characteristics and biological significance. *J. Controlled Release* **64**: 143-153 (2000).
- 5 F.-Q. Hu, X.-l. Wu, Y.-Z. Du, J. You, and H. Yuan. Cellular uptake and cytotoxicity of shell cross-linked stearic acid-grafted chitosan oligosaccharide micelles encapsulating doxorubicin. *Eur. J. Pharm. Biopharm.* **69**: 117-125 (2008).
- 6 Y.-Q. Ye, F.-L. Yang, F.-Q. Hu, Y.-Z. Du, H. Yuan, and H.-Y. Yu. Core-modified chitosan-based polymeric micelles for controlled release of doxorubicin. *Int. J. Pharm.* **352**: 294-301 (2008).
- 7 J. You, F.-Q. Hu, Y.-Z. Du, and H. Yuan. Improved cytotoxicity of doxorubicin by enhancing its nuclear delivery mediated via nanosized micelles. *Nanotechnology* **19**: 1-8 (2008).
- 8 J. D. Pruitt and W. G. Pitt. Sequestration and Ultrasound-Induced Release of Doxorubicin from Stabilized Pluronic P105 Micelles. *Drug Delivery* **9**: 253-258 (2002).

- 9 L. Y. Qiu and Y. H. Bae. Self-assembled polyethyleneimine-graft-poly(ϵ -caprolactone) micelles as potential dual carriers of genes and anticancer drugs. *Biomaterials* **28**: 4132-4142 (2007).
- 10 L. Liu, C. Li, X. Li, Z. Yuan, Y. An, and B. He. Biodegradable Poly(lactide)/Poly(ethylene glycol)/Poly(lactide) Triblock Copolymer Micelles as Anticancer Drug Carriers. *J. Appl. Polym. Sci.* **80**: 1976-1982 (2001).
- 11 F. Kohori, M. Yokoyama, K. Sakai, and T. Okano. Process design for efficient and controlled drug incorporation into polymeric micelle carrier systems. *J. Controlled Release* **78**: 155-163 (2002).
- 12 Z. G. Gao, D. H. Lee, D. I. Kim, and Y. H. Bae. Doxorubicin-loaded pH-sensitive micelle targeting acidic extracellular pH of human ovarian A2780 tumor in mice. *J. Drug Targeting* **13**: 391-397 (2005).
- 13 E. S. Lee, K. Na, and Y. H. Bae. Doxorubicin loaded pH-sensitive polymeric micelles for reversal of resistant MCF-7 tumor. *J. Controlled Release* **103**: 405-418 (2005).
- 14 E. R. Gillies and J. M. J. Frechet. pH-Responsive Copolymer Assemblies for Controlled Release of Doxorubicin. *Bioconjugate Chem.* **16**: 361-368 (2005).
- 15 C.-L. Lo, C.-K. Huang, K.-M. Lin, and G.-H. Hsiue. Mixed micelles formed from graft and diblock copolymers for application in intracellular drug delivery. *Biomaterials* **28**: 1225-1235 (2007).
- 16 H. Yin and Y. H. Bae. Physicochemical Aspects of Doxorubicin-loaded pH-sensitive Polymeric Micelle Formulations from Mixtures of Poly(L-histidine)-*b*-poly(ethylene glycol)/poly(L-lactide)-*b*-poly(ethylene glycol). *Eur. J. Pharm. Biopharm.* (2008).
- 17 G. S. Kwon, M. Naito, M. Yokoyama, T. Okano, Y. Sakurai, and K. Kataoka. Physical Entrapment of Adriamycin in AB Block Copolymer Micelles. *Pharm. Res.* **12**: 192-195 (1995).
- 18 Z.-G. Gao, H. D. Fain, and N. Rapoport. Controlled and targeted tumor chemotherapy by micellar-encapsulated drug and ultrasound. *J. Controlled Release* **102**: 203-222 (2005).

- 19 G. Kwon, M. Naito, M. Yokoyama, T. Okano, Y. Sakurai, and K. Kataoka. Block copolymer micelles for drug delivery: loading and release of doxorubicin. *J. Controlled Release* **48**: 195-201 (1997).
- 20 M. Kovar, L. Kovar, V. Subr, T. Etrych, K. Ulbrich, T. Mrkvan, J. Loucka, and B. Rihova. HPMA copolymers containing doxorubicin bound by a proteolytically or hydrolytically cleavable bond: comparison of biological properties in vitro. *J. Controlled Release* **99**: 301-314 (2004).
- 21 V. Omelyanenko, P. Kopeckova, C. Gentry, and J. Kopecek. Targetable HPMA copolymer-adriamycin conjugates. Recognition, internalization, and subcellular fate. *J. Controlled Release* **53**: 25-37 (1998).
- 22 P. Chytil, T. Etrych, C. Konak, M. Sirova, T. Mrkvan, J. Boucek, B. Rihova, and K. Ulbrich. New HPMA copolymer-based drug carriers with covalently bound hydrophobic substituents for solid tumour targeting. *J. Controlled Release* **127**: 121-130 (2008).
- 23 C. C. Lee, E. R. Gillies, M. E. Fox, S. J. Guillaudeu, J. M. J. Frechet, E. E. Dy, and F. C. Szoka. A single dose of doxorubicin-functionalized bow-tie dendrimer cures mice bearing C-26 colon carcinomas. *PNAS* **103**: 16649-16654 (2006).
- 24 H. R. Ihre, O. L. P. D. Jesus, J. Francis C. Szoka, and J. M. J. Frechet. Polyester Dendritic Systems for Drug Delivery Applications: Design, Synthesis, and Characterization. *Bioconjugate Chem.* **13**: 443-452 (2002).
- 25 D. Lu, X. Wen, J. Liang, Z. Gu, X. Zhang, and Y. Fan. A pH-sensitive nano drug delivery system derived from pullulan/doxorubicin conjugate. *J. Biomed. Mater. Res. B: Appl. Biomater.* (2008).
- 26 H. S. Yoo and T. G. Park. Biodegradable polymeric micelles composed of doxorubicin conjugated PLGA-PEG block copolymer. *J. Controlled Release* **70**: 63-70 (2001).
- 27 M. Yokoyama, S. Fukushima, R. Uehara, K. Okamoto, K. Kataoka, Y. Sakurai, and T. Okano. Characterization of physical entrapment and chemical conjugation of adriamycin in polymeric micelles and their design for in vivo delivery to a solid tumor. *J. Controlled Release* **50**: 79-92 (1998).

- 28 A. Mahmud, X.-B. Xiong, and A. Lavasanifar. Development of novel polymeric micellar drug conjugates and nano-containers with hydrolyzable core structure for doxorubicin delivery. *Eur. J. Pharm. Biopharm.* (2008).
- 29 J. H. Park, S. Lee, J.-H. Kim, K. Park, K. Kim, and I. C. Kwon. Polymeric nanomedicine for cancer therapy. *Prog. Polym. Sci.* **33**: 113-137 (2008).
- 30 R. Tong and J. Cheng. Anticancer Polymeric Nanomedicines. *Polym. Rev.* **47**: 345-381 (2007).
- 31 J. Khandare and T. Minko. Polymer-drug conjugates: Progress in polymeric prodrugs. *Prog. Polym. Sci.* **31**: 359-397 (2006).
- 32 K. Hoste, K. D. Winne, and E. Schacht. Polymeric prodrugs. *Int. J. Pharm.* **277**: 119-131 (2004).
- 33 H. Maeda, J. Wu, T. Sawa, Y. Matsumura, and K. Hori. Tumor vascular permeability and the EPR effect in macromolecular therapeutics: a review. *J. Controlled Release* **65**: 271-284 (2000).
- 34 G. Pasut and F. M. Veronese. Polymer-drug conjugation, recent achievements and general strategies. *Prog. Polym. Sci.* **32**: 933-961 (2007).
- 35 J. Djordjevic, M. Barch, and K. E. Uhrich. Polymeric Micelles Based on Amphiphilic Scorpion-like Macromolecules: Novel Carriers for Water-Insoluble Drugs. *Pharm. Res.* **22**: 24-32 (2005).
- 36 L. Tian, L. Yam, N. Zhou, H. Tat, and K. E. Uhrich. Amphiphilic Scorpion-like Macromolecules: Design, Synthesis, and Characterization. *Macromolecules* **37**: 538-543 (2004).
- 37 L. Tao and K. E. Uhrich. Novel amphiphilic macromolecules and their in vitro characterization as stabilized micellar drug delivery systems. *J. Colloid Interf. Sci.* **298**: 102-110 (2006).
- 38 J. Djordjevic, L. S. DelRosario, J. Wang, and K. E. Uhrich. Amphiphilic Scorpion-like Macromolecules as Micellar Nanocarriers. *J. Bioact. Compat. Polym.* **23**: 532-551 (2008).

- 39 K. Ulbrich, T. Etrych, P. Chytil, M. Jelinkova, and B. Rihova. HPMA copolymers with pH-controlled release of doxorubicin. In vitro cytotoxicity and in vivo antitumor activity. *J. Controlled Release* **87**: 33-47 (2003).
- 40 K. Ulbrich, T. Etrych, P. Chytil, M. Pechar, M. Jelinkova, and B. Rihova. Polymeric anticancer drugs with pH-controlled activation. *Int. J. Pharm.* **277**: 63-72 (2004).
- 41 R. Pola, M. Pechar, and K. Ulbrich. Polymer-Doxorubicin Conjugate with a Synthetic Peptide Ligand Targeted on Prostate Tumor. *J. Bioact. Compat. Polym.* **22**: 602-620 (2007).
- 42 H. S. Yoo, E. A. Lee, and T. G. Park. Doxorubicin-conjugated biodegradable polymeric micelles having acid-cleavable linkages. *J. Controlled Release* **82**: 17-27 (2002).
- 43 Y. Lee, S. Y. Park, H. Mok, and T. G. Park. Synthesis, Characterization, Antitumor Activity of Pluronic Mimicking Copolymer Micelles Conjugated with Doxorubicin via Acid-Cleavable Linkage. *Bioconjugate Chem.* **19**: 525-531 (2008).
- 44 M. Hruby, C. Konak, and K. Ulbrich. Polymeric micellar pH-sensitive drug delivery system for doxorubicin. *J. Controlled Release* **103**: 137-148 (2005).
- 45 Y. Bae, N. Nishiyama, S. Fukushima, H. Koyama, M. Yasuhiro, and K. Kataoka. Preparation and Biological Characterization of Polymeric Micelle Drug Carriers with Intracellular pH-Triggered Drug Release Property: Tumor Permeability, Controlled Subcellular Drug Distribution, and Enhanced in Vivo Antitumor Efficacy. *Bioconjugate Chem.* **16**: 122-130 (2005).
- 46 R. J. Christie and D. W. Grainger. Design strategies to improve soluble macromolecular delivery constructs. *Adv. Drug Delivery Rev.* **55**: 421-437 (2003).
- 47 T. Etrych, M. Jelinkova, B. Rihova, and K. Ulbrich. New HPMA copolymers containing doxorubicin bound via pH-sensitive linkage: synthesis and preliminary in vitro and in vivo biological properties. *J. Controlled Release* **73**: 89-102 (2001).
- 48 T. Etrych, P. Chytil, M. Jelinkova, B. Rihova, and K. Ulbrich. Synthesis of HPMA Copolymers Containing Doxorubicin Bound via a Hydrazone Linkage.

- Effect of Spacer on Drug Release and in vitro Cytotoxicity. *Macromol. Biosci.* **2**: 43-52 (2002).
- 49 T. K.-W. Lee, T. C.-M. Lau, and I. O.-L. Ng. Doxorubicin-induced apoptosis and chemosensitivity in hepatoma cell lines. *Cancer Chemother. Pharmacol.* **49**: 78-86 (2002).
- 50 A. V. Kabanov, E. V. Batrakova, and V. Y. Alakhov. Pluronic block copolymers as novel polymer therapeutics for drug and gene delivery. *Journal of Controlled Release* **82**: 189-212 (2002).
- 51 E. V. Batrakova, H. Han, D. W. Miller, and A. Kabanov. Effects of Pluronic P85 unimers and micelles on drug permeability in polarized BBMEC and Caco-2 cells. *Pharm. Res.* **15**: 1525-1531 (1998).
- 52 J. Szebeni, F. M. Muggia, and C. R. Alving. Complement Activation by Cremophor EL as a Possible Contributor to Hypersensitivity to Paclitaxel: an *In Vitro* Study. *J. National Cancer Institute* **90**: 300-306 (1998).
- 53 H. S. Yoo, K. H. Lee, J. E. Oh, and T. G. Park. In vitro and in vivo anti-tumor activities of nanoparticles based on doxorubicin-PLGA conjugates. *J. Controlled Release* **68**: 419-431 (2000).
- 54 T. Toyo'oka. *Modern Derivatization Methods for Separation Sciences*, John Wiley and Sons, New York, 1999.
- 55 O. Hovorka, M. St'astny, T. Etrych, V. Subr, J. Strohalm, K. Ulbrich, and B. Rihova. Differences in the intracellular fate of free and polymer-bound doxorubicin. *J. Controlled Release* **80**: 101-117 (2002).
- 56 K. K. Karukstis, E. H. Z. Thompson, J. A. Whiles, and R. J. Rosenfeld. Deciphering the fluorescence signature of daunomycin and doxorubicin. *Biophysical Chem.* **73**: 249-263 (1998).
- 57 M.-C. Jones and J.-C. Leroux. Polymeric micelles - a new generation of colloidal drug carriers. *Eur. J. Pharm. Biopharm.* **48**: 101-111 (1999).

- 58 Y. Hu, Y. Ding, D. Ding, M. Sun, L. Zhang, X. Jiang, and C. Yang. Hollow Chitosan/Poly(acrylic acid) Nanospheres as Drug Carriers. *Biomacromolecules* **8**: (2007).
- 59 A. David, P. Kopeckova, T. Minko, A. Rubinstein, and J. Kopecek. Design of a multivalent galactoside ligand for selective targeting of HPMA copolymer-doxorubicin conjugates to human colon cancer cells. *Eur. J. Cancer* **40**: 148-157 (2004).
- 60 B. Demirdirek. MS Thesis, *Department of Chemistry and Chemical Biology*, Rutgers University, Piscataway, 2009.

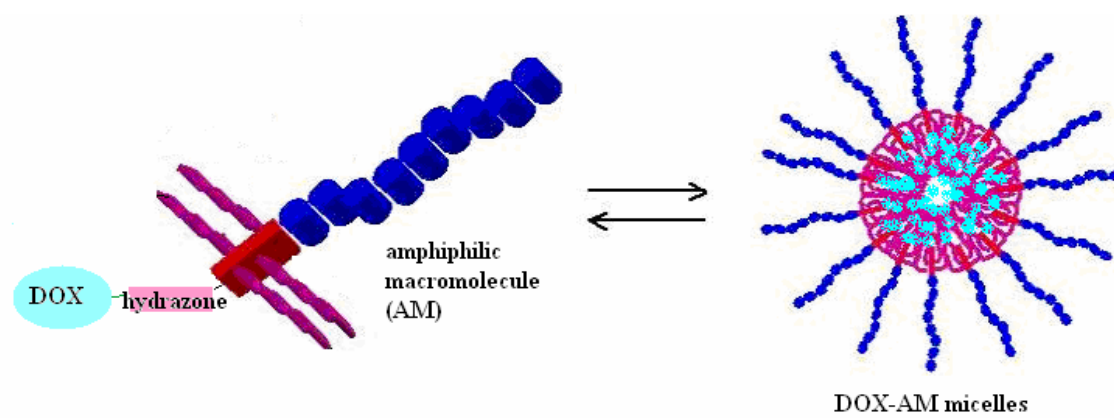


Figure 4-1. Cartoon of micelle formation from DOX-AM conjugates (cartoon adapted from Jelena Djordjevic with modification).

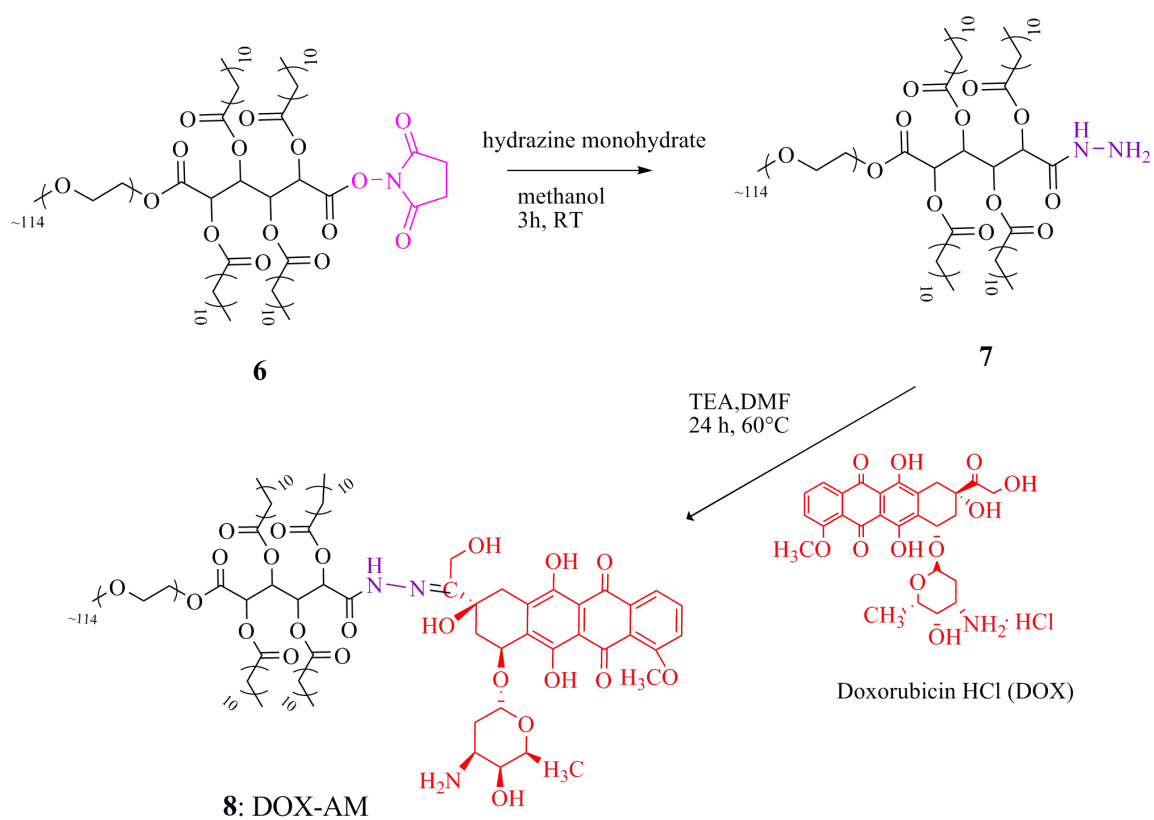


Figure 4-2. Preparation of DOX-AM conjugate (8).

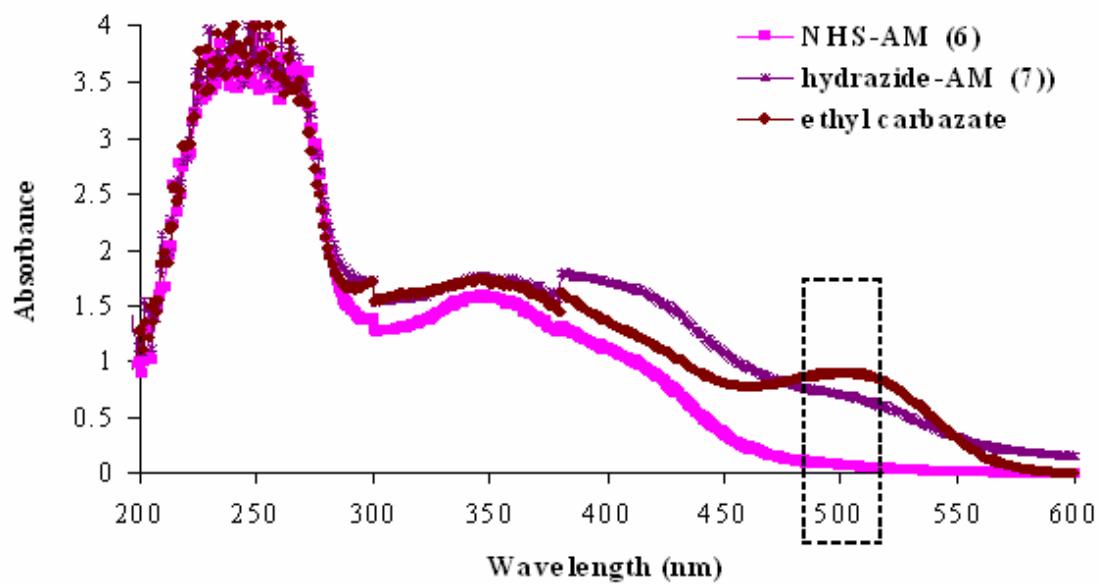


Figure 4-3. Detection of hydrazide end groups by TNBSA assay ($\lambda = 500$ nm).

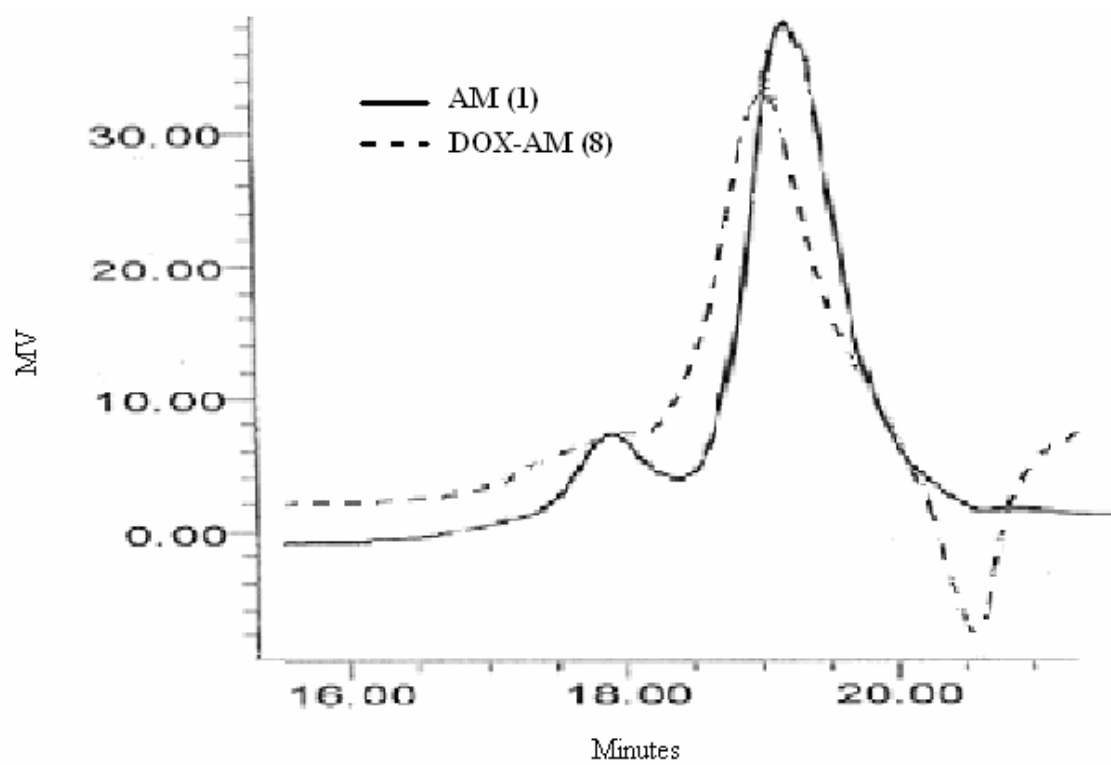


Figure 4-4. Gel permeation chromatograms before and after DOX conjugation.

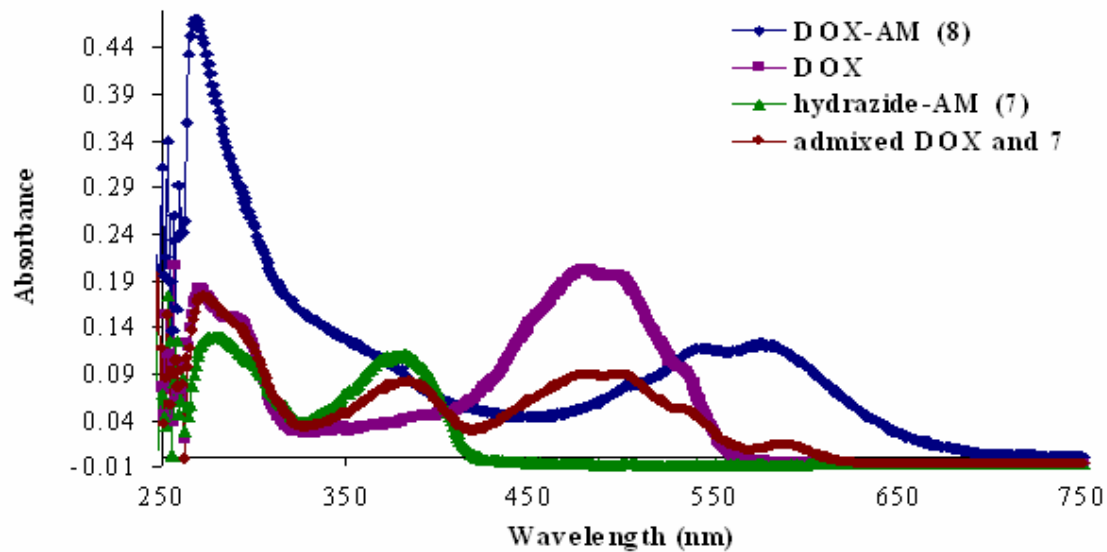


Figure 4-5. UV-vis absorption spectra of hydrazide-AM (7), free DOX, DOX conjugated to AM (8), and DOX physically admixed with AM.

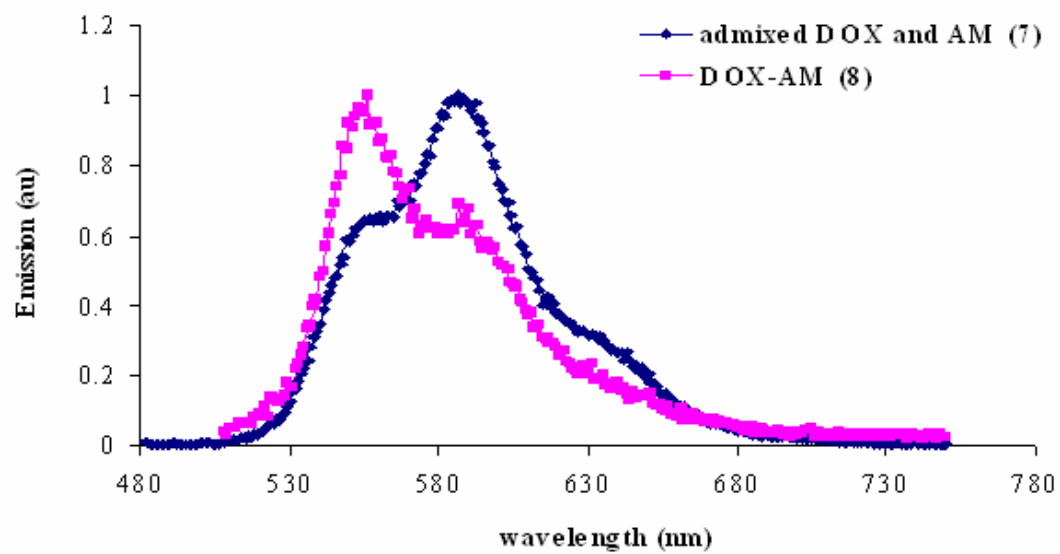


Figure 4-6. Spectrofluorophotometric spectra of DOX admixed with AM (7) (free drug) and DOX-AM (conjugated drug) (8).

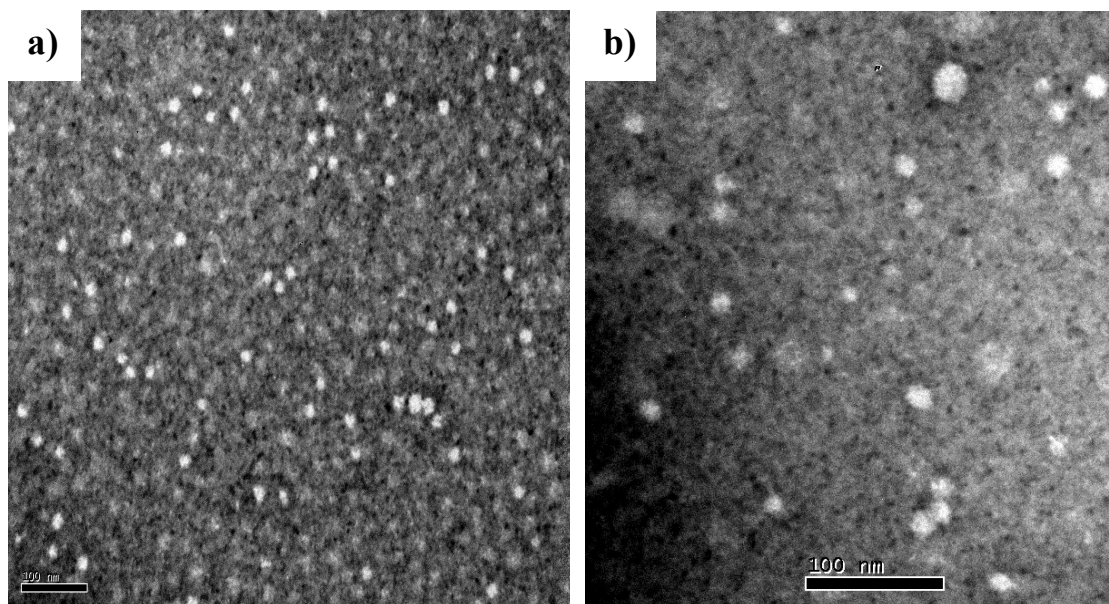


Figure 4-7. TEM images showing spherical morphology of (a) mixed micelles assembled from aqueous solutions (100 μM) of DOX-AM conjugates (**8**) containing unconjugated AMs and (b) AM micelles with physically encapsulated and chemically bound DOX.

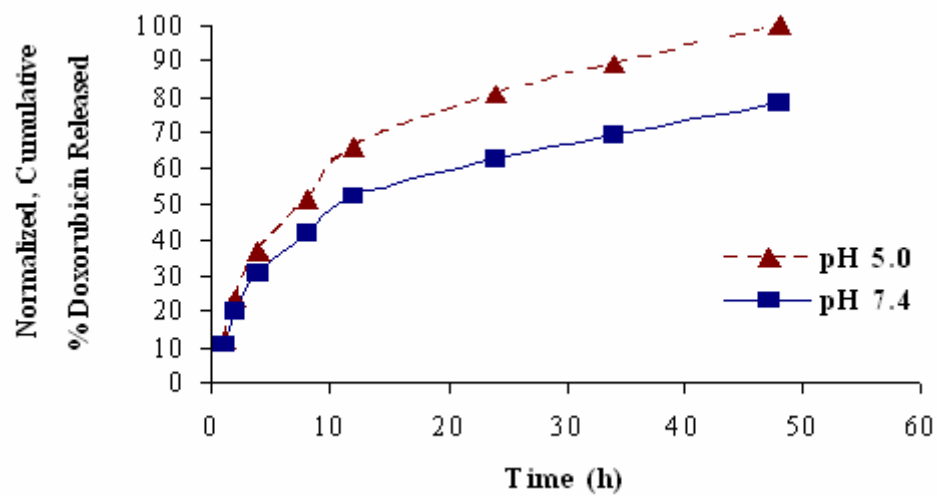


Figure 4-8. *In vitro* DOX release from DOX-AM (**8**) at 37°C (pH 7.4 and 5.0) [60].

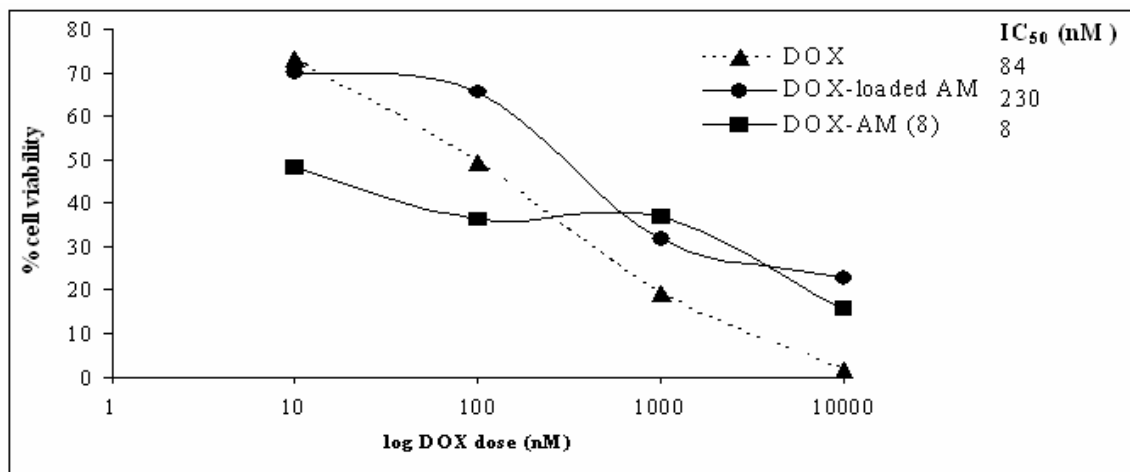


Figure 4-9. *In vitro* cytotoxicity of DOX in AM-based micelles against HepG2 cells after 72 h incubation. (S.D. < 1%)

Table 4-1. DOX encapsulation capability and micellar sizes of AM-based micelles.

Sample	DOX content (Total Wt %)	DLS Size (nm)
DOX-loaded AM (physically encapsulated DOX)	12 ± 1	16 ± 1
DOX-AM (chemically bound DOX)	6 ± 1	30 ± 1
DOX-loaded DOX-AScM (physically and chemically bound DOX)	24 ± 1	18 ± 2

Chapter 5

PHYSICALLY ENCAPSULATED AND CHEMICALLY BOUND CAMPTOTHECIN IN AMPHIPHILIC MACROMOLECULES-BASED MICELLES

5.1. Introduction

Camptothecin (CPT) is a plant alkaloid extracted from *Camptotheca acuminata* with potent antitumor activity to lung, ovarian, breast, pancreas, and stomach cancers, but with high water insolubility ($\log P = 1.74$) [1]. CPT exists in active lactone form in acidic environment but converted to inactive carboxylate form in neutral and basic conditions [2-4] (**Figure 5-1**). The inactive CPT carboxylate binds strongly with human serum albumin (HSA), further increasing CPT conversion to the inactive form [5, 6]. CPT lactone ring-opening results in decreased cellular interactions: cell membrane binding, membrane diffusibility, and intrinsic potency against target Topoisomerase I, each contribute to reduced activity [1]. Development of delivery systems such as micelles [7-13], liposomes [14], nanoparticles [15-17], and microspheres [18, 19] focus on both increasing CPT solubility and preserving CPT lactone bioactivity.

In this study, micelles assembled from amphiphilic macromolecules (AMs) were evaluated as CPT nanocarriers because they have good micellar characteristics: *i*) small size (~20 nm) [20], *ii*) low CMC values near 10^{-7} M [21, 22], *iii*) non-cytotoxicity [21] and *iv*) high encapsulation potential [21]. Poly(ethylene glycol) (PEG) chains reportedly decrease protein adsorption, opsonization and macrophageal uptake in blood circulation

[23-25]; likewise PEG shells of AM micelles are also expected to decrease HSA adsorption and reduce CPT binding.

Further, CPT was chemically conjugated *via* glycine linker to the AMs with the aim of enhancing CPT solubility and lactone stability. CPT-polymer conjugation offers several advantages compared to free CPT, mainly lactone stabilization [26] as the lactone functional group is essential for CPT-topoisomerase I inhibition [1, 27]. Furthermore, enhanced pharmacokinetics of CPT in blood and tumor, increased tumor localization, and increased bioavailability was previously described with CPT-polymer conjugates *in vivo* [28-31]. However, the CPT-AM micelles offer additional advantages as CPT nanocarriers from their nano sizes [20], biodegradability [32] and “protective” micellar core-shell structure [33] wherein the drug is possibly protected from hydrolysis and HSA adsorption with encapsulation. For illustration, **Figure 5-2a** shows a cartoon of CPT-AM micelles assembled from the conjugates, with CPT chemically bound in the micellar core. The glycine linker reportedly enhanced % CPT-polymer conjugation [31, 34-36] and was therefore used as CPT-AM linker.

The AM micelles were first evaluated by comparing physical encapsulation of CPT and chemical conjugation of CPT in terms of CPT content and *in vitro* cytotoxicity against human colon cancer cells. Then, AM micelles with both physically encapsulated and chemically bound CPT were analyzed. Finally, AM micelles were compared with known polymeric delivery systems: *i*) Pluronic P85, a commonly used micellar drug and

gene carrier [37, 38], and *ii*) Cremophor EL, a commonly used emulsifying agent for hydrophobic compounds [39].

5.2. Materials

(*S*)-(+)-Camptothecin (CPT), tBoc-glycine-OH, N,N'-dicyclohexylcarbodiimide (DCC) (1 M solution in dichloromethane), N-hydroxysuccinimide (NHS), diisopropylethylamine (DIPEA), N,N'-dimethylformamide (DMF), dimethylsulfoxide (DMSO), trifluoroacetic acid (TFA), human serum albumin (HSA), phosphate citrate buffer tablets (PCB), and phosphate buffered saline (PBS) tablets were purchased from Sigma-Aldrich (St. Louis, MO). Human colorectal adenocarcinoma cells (HT-29), McCoy's 5A medium, fetal bovine serum (FBS), penicillin-streptomycin solution, trypsin-EDTA solution (1x), MTT cell proliferation assay were purchased from American Tissue Culture Collection (ATCC) (Manassas, VA). Spectra/Por dialysis tubings (molecular weight cut-off MWCO 3.5 kDa), acrylic equilibrium dialysis cells (Scienceware, Bel-Art Products, NJ), Corning cell culture flasks, BD Falcon graduated tubes, BD Falcon 96-well plates, serological pipets, Vistalab reagent reservoirs, Corning surfactant-free cellulose acetate (SFCA) bottle-top filters, Whatman (PTFE, PVDF and regenerated cellulose) syringe filters, Dulbecco's PBS were purchased from Fisher Scientific (Atlanta, GA). Pluronic P85 and Cremophor EL were kindly given by BASF Corporation (Mount Olive, NJ). NHS-activated amphiphilic macromolecules (NHS-AM, **6**) and 4-(dimethylamino)pyridinium-*p*-toluene-sulfonate (DPTS) were synthesized according to previously reported methods [22, 40].

5.3. Methods

5.3.1. Cell Culture: Human Colon Cancer Cells

Human colorectal adenocarcinoma cells (HT-29) were grown in McCoy's 5A medium supplemented with 10% FBS and 1% penicillin-streptomycin solution. The cells were grown at 37 °C, 5% CO₂ for 2 passages prior to the 3-(4,5-dimethylthiazol-2-yl)-2,5-diphenyl-2H-tetrazolium bromide (MTT) experiment. The cells growing in the exponential phase, were seeded (10,000 cells/well) in 96-well plates for the MTT assay.

5.3.2. Chemical Characterization of CPT-AM

For NMR measurements in a 300 MHz Varian spectrometer, samples (10-50 mg) were dissolved in 0.75 mL DMSO-d₆ with TMS as the internal standard.

Gel permeation chromatography (GPC) was used for molecular weight determination, using a Waters 510 HPLC system equipped with a 5 µm gel precolumn, two PL columns with pore size 10³-10⁵ Å (Polymer Labs, UK), and Waters 410 Differential Refractometer. DMF containing 0.1 % v/v trifluoroacetic acid was used as the mobile phase (flow rate 0.8 mL/min) and solvent for sample dissolution (~10 mg/mL). The samples were filtered through a 0.45 µm PTFE filters before injection. Polystyrene standards (Polymer Labs, UK) were used to calibrate the GPC system and obtain number-average molecular weights and polydispersity indices (PDI).

UV-vis spectrophotometry was used to detect CPT lactone stabilization in aqueous solutions at physiological conditions (37 °C, pH 7.4) for 24 h. Samples were dissolved in

PBS (pH 7.4), incubated at 37 °C for 24 h, and then analyzed for slight peak shift in CPT spectra (355 nm to 363 nm), considered a sign of CPT lactone hydrolysis as reported by Zhao *et al.* [26]

5.3.3. Synthesis of CPT-AM (10)

CPT-glycine (**9**) was prepared similar to methods reported by Cheng *et al.* [34] and Paranjpe *et al.* [36], except that DPTS was used instead of DMAP and DMF was added to the reaction mixture (**Figure 5-3**). t-Boc-glycine-OH (0.26 g, 1.5 mmol) was dissolved in 50 mL anhydrous CH₂Cl₂ at room temperature. The reaction flask was immersed in an ice bath and the other reagents were sequentially added: DPTS (0.092 g), CPT (0.17 g, 0.48 mmol), DMF (0.5 mL) and DCC (1.5 mmol, 1.5 mL of 1 M in CH₂Cl₂). The reaction mixture was warmed to room temperature and continuously stirred for 24 h under argon. After removal of the by-product N,N-dicyclohexylurea (DCU) by suction filtration, the filtrate was washed with cold 0.1 N HCl (25 mL), 50:50 brine:water (3 x 25 mL), and dried over anhydrous MgSO₄. Solvents were removed by rotary evaporation and the tBoc-glycine-CPT product recrystallized in 10 mL methanol as light yellow solids (65 % yield) that displayed similar ¹H NMR (DMSO-d₆) as reported by Cheng *et al.* [34]. tBoc-glycine-CPT was deprotected by dissolving in 20 mL CH₂Cl₂ and adding 20 mL TFA dropwise at 0 °C. The reaction mixture was stirred for 1 h and the solvents removed by rotary evaporation. CPT-glycine (**9**) was recrystallized from diethyl ether (90 % yield) and displayed similar ¹H NMR (DMSO-d₆) as reported by Cheng *et al.* [34]. Furthermore, 406 (M + H) was found from ESI/MS (m/z) analysis as reported likewise by Cheng *et al.* [34] and Paranjpe *et al.* [36].

CPT-glycine (**9**) (0.48 g, 1.2 mmol) was dissolved in 15:1 v/v CH₂Cl₂:DMSO, to which NHS-AM (**6**) (0.70 g, 0.12 mmol) dissolved in 5 mL CH₂Cl₂, and DIPEA (0.45 mL) was added. The reaction proceeded for 5 h at room temperature, then the reaction mixture was washed with 50:50 brine:water (25 mL) and dried over anhydrous MgSO₄. After solvent removal by rotary evaporation, the CPT-AM conjugate (**10**) was isolated by precipitation in 1:10 CH₂Cl₂:diethyl ether, centrifugation (Zettrifugen, Germany) (3000 RPM, 5 min), decantation, and air-drying. CPT-AM conjugates (**10**) were re-dissolved in 500 mL HPLC-grade water, filtered through 0.22 μm SFCA filters, and lyophilized for 72 h (-50 °C, 65 x 10⁻³ mbar, FreeZone 4.5 Benchtop and Console Freeze Dry System, Labconco, Kansas City, Missouri) to obtain a yellowish white solid (0.64 g, 54 % yield). ¹H NMR (DMSO-d₆): δ 7.7 – 8.8 (m, 5H, **CPT** Ar-H), 7.29 (s, 1H, **CPT** Ar-H), 5.59 (s, 2H, **CPT** CH₂O), 5.50 (m, 2H, **AM** CH), 5.35 (s, 2H, **CPT** CH₂N), 5.10 (m, 2H, **AM** CH), 4.19 (m, **glycine** CH₂) 3.50 (m, ~0.4 kHz, **AM** CH₂O), 2.40 (t, 4H, **AM** CH₂), 2.30 (t, 4H, **AM** CH₂), 2.20 (m, 2H, **CPT** CH₂), 1.59 (m, 4H, **AM** CH₂), 1.51 (m, 4H, **AM** CH₂), 1.21 (m, 64H, **AM** CH₂), 0.95 (t, 3H, **CPT** CH₃), 0.89 (t, 12H, **AM** CH₃). GPC: Mw: 7100; PDI: 1.0.

5.3.4. Size Analysis of CPT-AM Micelles

Dynamic light scattering (DLS) measurements were used to determine particle size distribution. CPT-AM micelles were analyzed in a Malvern Instruments Zetasizer Nano ZS-90 instrument (Southboro, MA) using automeasurement method (12 runs) at a 90° scattering angle and 37 °C reading temperature. CPT-AM micelles were prepared in

deionized water (1 mg/mL) or PBS buffer (pH 7.4) and filtered using 0.22 μm poly(vinylidene fluoride) (PVDF) syringe filters prior to DLS analysis.

Transmission electron microscopy (TEM) was used to determine CPT-AM micellar morphology using a JEM-100 CXII (Jeol Ltd, Japan) microscope. Lyophilized solids of CPT-AM were dissolved (1 mg/mL) in HPLC-grade water, filtered using 0.22 μm PVDF syringe filters and incubated for 20 min at 37 °C. A drop of the sample was placed onto a wax dental plate (Electron Microscopy Sciences, Hatfield, PA). A UV-activated circular copper grid (Formvar/carbon film, Electron Microscopy Sciences, Hatfield, PA) was placed on the sample drop for 1 min. Then the grid was removed, tapped with filter paper to remove excess water, and negatively stained using 1 % aqueous solution of uranyl acetate (Electron Microscopy Sciences, Hatfield, PA) for 1 min. The grid was air dried for 20 min and then analyzed under the electron microscope at 80 kV. Analysis of the samples was done in triplicate.

5.3.5. CPT-Loading by Solvent Evaporation

This experiment was done with the assistance of Bahar Demirdirek.

Camptothecin was loaded into polymeric micelles following the method reported by Watanabe *et al.* [41] with modifications and illustrated in **Figure 5-2b**. Using 1:13 w/w drug:polymer ratio, CPT and polymer sample were dissolved in a solution of methanol:chloroform (4:1 v/v). Solvents were then removed by rotary evaporation at room temperature. PBS (pH 7.4) was added to a 1.5 mg/mL final polymer concentration. The solution was sonicated at room temperature for 5 min, then stirred for 4 h at 37 °C.

The resulting mixtures were filtered through 0.45 μm PVDF syringe filters. CPT concentration was determined from UV-vis absorption (Beckman DU520 UV/VIS Spectrophotometer, Fullerton, CA) at 365 nm as reported elsewhere [9, 41] after dilution with dimethylsulfoxide (DMSO) (9:1). Encapsulation experiments were performed in triplicate. Weight % loading, encapsulated efficiency (%) and solubility enhancement (-fold) were calculated as follows:

$$\text{Weight \% loading} = \frac{\text{Concentration of free drug detected}}{\text{Concentration of polymer}} \times 100$$

$$\text{Solubility enhancement (-fold)} = \frac{\text{Solubility of drug in presence of polymer}}{\text{Solubility of free drug}} \times 100$$

5.3.6. Impact of HSA on CPT Release *In Vitro*

This experiment was done with the assistance of Bahar Demirdirek.

Polymer samples in PBS were mixed with 4% w/v HSA in PBS. Aliquots (5 mL) of the resulting solutions were placed in donor cells of acrylic equilibrium dialysis cells separated from receptor cells by regenerated cellulose acetate membranes (Spectra/Por flat sheets MWCO 3.5 kDa). In the receptor cells, 5 mL PBS pH 7.4 were added. The dialysis cells were incubated at 37 °C for 48 h. At specific time intervals, receptor cell solutions (5 mL) were withdrawn and replaced with fresh buffer (5 mL). CPT quantification was performed by UV-vis spectrophotometry at λ 365 nm. Experiments were performed in triplicate.

5.3.7. Cytotoxicity Assay against Human Liver Cancer Cells

Using the MTT cell proliferation assay, polymer samples were compared with CPT control against human colorectal carcinoma cells (HT-29). The MTT assay is based on the reduction of 3-(4,5-dimethylthiazol-2-yl)-2,5-diphenyl-2H-tetrazolium bromide (MTT) reagent to formazan salts by mitochondrial dehydrogenase enzymes in viable cells (ATCC, Manassas, VA). Briefly, HT-29 cells (10,000 cells/well) were plated in 96-well tissue culture plates and incubated at 37°C, 5% CO₂ for 24 h. Samples were dissolved in sterile Dulbecco's PBS (DPBS) to a final CPT concentration of 10 µM. Samples were then serially diluted in complete media to obtain up to 1 nM CPT concentration range. Sample solutions were added to the wells and incubated for an additional 72 h. MTT reagent was then added to the wells, incubated for 3 h, followed by addition of the MTT detergent and incubation for 2 h at room temperature in the dark. Absorbance values were obtained from the EL808 Ultra Microplate Reader (Biotek Instruments, Winooski, VT) at 570 nm using the KC Junior program. Four replicates were performed at each concentration for each sample.

5.3.8. Analysis of CPT-loaded CPT-AM Micelles

*CPT-AM micelles were loaded with additional CPT using the solvent evaporation method described in **Section 5.3.4** and performed by Bahar Demirdirek. The resulting micelles consisted of both physically encapsulated and chemically bound drug and referred to as CPT-loaded CPT-AM micelles.* Using the same methods described in **Section 5.3.7**, the *in vitro* cytotoxicity of CPT-loaded CPT-AM micelles were analyzed against HT-29 cells.

5.3.9. Comparison with Pluronic P85 and Cremophor EL

This experiment was done with the assistance of Bahar Demirdirek.

The two polymeric drug delivery systems, Pluronic P85 and Cremophor EL, were loaded with CPT using the methods described in **Section 5.3.4**. The resulting samples were used to study HSA impact on CPT release using methods described in **Section 5.3.6**. CPT-loaded polymer solutions were also analyzed for *in vitro* cytotoxicity against HT-29 cells using the methods described in **Section 5.3.7**.

5.3.10. Statistical Analysis of Data

Data are reported as means \pm standard deviation. Differences among the % cell viability results for CPT \pm polymer samples were compared using univariate analysis of variance (ANOVA) and Tukey and LSD post hoc tests for multiple comparisons at each CPT concentration using SPSS for Windows v.16 (SPSS, Chicago, IL), with the level of significance set at $\alpha = 0.05$.

5.4. Results and Discussion

5.4.1. Synthesis and Characterization of CPT-AM Conjugates

The lactone ring is crucial in CPT anticancer activity [27, 42], thus the CPT delivery system should strive to preserve the bioactive CPT lactone. Polymeric micelles reportedly preserve the CPT lactone *in vitro* via physical encapsulation [9, 10], whereas CPT-polymer conjugation by acylation of CPT effectively stabilized CPT lactone *in vivo* [30, 31]. The CPT-AM micelles delivery system combines these two advantages: CPT

acylation to AM unimers can stabilize the lactone ring, while the core-shell structure of CPT-AM micelles can protect the drug from hydrolysis. CPT-AM conjugates (**10**) were synthesized from NHS-AM (**6**) and CPT-glycine (**9**) shown in **Figure 5-3**.

CPT lactone stabilization is achieved upon acylation of carbon 20 of CPT [26]. CPT was successfully acylated to AMs *via* glycine linker at the carbon 20 as shown by the almost complete disappearance of CPT hydroxyl proton peak at 6.5 ppm in the ^1H NMR spectrum. Furthermore, UV analysis showed similar spectra of CPT-AM to CPT lactone after incubation for 24 h at 37 °C, pH 7.4 (**Figure 5-4**). In contrast, free CPT showed a slight λ shift (355 to 363 nm) after incubation in the same conditions, indicative of CPT lactone hydrolysis to carboxylate as similarly reported by Zhao *et al.* [26] (**Figure 5-4**).

CPT-AM conjugation was further confirmed from GPC analysis; AM alone has a retention time of 20.25 min whereas CPT-AM has a retention time of 19.75 min. UV analysis determined the extent of CPT conjugation to AMs; based on CPT calibration curves, 54 % of the NHS-activated AM (**6**) was converted to CPT-AM conjugates (**10**). Given that these structurally similar polymers could not be readily separated, subsequent experiments utilized the ~ 50:50 AM:CPT-AM mixture.

5.4.2. Size Analysis of CPT-AM Micelles

CPT-AMs assembled into mixed micelles of 22 nm sizes as detected by dynamic light scattering analysis. TEM images (**Figure 5-5**) showed spherical morphologies and micellar sizes of CPT-AM mixed micelles similar to the DLS data (1 mg/mL).

5.4.3. CPT Content in AM micelles vs CPT-AM micelles

CPT was physically encapsulated in the AM micelles using the solvent evaporation method. Comparison of CPT content (**Table 5-1**) showed higher CPT chemically bound in CPT-AM (**10**) micelles (3 wt %) compared to CPT physically encapsulated in AM micelles (0.4 wt %). Likewise, CPT solubility enhancement was higher in CPT-AM micelles (300-fold) compared to AM micelles (2-fold).

5.4.4. Impact of HSA on CPT Release *In Vitro*

In the presence of HSA, a decrease in CPT *in vitro* release is an indirect indication of the inactive carboxylate form of CPT binding to HSA, as only the active lactone of CPT can pass through the dialysis membrane. Using a method demonstrated by Opanasopit *et al.*, [9] the amount of free CPT was drastically lowered in the presence of HSA (6 %), indicating a significant amount of binding to HSA (**Figure 5-6**). Notably, the AM-based polymeric micelles “protected” the CPT, likely due to decreased protein adsorption by the PEG micellar shells. For example, CPT loaded in AM micelles showed 64 % CPT release at 48 h; CPT release decreased to 23 % in the presence of HSA (**Figure 5-6**) indicating a difference of 41% released CPT. In contrast, the difference in released CPT was 94% if the drug alone was in the presence of HSA. Slower CPT release from the CPT-AM micelles compared to CPT-loaded AM micelles was observed due to slow ester hydrolysis at experimental conditions (pH 7.4, 37 °C, 48 h).

5.4.5. *In Vitro* Cytotoxicity Assay

The human colorectal carcinoma cell line (HT-29) is commonly used to assess efficacy of CPT-based delivery systems in cell proliferation assays *in vitro* [34, 43] and in animal xenografts *in vivo* [35, 43, 44]. The MTT assay of CPT-loaded AM micelles and CPT-AM micelles showed comparable cytotoxicities to CPT alone against HT-29 cells (**Figure 5-7**). Increased CPT-AM cytotoxicity was expected against HT-29 cells compared to CPT alone, as increased CPT solubility and CPT lactone stability was observed in CPT-AMs. Furthermore, upon endocytosis of CPT-AMs in HT-29 cells, esterases in lysosomes were expected to hydrolyze ester bonds between CPT and glycine-AM, resulting to CPT release from CPT-AMs. However, inside HT-29 cells, ester hydrolysis might have been too slow even in acidic pH ~ 5.0 of the lysosomes. In addition, the esterases might have been hindered by the AM micellar shells, as CPT-AMs possibly existed as micelles inside the lysosomes and the ester bonds were not accessible for esterase activity.

5.4.6. Analysis of CPT-loaded CPT-AM Micelles

AM micelles with both physically encapsulated and chemically bound CPT were analyzed for CPT content and *in vitro* cytotoxicity against HT-29 cells. Although AM micelles with both physically encapsulated and chemically bound CPT had higher CPT content (10 wt % total CPT) than CPT-loaded AM micelles (0.4 wt %) or CPT-AM micelles (3 wt %), equivalent CPT concentrations in the different micelle systems were used against HT-29 cells in the MTT assay. Results showed the cytotoxicity of all AM-based micelles were comparable ($IC_{50} \sim 2.6$ nM) to each other.

5.4.7. Comparison with Pluronic P85 and Cremophor EL

CPT loaded in AM micelles (0.4 wt %) were comparable to Pluronic P85 (0.7 wt %) and Cremophor EL (0.6 wt %). HSA impact on CPT release from the polymeric carriers was also analyzed. In the presence of HSA, the decrease in CPT release from Pluronic P85 (49 %), Cremophor EL (35 %) and AM (41 %) were lowered compared to free CPT (94 %). These results indicate the drug “protecting” capability of the polymeric drug carriers. MTT assay data showed comparable cytotoxicity of CPT-loaded polymeric carriers with the CPT-loaded AM-based micelles ($IC_{50} \sim 2.6$ nM).

5.5. Conclusions

Chemical conjugation of CPT to AM micelles showed higher CPT solubility enhancement and slower CPT release compared to physical encapsulation. The polymeric drug carriers, Pluronic P85 and Cremophor EL, showed comparable CPT loadings to AM micelles (but lower than the CPT-AM micelles), similar drug “protecting” capabilities in reducing HSA impact on CPT release, and comparable cytotoxicity against HT-29 cells.

5.6. References

- 1 A. Hatefi and B. Amsden. Camptothecin delivery methods. *Pharmaceutical Research* **19**: 1389-1399 (2002).
- 2 I. Chourpa, J.-M. Millot, G. D. Sockalingum, J.-F. Riou, and M. Manfait. Kinetics of lactone hydrolysis in antitumor drugs of camptothecin series as studied by fluorescence spectroscopy. *Biochimica et Biophysica Acta* **1379**: 353-366 (1998).
- 3 K. Akimoto, A. Kawai, and K. Ohya. Kinetic Studies of the Hydrolysis and Lactonization of Camptothecin and Its Derivatives, CPT-11 and SN-38, in Aqueous Solution. *Chem. Pharm. Bull.* **42**: 2135-2138 (1994).
- 4 J. Fassberg and V. J. Stella. A kinetic and mechanistic study of the hydrolysis of camptothecin and some analogues. *Journal of Pharmaceutical Sciences* **81**: 676-684 (1992).
- 5 T. G. Burke and Z. Mi. The Structural Basis of Camptothecin Interactions with Human Serum Albumin: Impact on Drug Stability. *Journal of Medicinal Chemistry* **37**: 40-46 (1994).
- 6 Z. Mi and T. G. Burke. Marked interspecies variations concerning the interactions of camptothecin with serum albumins: a frequency-domain fluorescence spectroscopy study. *Biochemistry* **33**: 12540-12545 (1994).
- 7 P. Opanasopit, M. Yokoyama, M. Watanabe, K. Kawano, Y. Maitani, and T. Okano. Block Copolymer Design for Camptothecin Incorporation into Polymeric Micelles for Passive Tumor Targeting. *Pharmaceutical Research* **21**: 2001-2008 (2004).
- 8 P. Opanasopit, T. Ngawhirunpat, T. Rojanarata, C. Choochottiros, and S. Chirachanchai. Camptothecin-incorporating N-phthaloylchitosan-g-mPEG self-assembly micellar system: Effect of degree of deacetylation. *Colloids and Surfaces B: Biointerfaces* **60**: 117-124 (2007).
- 9 P. Opanasopit, M. Yokoyama, M. Watanabe, K. Kawano, Y. Maitani, and T. Okano. Influence of serum and albumins from different species on stability of camptothecin-loaded micelles. *Journal of Controlled Release* **104**: 313-321 (2005).

- 10 R. Barreiro-Iglesias, L. Bromberg, M. Temchenko, T. A. Hatton, A. Concheiro, and C. Alvarez-Lorenzo. Solubilization and stabilization of camptothecin in micellar solutions of pluronic-g-poly(acrylic acid) copolymers. *Journal of Controlled Release* **97**: 537-549 (2004).
- 11 T. Yamamoto, M. Yokoyama, P. Opanasopit, A. Hayama, K. Kawano, and Y. Maitani. What are the determining factors for stable drug incorporation into polymeric micelle carriers? Consideration on physical and chemical characters of the micelle inner core. *Journal of Controlled Release* **123**: 11-18 (2007).
- 12 L. Li and Y. B. Tan. Preparation and properties of mixed micelles made of Pluronic polymer and PEG-PE. *Journal of Colloid and Interface Science* **317**: 326-331 (2008).
- 13 K. Kawano, M. Watanabe, T. Yamamoto, M. Yokoyama, P. Opanasopit, T. Okano, and Y. Maitani. Enhanced antitumor effect of camptothecin loaded in long-circulating polymeric micelles. *Journal of Controlled Release* **112**: 329-332 (2006).
- 14 M. Watanabe, K. Kawano, K. Toma, Y. Hattori, and Y. Maitani. In vivo antitumor activity of camptothecin incorporated in liposomes formulated with an artificial lipid and human serum albumin. *Journal of Controlled Release* **127**: 231-238 (2008).
- 15 L. Zhang, Y. Hu, X. Jiang, C. Yang, W. Lu, and H. H. Yang. Camptothecin derivative-loaded poly(caprolactone-co-lactide)-b-PEG-b-poly(caprolactone-co-lactide) nanoparticles and their biodistribution in mice. *Journal of Controlled Release* **96**: 135-148 (2004).
- 16 K. H. Min, K. Park, Y.-S. Kim, S. M. Bae, S. Lee, H. G. Jo, R.-W. Park, I.-S. Kim, S. Y. Jeong, K. Kim, and I. C. Kwon. Hydrophobically modified glycol chitosan nanoparticles-encapsulated camptothecin enhance the drug stability and tumor targeting in cancer therapy. *Journal of Controlled Release* **127**: 208-218 (2008).
- 17 R. Kunii, H. Onishi, K.-i. Ueki, K.-i. Koyama, and Y. Machida. Particle characteristics and biodistribution of camptothecin-loaded PLA/(PEG-PPG-PEG) nanoparticles. *Drug Delivery* **15**: 3-10 (2008).

- 18 B. Ertl, P. Platzter, M. Wirth, and F. Gabor. Poly(D,L-lactic-co-glycolic acid) microspheres for sustained delivery and stabilization of camptothecin. *Journal of Controlled Release* **61**: 305-317 (1999).
- 19 A. Shenderova, T. G. Burke, and S. P. Schwendeman. The Acidic Microclimate in Poly(lactide-co-glycolide) Microspheres Stabilizes Camptothecins. *Pharmaceutical Research* **16**: 241-248 (1999).
- 20 L. Tao and K. E. Uhrich. Novel amphiphilic macromolecules and their in vitro characterization as stabilized micellar drug delivery systems. *Journal of Colloid and Interface Science* **298**: 102-110 (2006).
- 21 J. Djordjevic, M. Barch, and K. E. Uhrich. Polymeric micelles based on amphiphilic scorpion-like macromolecules: novel carriers for water insoluble drugs. *Pharmaceutical Research* **22**: 24-32 (2005).
- 22 L. Tian, L. Yam, N. Zhou, H. Tat, and K. E. Uhrich. Amphiphilic scorpion-like macromolecules: design, synthesis and characterization. *Macromolecules* **37**: 538-543 (2004).
- 23 R. Gref, M. Luck, P. Quellec, M. Marchand, E. Dellacherie, S. Harnisch, T. Blunk, and R. H. Muller. 'Stealth' corona-core nanoparticles surface modified by polyethylene glycol (PEG): influences of the corona (PEG chain length and surface density) and of the core composition on phagocytic uptake and plasma protein adsorption. *Colloids and Surfaces B: Biointerfaces* **18**: 301-313 (2000).
- 24 V. P. Torchilin. Structure and design of polymeric surfactant-based drug delivery systems. *Journal of Controlled Release* **73**: 137-172 (2001).
- 25 A. Vonarbourg, C. Passirani, P. Saulnier, and J. P. Benoit. Parameters influencing the stealthiness of colloidal drug delivery systems. *Biomaterials* **27**: 4356-4373 (2006).
- 26 H. Zhao, C. Lee, P. Sai, Y. Choe, M. Boro, A. Pendri, S. Guan, and R. B. Greenwald. 20-O-Acylcamptothecin derivatives: evidence for lactone stabilization. *Journal of Organic Chemistry* **65**: 4601-4606 (2000).
- 27 B. C. Giovanella, N. Harris, J. Mendoza, Z. Cao, J. Liehr, and J. S. Stehlin. Dependence of anticancer activity of camptothecins on maintaining their lactone function. *Annals of New York Academy of Sciences* **922**: 27-35 (2000).

- 28 R. Bhatt, P. d. Vries, J. Tulinsky, G. Bellamy, B. Baker, J. W. Singer, and P. Klein. Synthesis and in Vivo Antitumor Activity of Poly(L-glutamic acid) Conjugates of 20(S)-Camptothecin. *Journal of Medicinal Chemistry* **46**: 190-193 (2003).
- 29 V. R. Caiolfa, M. Zamai, A. Fiorino, E. Frigerio, C. Pellizzoni, R. d'Argy, A. Ghiglieri, M. G. Castelli, M. Farao, E. Pesenti, M. Gigli, F. Angelucci, and A. Suarato. Polymer-bound camptothecin: initial biodistribution and antitumour activity studies. *Journal of Controlled Release* **65**: 105-119 (2000).
- 30 D. Yu, P. Peng, S. S. Dharap, Y. Wang, M. Mehlig, P. Chandna, H. Zhao, D. Filpula, K. Yang, V. Borowski, G. Borchard, Z. Zhang, and T. Minko. Antitumor activity of poly(ethylene glycol)-camptothecin conjugate: the inhibition of tumor growth in vivo. *Journal of Controlled Release* **110**: 90-102 (2005).
- 31 J. W. Singer, R. Bhatt, J. Tulinsky, K. R. Buhler, E. Heasley, P. Klein, and P. de Vries. Water-soluble poly(L-glutamic acid)-gly-camptothecin conjugates enhance camptothecin stability and efficacy in vivo. *Journal of Controlled Release* **74**: 243-247 (2001).
- 32 B. Demirdirek and K. E. Uhrich. Biodegradation of amphiphilic macromolecules (manuscript in preparation).
- 33 J. Wang, L. S. d. Rosario, B. Demirdirek, A. Bae, and K. E. Uhrich. Comparison of PEG chain length and density on amphiphilic macromolecular nanocarriers: self-assembled and unimolecular micelles. *Acta Biomaterialia*.
- 34 J. Cheng, K. T. Khin, G. S. Jensen, A. Liu, and M. E. Davis. Synthesis of linear, β -cyclodextrin-based polymers and their camptothecin conjugates. *Bioconjugate Chemistry* **14**: 1007-1017 (2003).
- 35 C. D. Conover, R. B. Greenwald, A. Pendri, C. W. Gilbert, and K. L. Shum. Camptothecin delivery systems: enhanced efficacy and tumor accumulation of camptothecin following its conjugation to polyethylene glycol via a glycine linker. *Cancer Chemotherapeutics and Pharmacology* **42**: 407-414 (1998).
- 36 P. V. Paranjpe, Y. Chen, V. Kholodovych, W. Welsh, S. Stein, and P. J. Sinko. Tumor-targeted bioconjugate based delivery of camptothecin: design, synthesis and in vitro evaluation. *Journal of Controlled Release* **100**: 275-292 (2004).

- 37 A. V. Kabanov, E. V. Batrakova, and V. Y. Alakhov. Pluronic block copolymers as novel polymer therapeutics for drug and gene delivery. *Journal of Controlled Release* **82**: 189-212 (2002).
- 38 E. V. Batrakova, H. Han, D. W. Miller, and A. Kabanov. Effects of Pluronic P85 unimers and micelles on drug permeability in polarized BBMEC and Caco-2 cells. *Pharm. Res.* **15**: 1525-1531 (1998).
- 39 J. Szebeni, F. M. Muggia, and C. R. Alving. Complement Activation by Cremophor EL as a Possible Contributor to Hypersensitivity to Paclitaxel: an *In Vitro* Study. *Journal of National Cancer Institute* **90**: 300-306 (1998).
- 40 J. Djordjevic, L. S. del Rosario, J. Wang, and K. E. Uhrich. Amphiphilic scorpion-like macromolecules as micellar nanocarriers. *Journal of Bioactive and Compatible Polymers* **23**: 532-551 (2008).
- 41 M. Watanabe, K. Kawano, M. Yokoyama, P. Opanasopit, T. Okano, and Y. Maitani. Preparation of camptothecin-loaded polymeric micelles and evaluation of their incorporation and circulation stability. *International Journal of Pharmaceutics* **308**: 183-189 (2006).
- 42 L. F. Liu, S. D. Desai, T.-K. Li, Y. Mao, M. Sun, and S.-P. Sim. Mechanism of Action of Camptothecin. *Annals of New York Academy of Sciences* 1-10.
- 43 A. V. Yurkovetskiy, A. Hiller, S. Syed, M. Yin, X. M. Lu, A. J. Fischman, and M. I. Papisov. Synthesis of a Macromolecular Camptothecin Conjugate with Dual Phase Drug Release. *Molecular Pharmaceutics* **1**: 375-382 (2004).
- 44 R. B. Greenwald, A. Pendri, C. D. Conover, C. Lee, Y. H. Choe, C. Gilbert, A. Martinez, J. Xia, D. Wu, and M.-m. Hsue. Camptothecin-20-PEG Ester Transport Forms: the Effect of Spacer Groups on Antitumor Activity. *Bioorganic and Medicinal Chemistry* **6**: 551-562 (1998).

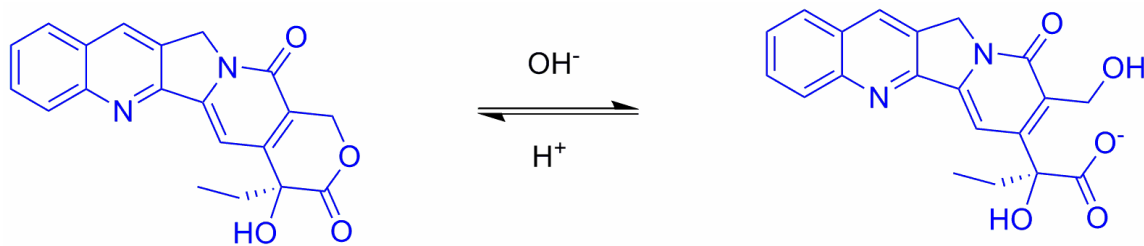


Figure 5-1. Chemical structures of CPT lactone (left) and CPT carboxylate (right) [29]

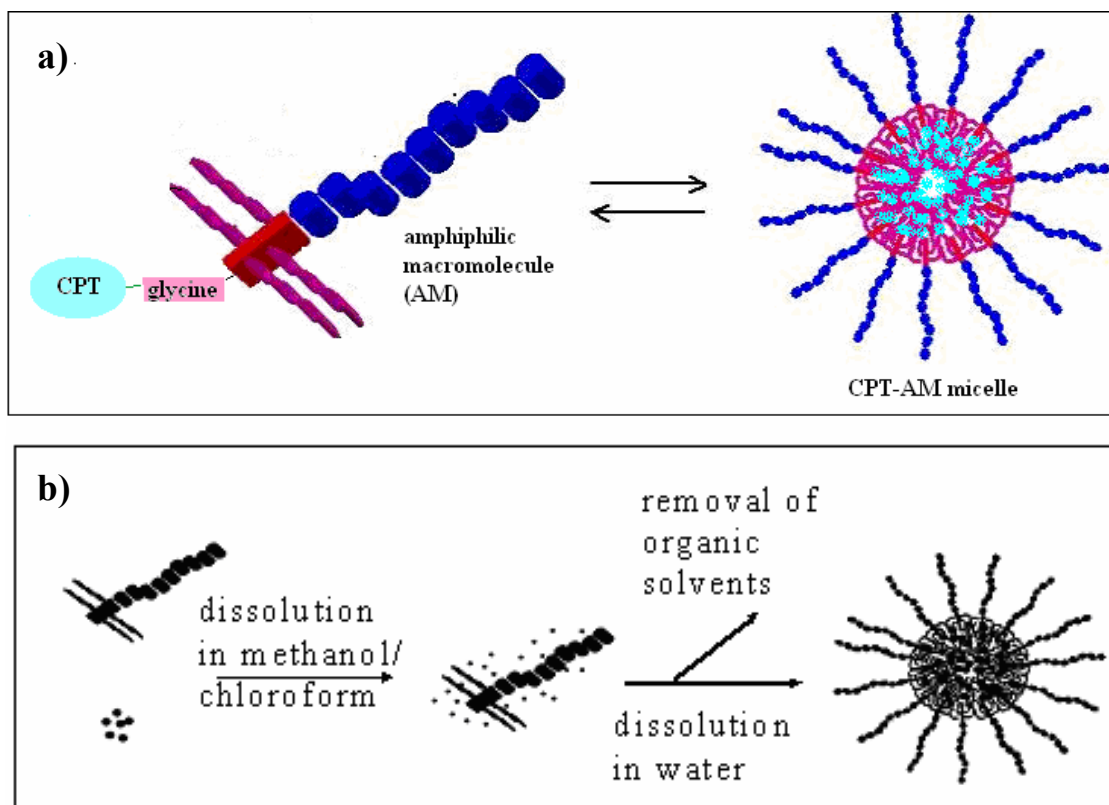


Figure 5-2. Cartoons of micelle assembly: (a) from CPT-AM conjugates (**10**) (CPT chemical conjugation); and (b) CPT loading in AM micelles by solvent evaporation (CPT physical encapsulation). Cartoons adapted from Jelena Djordjevic with modifications.

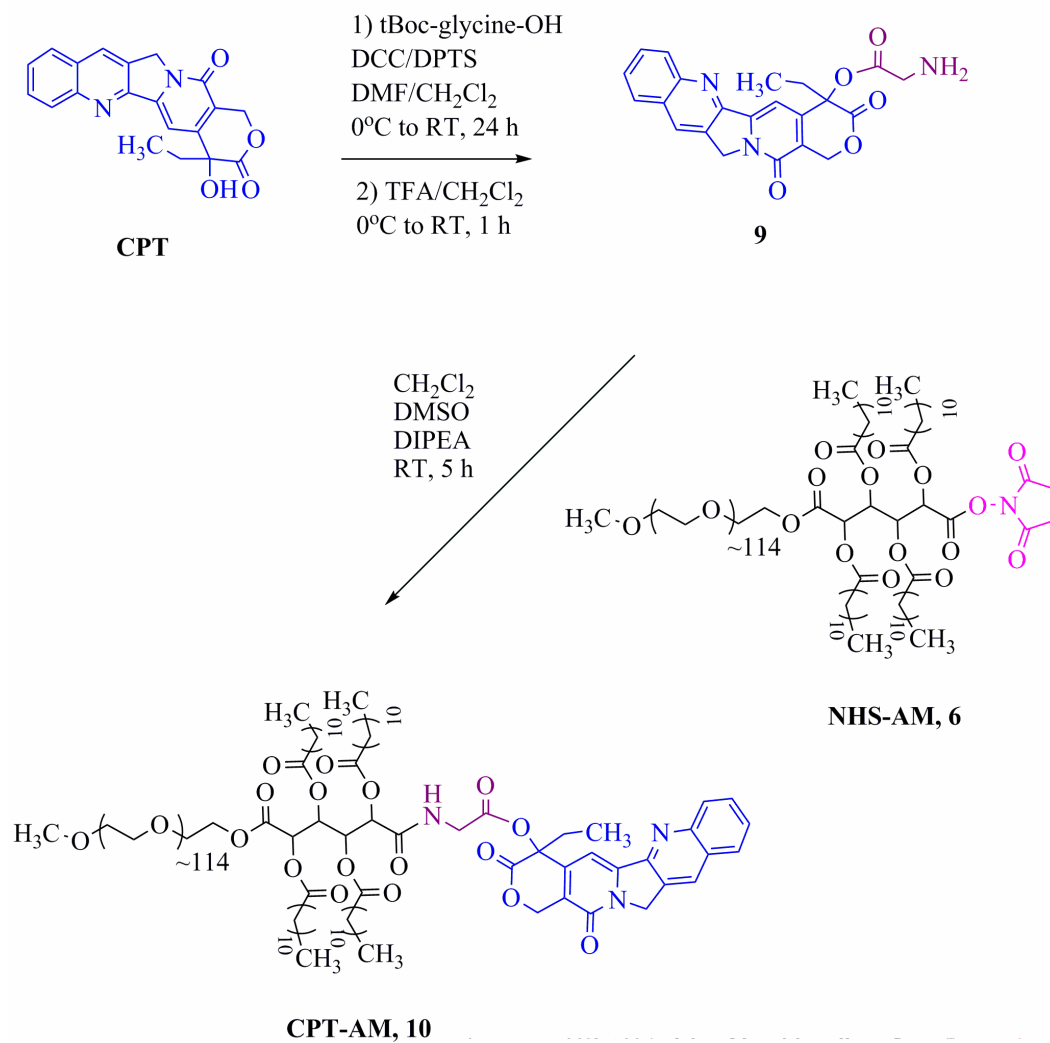


Figure 5-3. Synthesis of CPT-AM conjugates (**10**).

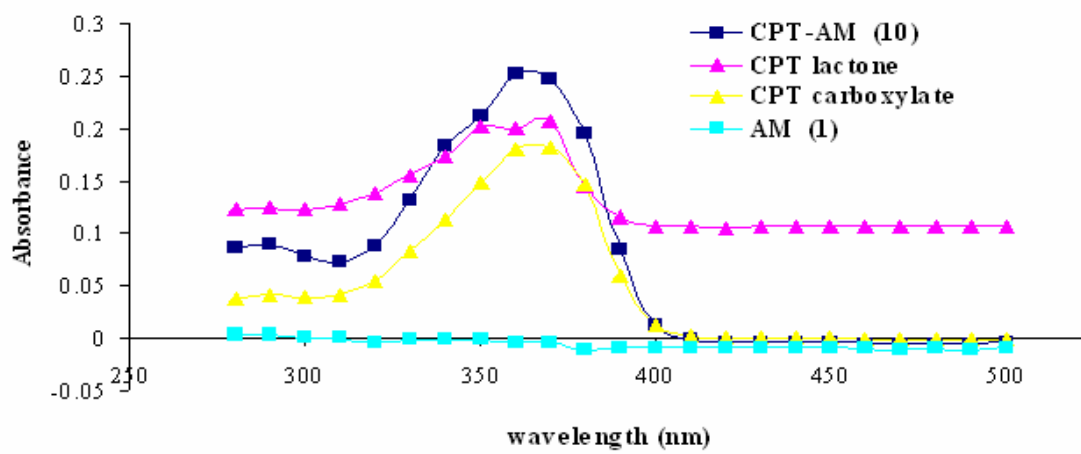


Figure 5-4. UV spectra of CPT derivatives and AM alone (1).

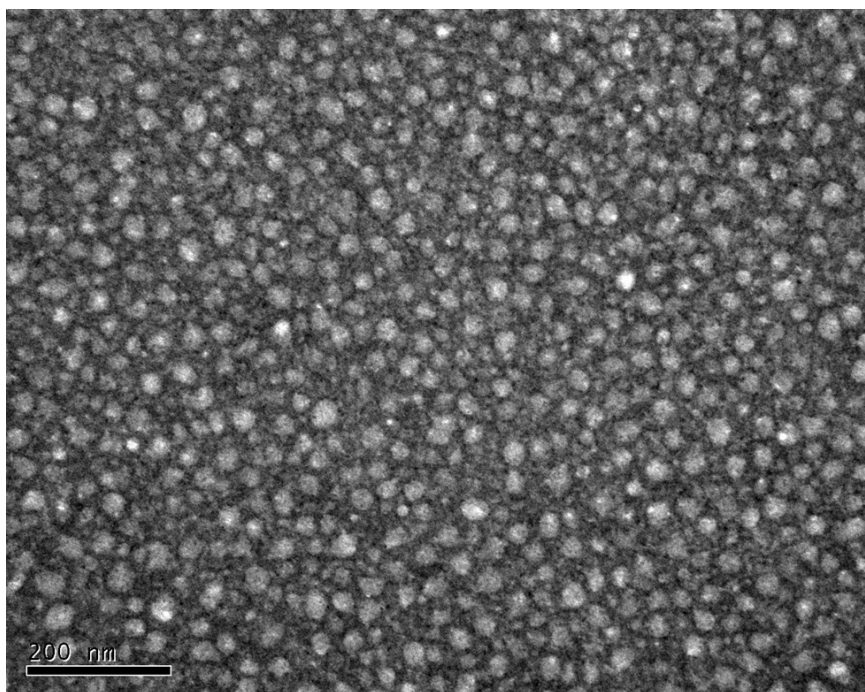


Figure 5-5. Transmission electron micrograph of CPT-AM (10)/AM mixed micelles in water (1 mg/mL) negatively stained with 1% uranyl acetate.

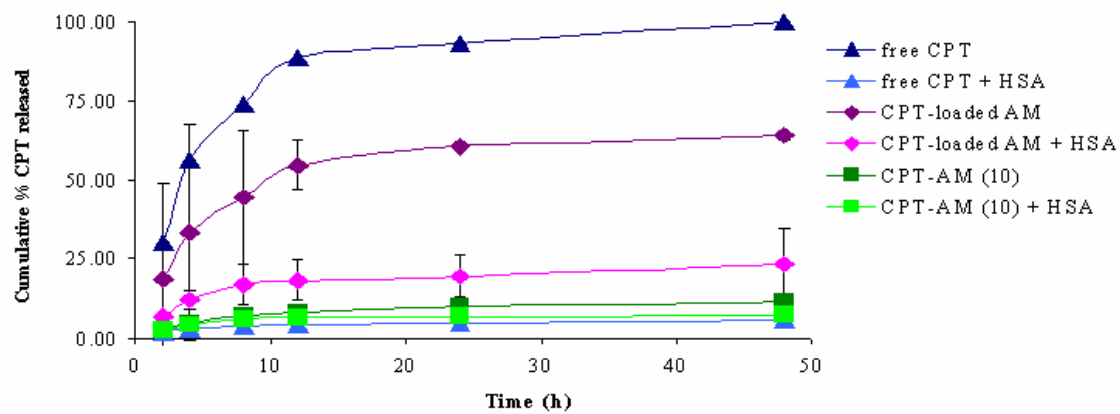


Figure.5-6. Impact of HSA on CPT release from AM-based micelles.

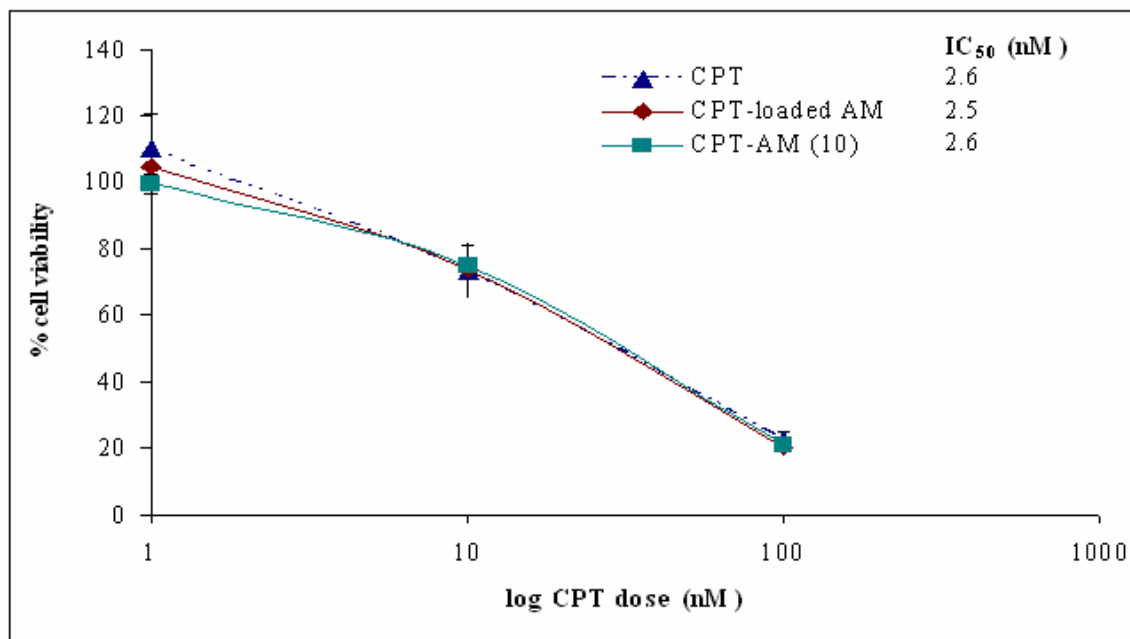


Figure 5-7. *In vitro* cytotoxicity of CPT and CPT-carrier versions against HT-29 cells after 72 h incubation.

Table 5-1. CPT encapsulation capability and solubility enhancement of AM-based micelles.

Sample	CPT content (Wt %)	CPT Solubility Enhancement (-fold)
CPT-loaded AM (physically encapsulated CPT)	0.4 ± 0.08	2
CPT-AM (10) (chemically bound CPT)	3 ± 1	300

Chapter 6

CAMPTOTHECIN-CONJUGATED AMPHIPHILIC MACROMOLECULES: CPT-MUCIC-AM VS CPT-ALKYL-AM

6.1. Introduction

Camptothecin (CPT) conjugation to carboxylic end groups of polymer chain ends or side chains is usually performed *via* carbodiimide coupling reagents to prepare CPT-polymer conjugates [1-4]. Commonly used reagents include *N*-(3-dimethylaminopropyl)-*N*-ethylcarbodiimide (EDC) [1-3] and 4-(methylamino)-pyridine (DMAP) (as catalyst). Recently, CPT conjugation to functional aliphatic polyesters was reported *via* click cycloaddition chemistry [5]. Click chemistry, the reaction of copper(I)-catalyzed 1,2,3-triazole formation from azides and terminal acetylenes, is interesting due to its high conversion, complete specificity and biocompatibility of the reactants [6]. Applications of this click chemistry reaction was shown in the preparation of end-functionalized polymers [7], in preparation of novel conjugated polymers [8] and in functionalization of micelles and shell-crosslinked nanoparticles [9].

As outlined in Chapter 5, the lactone form of CPT is desirable for many reasons. In this chapter, CPT was chemically bound to amphiphilic macromolecules using both the carbodiimide coupling and click chemistry methods, with each method utilizing one site of attachment to the AM: the mucic acid carboxylic end or the functionalized acyl chain end (**Figure 6-1**). *N,N'*-dicyclohexylcarbodiimide (DCC) was used as the coupling agent as it consistently showed good yields in PEGylation reactions used to prepare AMs [10]. DCC was used to conjugate CPT to the mucic acid to form CPT-mucic-AM conjugates

(**Figure 11**); copper/sodium ascorbate reagents were used to conjugate CPT to the acyl side chains of the mucic acid backbone to yield CPT-alkyl-AM conjugates (**Figure 6-3**). The conjugates were then compared based on overall conjugation yield, HSA impact on CPT release, and micellar sizes *in vitro*. The CPT-conjugated forms were also compared to CPT physically encapsulated in AM micelles.

6.2. Materials

(*S*)-(+)-Camptothecin (CPT), 6-heptynoic acid, 4-dimethylamino-pyridine (DMAP), N,N'-dicyclohexylcarbodiimide (DCC) (1 M solution in dichloromethane), anhydrous N,N'-dimethylformamide (DMF), anhydrous dichloromethane (CH₂Cl₂), dimethylsulfoxide (DMSO), tetrahydrofuran (THF), copper sulfate pentahydrate (CuSO₄·5H₂O), sodium ascorbate, human serum albumin (HSA), and phosphate buffered saline (PBS) tablets were purchased from Sigma-Aldrich (St. Louis, MO). Spectra/Por regenerated cellulose membranes (flat sheets, molecular weight cut-off MWCO 3.5 kDa) and acrylic equilibrium dialysis cells (Scienceware, Bel-Art Products, NJ) were purchased from Fisher Scientific (Atlanta, GA). NHS-activated amphiphilic macromolecules (NHS-AM, **6**) and 4-(dimethylamino)pyridinium-*p*-toluene-sulfonate (DPTS) were synthesized according to previously reported methods [10, 11]. Azide-terminated amphiphilic macromolecules (**13**) were synthesized by Sarah Sparks.

6.3. Methods

6.3.1. Chemical Characterization of CPT-Mucic/Alkyl-AM Conjugates

For NMR measurements using a 300 MHz Varian spectrometer, samples (10-50 mg) were dissolved in 0.75 mL DMSO-d₆ with TMS as the internal standard. For IR measurements using an FT-IR spectrometer, samples (~10 mg) were dissolved in dichloromethane and placed dropwise onto KBr plates, and the solvent evaporated by air drying.

Gel permeation chromatography (GPC) was used for molecular weight determination, using a Waters Alliance Series 2695 Separations Module connected with Styragel® HR3 THF column (7.8 mm x 300 mm), and Waters RI Detector. THF was used as the eluent solvent (1 mL/min) and solvent for samples (~ 10 mg/mL) that were filtered through 0.22 µm PTFE syringe filters (Whatman, Clifton, NJ) prior to GPC injection. Narrow MW Waters PEG standards were used to calibrate the column.

UV-vis spectrophotometry was used to detect CPT lactone stabilization in aqueous solutions at physiological conditions (37 °C, pH 7.4) for 24 h. Samples were dissolved in PBS (pH 7.4), incubated at 37 °C for 24 h, and then analyzed for a peak shift in the CPT spectra (355 nm to 363 nm), considered a sign of CPT lactone hydrolysis as reported by Zhao *et al.* [12]

6.3.2. Preparation of CPT-Mucic-AM Conjugates by Direct Conjugation

Prior to further reaction, AM (**1**) was vacuum oven-dried overnight. AM (**1**) (0.50 g, 0.084 mmol) and DPTS (0.025 g) were dissolved in 3 mL anhydrous CH₂Cl₂. CPT (0.059 g, 0.17 mmol) was added, and the reaction flask capped and attached with an argon balloon. The remaining reagents were sequentially added *via* syringe: DMF (5 mL) and DCC (0.40 mL of 1 M in CH₂Cl₂, 0.40 mmol). The reaction mixture was continuously stirred for 48 h at room temperature under argon in the dark. After removal of the by-product N,N-dicyclohexylurea (DCU) by suction filtration (2x), the filtrate was washed with cold 0.1 N HCl (10 mL), 50:50 brine:water (2 x 10 mL), brine (3 x 20 mL) and dried over anhydrous MgSO₄. Solvent was removed by rotary evaporation and the CPT-mucic-AM conjugates (**11**) were precipitated in 10 volume excess diethyl ether (3x) and isolated by centrifugation (3500 RPM, 5 min) followed by decanting off supernatant. The isolated solids were redissolved in deionized water (~150 mL), syringe-filtered using 0.22 μm PVDF filters and lyophilized for 48 h (-50 °C, 65 x 10⁻³ mbar, FreeZone 4.5 Benchtop and Console Freeze Dry System, Labconco, Kansas City, Missouri) to obtain a white solid (0.26 g, 4 % yield). ¹H NMR (CDCl₃): δ 7.6 – 8.4 (m, 5H, **CPT** Ar-H), 7.20 (s, 1H, **CPT** Ar-H), 5.70 (m, 2H, **AM** CH), 5.52 (s, 2H, **CPT** CH₂-O), 5.35 (s, H, **CPT** CH₂-N), 5.20 (m, 2H, **AM** CH), 3.70 (m, ~0.4 kH, **AM** CH₂O), 2.50 (t, 4H, **AM** CH₂), 2.30 (t, 4H, **AM** CH₂), 1.65 (m, 4H, **AM** CH₂), 1.55 (m, 4H, **AM** CH₂), 1.30 (m, 64H, **AM** CH₂), 0.95 (t, 12H, **AM** CH₃). GPC: Mw: 5500; PDI: 1.2

6.3.3. Preparation of CPT-Alkyl-AM Conjugates by Click Chemistry

Alkyne-terminated CPT (**12**) was prepared by dissolving CPT (0.10 g, 0.30 mmol), 6-heptynoic acid (0.07 mL, $\rho = 1.004$ g/mL, 0.56 mmol) and DMAP (5.0 mg) in anhydrous CH_2Cl_2 (10 mL), then the reaction flask was capped and an argon balloon attached. The remaining reagents were added *via* syringe: DMF (1 mL) and DCC (1.1 mL of 1 M in CH_2Cl_2 , 1.1 mmol). The reaction mixture was stirred continuously for 50 h at room temperature in the dark. After removal of the by-product N,N-dicyclohexylurea (DCU) by suction filtration (2x), the solvent was removed by rotary evaporation. The solids were washed with diethyl ether to remove unreacted 6-heptynoic acid, and then suction filtered. The residue was washed with 50:50 brine:water (3 x 10 mL) and dried over anhydrous MgSO_4 . Solvent was removed by rotary evaporation to obtain alkyne-terminated CPT (**12**) as a yellow solid (0.048 g, 36 % yield). ^1H NMR (DMSO-d_6): δ 7.6 – 8.8 (m, 5H, **CPT** Ar-H), 7.09 (s, 1H, **CPT** Ar-H), 5.52 (s, 2H, **CPT** CH₂-O), 5.35 (s, H, **CPT** CH₂-N), 2.79 (t, 1H, **alkynyl** H), 2.60 (m, 2H, **heptynoyl** CH₂), 2.20 (m, 2H, **heptynoyl** CH₂), 2.10 (m, 2H, **CPT** CH₂), 1.70 (m, 2H, **heptynoyl** CH₂), 1.55 (m, 2H, **heptynoyl** CH₂), 0.90 (t, 3H, **CPT** CH₃). FT-IR (KBr, cm^{-1}): 2104 (alkynyl C-C).

Alkyne-terminated CPT (**12**) (0.048 g, 0.11 mmol) dissolved in 3 mL DMSO was added to the reaction mixture containing azide-terminated AM (**13**) (0.080 g, 0.013 mmol), copper sulfate pentahydrate (0.017 g, 0.069 mmol) and sodium ascorbate (0.028 g, 0.14 mmol) dissolved in 3 mL H_2O . The resulting mixture was stirred continuously for 48 h at room temperature in the dark. The reaction mixture was exhaustively dialyzed against 1:100 DMSO/ H_2O and then against H_2O to remove all other reagents, using

Spectra/Por dialysis membranes (MWCO 3.5 kDa). The solutions remaining in the dialysis bags were frozen and lyophilized for 48 h (-50 °C, 65×10^{-3} mbar, FreeZone 4.5 Benchtop and Console Freeze Dry System, Labconco, Kansas City, Missouri) to obtain CPT-alkyl-AM (**14**) as a whitish yellow solid (0.087 g, 83 % yield).

(Characterization of CPT-alkyl-AM (14) was done with the assistance of Sarah Sparks:

*$^1\text{H NMR}$ (CDCl_3): δ 7.6 – 8.4 (m, 5H, **CPT Ar-H**), 7.20 (s, 1H, **CPT Ar-H**), 5.70 (m, 2H, **AM CH**), 5.40 (m, 2H, **AM CH**), 5.30 (s, 4H, **CPT CH₂**), 3.65 (m, ~0.4 kHz, **AM CH₂O**), 2.50 (m, 2H, **heptynoyl CH₂**), 2.30 (m, 2H, **heptynoyl CH₂**), 2.20 (m, 2H, **CPT CH₂**), 1.90 (t, 4H, **AM CH₂**), 1.55 (m, 12H, **AM CH₂**), 1.25 (t, 4H, **AM CH₂**), 0.95 (t, 3H, **CPT CH₃**). GPC: M_w : 6300; PDI: 1.2)*

6.3.4. Impact of HSA on CPT Release *In Vitro*

CPT-AM conjugates dissolved in PBS were mixed with 4% w/v HSA in PBS. Aliquots (5 mL) of the resulting solutions were placed in donor cells of acrylic equilibrium dialysis cells separated from receptor cells by regenerated cellulose acetate membranes (Spectra/Por flat sheets MWCO 3.5 kDa). In the receptor cells, 5 mL PBS pH 7.4 were added. The dialysis cells were incubated at 37 °C for 48 h. At specific time intervals, receptor cell solutions (5 mL) were withdrawn and replaced with fresh buffer (5 mL). Quantification of CPT release was performed by UV-vis spectrophotometry at λ 365 nm. Experiments were performed in triplicate.

6.3.5. Impact of HSA on CPT-Mucic/Alkyl-AM Micellar Sizes *In Vitro*

Dynamic light scattering (DLS) measurements were used to determine particle size distribution of CPT-mucic/alkyl-AM micelles mixed with 4% w/v HSA in PBS. Samples were analyzed using a Malvern Instruments Zetasizer Nano ZS-90 instrument (Southboro, MA) set at automeasurement method (12 runs) at a 90° scattering angle and 37 °C reading temperature. Samples were filtered using 0.22 µm poly(vinylidene fluoride) (PVDF) syringe filters prior to DLS analysis.

6.4. Results and Discussion

6.4.1. Synthesis and Characterization of CPT-Mucic/Alkyl-AM Conjugates

As discussed in Chapter 5, the lactone ring of CPT is crucial in its anticancer activity [13, 14]. The CPT delivery system should preserve the bioactive CPT lactone until reaching the target site. In polymer-CPT conjugation, CPT lactone stabilization is typically achieved upon acylation of carbon 20 of CPT [12]. In this chapter, CPT was acylated to AMs *via* two methods: *i*) mucic acid carboxylic group, or *ii*) functionalized alkyl side chains of AM (**Figure 6-1**).

Preparation of CPT-mucic-AM (**11**) was done by carbodiimide coupling reaction (**Figure 6-2**) with no prior modification of polymer nor drug. CPT conjugation was observed from GPC analysis, with an increase of MW from 5300 Da to 5500 Da, using PEG calibration standards. UV analysis was used to determine the extent of CPT conjugation to AMs. Based on CPT calibration curves, only 4 % of the AM (**1**) was converted to CPT-mucic-AM (**11**) likely due to the steric hindrance of mucic acid

carboxylic end groups. As AM (**1**) and CPT-mucic-AM (**11**) were structurally similar polymers and could not be readily separated, subsequent experiments utilized the ~ 96:4 AM:CPT-mucic-AM mixture.

Alkyne-terminated CPT (**12**) was first prepared and then reacted with azide-terminated AM (**13**) to obtain CPT-alkyl-AM (**14**) by click chemistry (**Figure 6-3**). Evidence of CPT alkyne-functionalization was observed with ^1H NMR analysis: *i*) appearance of alkynyl proton peak at 2.79 ppm, and *ii*) disappearance of the carboxylate proton of heptynoic acid at 12.0 ppm. Furthermore, the alkynyl carbon-carbon triple bond absorption peak appeared at 2104 cm^{-1} based on FT-IR analysis. CPT conjugation to AM was also observed from GPC analysis (*performed by Sarah Sparks*), with an increase of MW from 6000 Da to 6300 Da (indicating one CPT attached per AM) using PEG calibration standards. From UV analysis, 83 % of azide-functionalized AM (**13**) was converted to CPT-alkyl-AM (**14**). The higher coupling efficiency is likely due to the more flexible alkyl side chains of the mucic acid AM backbone compared to the carboxylate end group of mucic acid. As this conjugation consisted of only one CPT attached per AM, subsequent experiments explored the optimization of the click chemistry methods (different solvents, reagents, etc) to attach more CPT molecules.

UV analysis showed CPT lactone stabilization in both CPT-mucic-AM (**11**) (**Figure 6-4**) and CPT-alkyl-AM (**14**) (**Figure 6-5**) based on the similarity of their UV spectra with CPT lactone at the 325 – 400 nm region after incubation for 24 h at 37 °C, pH 7.4. In contrast, lactone hydrolysis of free CPT shows a slight λ shift (355 to 363 nm) after

incubation in the same conditions; this wavelength shift was similarly reported by Zhao *et al.* [12].

6.4.2. Impact of HSA on CPT Release *In Vitro*

Similar to the experiments in Chapter 5, a decrease in CPT *in vitro* release in the presence of HSA served as an indirect indication of CPT carboxylate binding to HSA [15]. For comparison, CPT-loaded AM micelles were prepared using the same method described in **Section 5.3.5**. Using the dialysis membrane method, HSA impact on CPT release (**Table 6-1**) was highest for CPT physically encapsulated in AMs, showing a 20 % decrease in CPT release. CPT that was chemically bound *via* the mucic acid (**11**) was less affected by HSA. This difference suggests the positive impact of CPT attachment on lactone stability: CPT attached to the micellar core is protected compared to CPT attached to the alkyl side chains, such that lactone hydrolysis and HSA binding is reduced.

6.4.3. Impact of HSA on CPT-Mucic/Alkyl-AM Micellar Sizes *In Vitro*

Interactions of drug carriers with serum proteins influence their *in vivo* fate as systemic drug delivery systems [16]. Yet the presence of PEG stabilizes the micellar interface [17] and decreases protein adsorption to the carrier [16-18]. In this chapter, HSA adsorption to AM-based micelles was also analyzed by dynamic light scattering. A reduction in micellar sizes of AM-based micelles was observed (**Table 6-2**) regardless of CPT loading method (physically encapsulated *vs* chemically bound). This data shows that although HSA impact on CPT *in vitro* release was reduced, the stability of AM-based

micelles in the presence of biological components (e.g. in plasma or blood) requires further evaluation (see **FUTURE WORK**).

6.5. Conclusions

CPT conjugation (4 %) *via* the mucic acid carboxylate end groups was sterically hindered. In contrast, higher CPT conjugation was achieved (83 %) *via* the flexible alkyl chains (**Figure 6-1**). Dialysis experiments showed that CPT attachment correlates with the influence of HSA: CPT attached to the micellar core are less influenced by HSA than CPT attached to the alkyl chain ends. The highest HSA impact was on physically encapsulated CPT. From DLS analysis, however, HSA reduced the micellar sizes by more than half, suggesting instability of the AM-based micelles. Further studies are necessary to understand these observations.

6.6. References

- 1 N.-J. Lee, S.-S. Ju, W.-J. Cho, S.-H. Kim, K.-T. Kang, T. Brady, and E. A. Theodorakis. Synthesis and biological activity of medium molecular weight polymers of camptothecin. *European Polymer Journal* **39**: 367-374 (2003).
- 2 J. J. Khandare, P. Chandna, Y. Wang, V. P. Pozharov, and T. Minko. Novel polymeric prodrug with multivalent components for cancer therapy. *The Journal of Pharmacology and Experimental Therapeutics* **317**: 929-937 (2006).
- 3 J. Cheng, K. T. Khin, G. S. Jensen, A. Liu, and M. E. Davis. Synthesis of linear, β -cyclodextrin-based polymers and their camptothecin conjugates. *Bioconjugate Chemistry* **14**: 1007-1017 (2003).
- 4 R. Bhatt, P. d. Vries, J. Tulinsky, G. Bellamy, B. Baker, J. W. Singer, and P. Klein. Synthesis and in Vivo Antitumor Activity of Poly(L-glutamic acid) Conjugates of 20(S)-Camptothecin. *Journal of Medicinal Chemistry* **46**: 190-193 (2003).
- 5 B. Parrish and T. Emrick. Soluble Camptothecin Derivatives Prepared by Click Cycloaddition Chemistry on Functional Aliphatic Polyesters. *Bioconjugate Chemistry* **18**: 263-267 (2007).
- 6 H. C. Kolb and K. B. Sharpless. The growing impact of click chemistry on drug discovery. *Drug Discovery Today* **8**: 1128-1137 (2003).
- 7 J.-F. Lutz, H. G. Borner, and K. Weichenhan. Combining atom transfer radical polymerization and click chemistry: a versatile method for the preparation of end-functional polymers. *Macromolecular Rapid Communications* **26**: 514-518 (2005).
- 8 D. J. V. C. v. Steenis, O. R. P. David, G. P. F. v. Strijdonck, J. H. v. Maarseveen, and J. N. H. Reek. Click-chemistry as an efficient synthetic tool for the preparation of novel conjugated polymers. *Chemical Communications* 4333-4335 (2005).
- 9 R. K. O'Reilly, M. J. Joralemon, K. L. Wooley, and C. J. Hawker. Functionalization of micelles and shell cross-linked nanoparticles using click chemistry. *Chem Materials* **17**: 5976-5988 (2005).

- 10 L. Tian, L. Yam, N. Zhou, H. Tat, and K. E. Uhrich. Amphiphilic scorpion-like macromolecules: design, synthesis and characterization. *Macromolecules* **37**: 538-543 (2004).
- 11 J. Djordjevic, L. S. del Rosario, J. Wang, and K. E. Uhrich. Amphiphilic scorpion-like macromolecules as micellar nanocarriers. *Journal of Bioactive and Compatible Polymers* **23**: 532-551 (2008).
- 12 H. Zhao, C. Lee, P. Sai, Y. Choe, M. Boro, A. Pendri, S. Guan, and R. B. Greenwald. 20-*O*-Acylcamptothecin derivatives: evidence for lactone stabilization. *Journal of Organic Chemistry* **65**: 4601-4606 (2000).
- 13 L. F. Liu, S. D. Desai, T.-K. Li, Y. Mao, M. Sun, and S.-P. Sim. Mechanism of Action of Camptothecin. *Annals of New York Academy of Sciences* 1-10.
- 14 B. C. Giovanella, N. Harris, J. Mendoza, Z. Cao, J. Liehr, and J. S. Stehlin. Dependence of anticancer activity of camptothecins on maintaining their lactone function. *Annals of New York Academy of Sciences* **922**: 27-35 (2000).
- 15 P. Opanasopit, M. Yokoyama, M. Watanabe, K. Kawano, Y. Maitani, and T. Okano. Influence of serum and albumins from different species on stability of camptothecin-loaded micelles. *Journal of Controlled Release* **104**: 313-321 (2005).
- 16 J. Liu, F. Zeng, and C. Allen. Influence of serum protein on polycarbonate-based copolymer micelles as a delivery system for a hydrophobic anti-cancer agent. *Journal of Controlled Release* **103**: 481-497 (2005).
- 17 A. Lavasanifar, J. Samuel, and G. S. Kwon. Poly(ethylene oxide)-*block*-poly(L-amino acid) micelles for drug delivery. *Advanced Drug Delivery Reviews* **54**: 169-190 (2002).
- 18 G. S. Kwon and K. Kataoka. Block copolymer micelles as long-circulating drug vehicles. *Advanced Drug Delivery Reviews* **16**: 295-309 (1995).

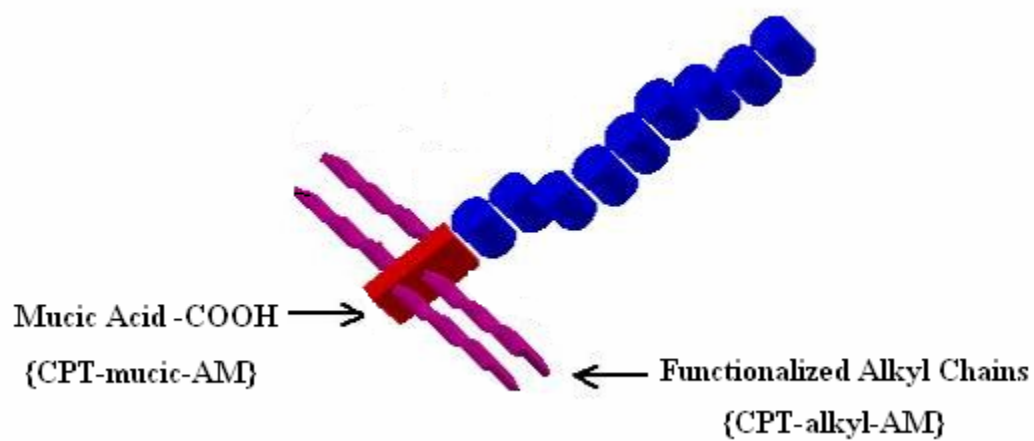


Figure 6-1. Cartoon of AM showing possible sites of CPT attachment (cartoon adapted from Jelena Djordjevic).

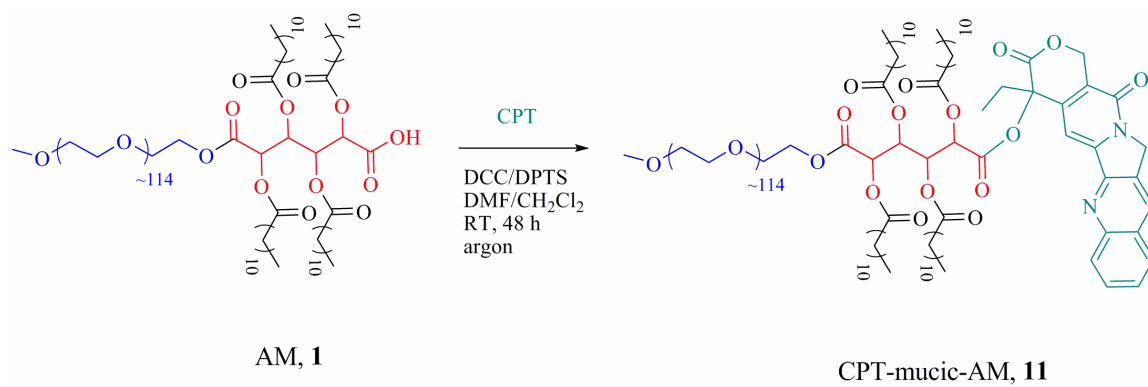


Figure 6-2. Preparation of CPT-mucic-AM (**11**).

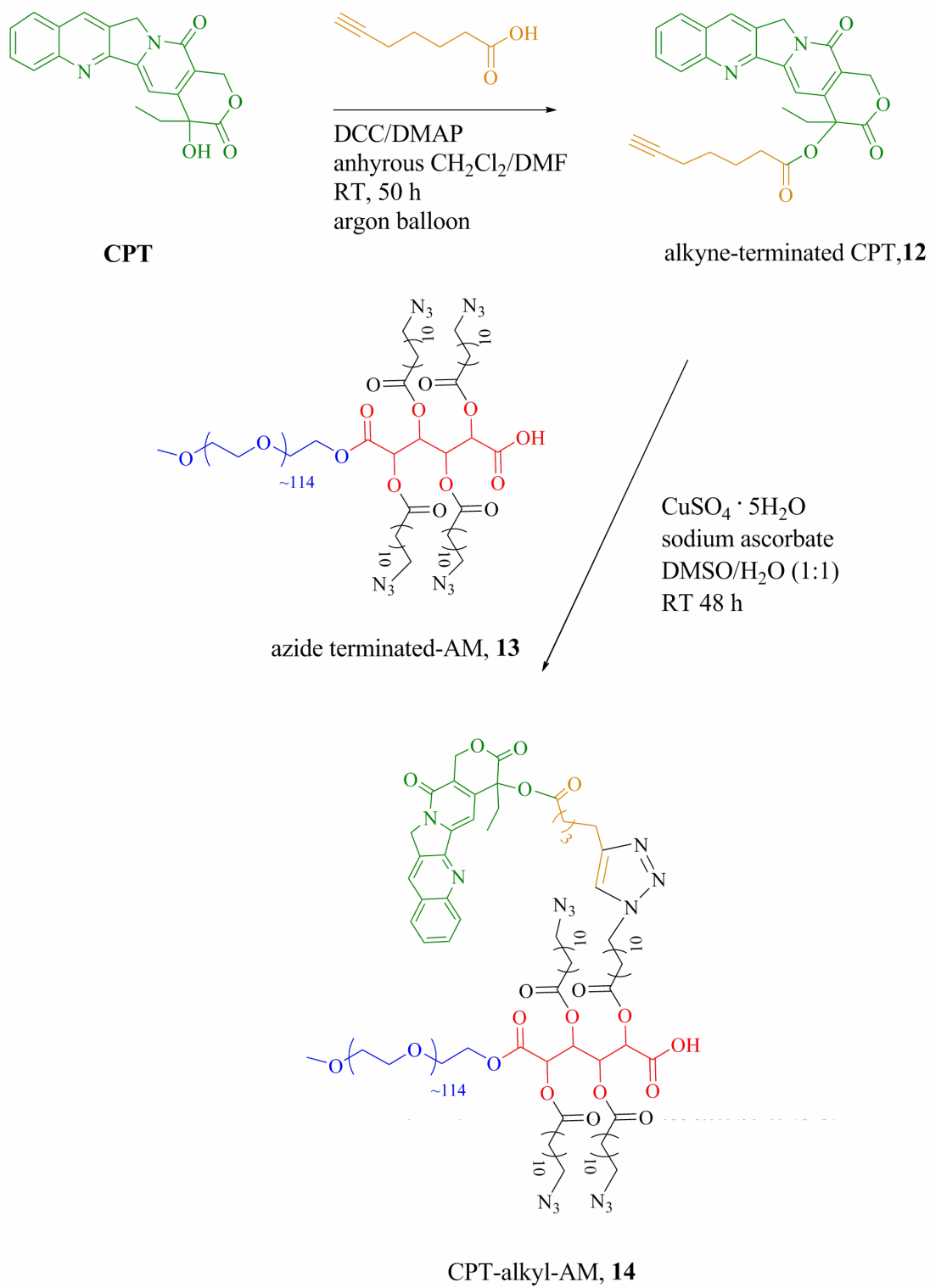


Figure 6-3. Preparation of CPT-alkyl-AM (14).

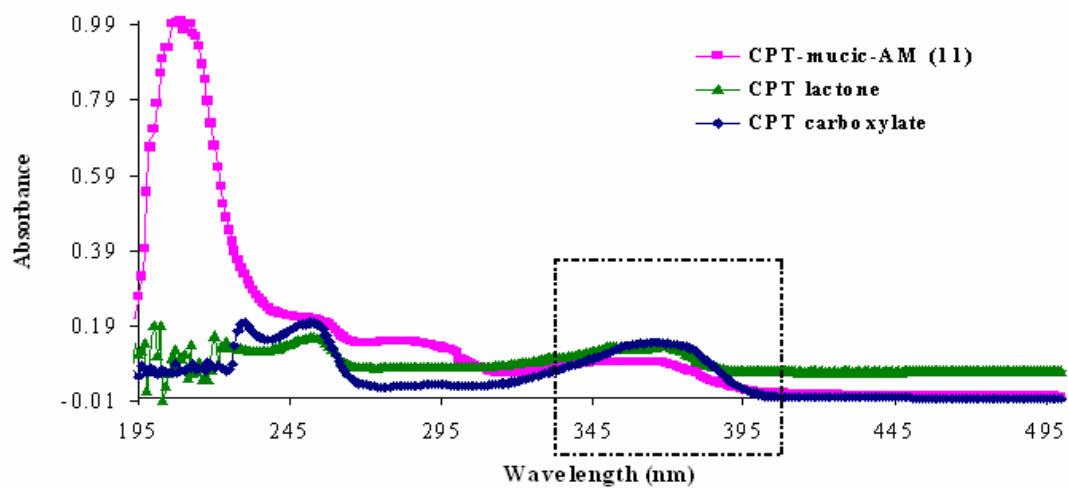


Figure 6-4. UV spectra of the two CPT forms and CPT-mucic-AM (11).

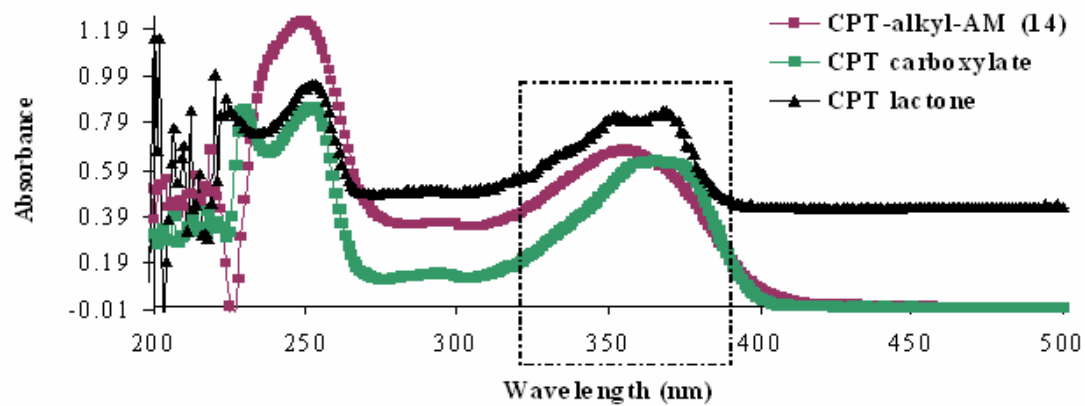


Figure 6-5. UV spectra of the two CPT forms and CPT-alkyl-AM (**14**).

Table 6-1. Impact of HSA on CPT *in vitro* release from AM-based micelles.

Sample	% CPT Cumulative Release (48h, 37°C)	
	Without HSA	With HSA
CPT-mucic-AM (11) (chemically bound drug)	24 %	20 %
CPT-alkyl-AM (14) (chemically bound drug)	25 %	14 %
CPT-loaded AM (physically encapsulated drug)	22 %	2 %

Table 6-2. Impact of HSA on micellar sizes of AM-based CPT micelle carriers.

Sample	Average Micellar Sizes (nm)	
	Without HSA	With HSA
CPT-mucic-AM (11) (chemically bound drug)	23	7
CPT-alkyl-AM (14) (chemically bound drug)	20	9
CPT-loaded AM (physically encapsulated drug)	22	8

FUTURE WORK

Use of Catalyst for Higher DOX Conjugation to AMs

DOX was conjugated to amphiphilic macromolecules (AMs) via hydrazone linkage resulting in a 29 % overall yield (Chapter 4). To obtain higher DOX conjugation, 1-5 mol % trifluoroacetic acid can be used as a catalyst (similar to the use of acetic acid [1]) in the reaction between hydrazide-AM (7) and DOX·HCl (see **Figure 4-2**) to obtain DOX-AMs (8).

In Vitro Drug Release from Drug-AM Conjugates

Further investigation of *in vitro* drug release from drug-AM conjugates is recommended:

a) The kinetics of DOX release from DOX-AMs (see Chapter 4, **Figure 4-8**) can be investigated to determine the kinetics of hydrazone bond cleavage at different pH values, and explore the extent of buffering capability of the buffers used, phosphate buffered saline (pH 6 - 9) and phosphate citrate buffer (pH 2.5 – 5.6) [2]. Furthermore, the release of physically encapsulated DOX in AM micelles can be evaluated at pH 5.0 and pH 7.4 to compare with DOX-AMs (chemically bound DOX) and further verify the pH-sensitivity of hydrazone linkage between DOX and AMs.

b) It is possible that human serum albumin (HSA) adsorbed to the regenerated cellulose dialysis membrane, blocking CPT release. If this is true, then CPT-HSA binding cannot be correlated with reduced CPT release, and the conclusions on HSA impact on CPT release from AM micelles (see Chapter 5, **Figure 5-6**) was incorrect. To

investigate this possibility, HSA in PBS can be incubated in the donor cells of the dialysis set-up (see **Section 5.3.6.**) for 48 h, then the HSA solution is replaced with CPT solutions in PBS (CPT alone, or CPT-loaded AMs or CPT-AMs). Comparison of the CPT release profiles will confirm whether HSA adsorbed to the membranes or not.

c) The anticancer activity of CPT is dependent on its closed lactone ring, thus release of intact CPT from CPT-AMs is of utmost importance. *In vitro* CPT release from CPT-AMs was very slow (see Chapter 5, **Figure 5-6**) possibly due to the slow ester bond hydrolysis between drug and glycine-AM. This slow CPT release is possibly one reason for no increased cytotoxicity of CPT-AMs compared to CPT alone. Further investigation of CPT release (e.g. extreme pH conditions, in presence of lysosomal enzymes) from CPT-AMs is therefore necessary to fully explore the potential of CPT-AMs as CPT nanocarriers.

Note: In the drug release experiments, it is important to always determine drug distribution (in donor cells, in receptor cells, or if adsorbed to membrane or dialysis cells) such that drug concentrations all add up to 100 %.

Cell Studies

Using confocal scanning microscopy, the pH sensitivity of the hydrazone linkages in DOX-AM conjugates can be further evaluated inside cancer cells. Addition of Bafilomycin A1 will inhibit endo/lysosomal acidification [3]. Intracellular DOX release from DOX-AMs, in the presence and absence of Bafilomycin A1, can be analyzed by comparing accumulation of DOX (a naturally fluorescent molecule) in cell nuclei stained with fluorescent markers (e.g. DAPI).

Micellar Stability in the Presence of Serum Proteins

Interactions of polymeric carriers with serum proteins reportedly influenced their *in vivo* fate as systemic drug delivery systems [4]. For block copolymer micelles, proteins are postulated to *i*) adsorb to the surface (especially if charged or hydrophobic) and cause opsonization leading to rapid RES clearance; or *ii*) accelerate the drug release from the micelles (if drug-protein affinity is high) and reduce drug accumulation at the tumor site [4]. The presence of PEG or PEO at the surface of drug delivery systems induces steric repulsive forces, stabilizing the micellar interface [5], and decreases the protein adsorption to the carrier [4-6]. However, AM micellar sizes were reduced in the presence of human serum albumin (Chapter 6) indicating micellar instability. Thus the stability of drug-loaded AM-based micelles in serum or blood needs to be further investigated.

***In Vivo* Studies**

Furthermore, *in vivo* studies are necessary to explore the potential of the AM-based micelles for anticancer drug delivery. In particular, drug-loaded or drug-conjugated AM micelles should be evaluated for prolonged blood circulation and accumulation in tumors *in vivo*.

References

- 1 T. Etrych, M. Jelinkova, B. Rihova, and K. Ulbrich. New HPMA copolymers containing doxorubicin bound via pH-sensitive linkage: synthesis and preliminary in vitro and in vivo biological properties. *Journal of Controlled Release* **73**: 89-102 (2001).
- 2 http://en.wikipedia.org/wiki/Buffer_solution.
- 3 P. Watson, A. Jones, and D. Stephens. Intracellular trafficking pathways and drug delivery: fluorescence imaging of living and fixed cells. *Adv. Drug Del. Rev.* **57**: 43-61 (2005).
- 4 J. Liu, F. Zeng, and C. Allen. Influence of serum protein on polycarbonate-based copolymer micelles as a delivery system for a hydrophobic anti-cancer agent. *Journal of Controlled Release* **103**: 481-497 (2005).
- 5 A. Lavasanifar, J. Samuel, and G. S. Kwon. Poly(ethylene oxide)-*block*-poly(L-amino acid) micelles for drug delivery. *Advanced Drug Delivery Reviews* **54**: 169-190 (2002).
- 6 G. S. Kwon and K. Kataoka. Block copolymer micelles as long-circulating drug vehicles. *Advanced Drug Delivery Reviews* **16**: 295-309 (1995).

CURRICULUM VITA

LEILANI SINGSON DEL ROSARIO

EDUCATION

- 09/2004-05/2009 Ph.D. Biochemistry
Department of Chemistry and Chemical Biology
Rutgers University, Piscataway, NJ, USA
- 06/1996-11/2001 B.S. Agricultural Chemistry, *magna cum laude*
Institute of Chemistry, College of Arts and Sciences
University of the Philippines Los Baños
College, Laguna, Philippines

TEACHING EXPERIENCE

- 09/2004-08/2005 Teaching Assistant (Chem 171, Chem 311, Chem 307)
Department of Chemistry and Chemical Biology
Rutgers University, Piscataway, NJ

PUBLICATIONS

- Jinzhong Wang, **Leilani S. del Rosario**, Bahar Demirdirek, Angela Bae, Kathryn E. Uhrich. "Comparison of PEG Chain Length and Density on Amphiphilic Macromolecular Nanocarriers: Self-assembled and Unimolecular Micelles." *Acta Biomateriala*, {invited} **2009**, 5, 883-892.
- Jelena Djordjevic, **Leilani S. del Rosario**, Jinzhong Wang, Kathryn E. Uhrich. "Amphiphilic Scorpion-like Macromolecules as Micellar Nanocarriers." *J. Bioactive and Compatible Polymers*, **2008**, 23, 532-551.